DYNAMIC RESPONSES TO SOCIAL SIGNALS

A Dissertation

Presented to the Faculty of the Graduate School

of Cornell University

In Partial Fulfillment of the Requirements for the Degree of

Doctor of Philosophy

by

Caitlin Hope Miller

August 2022

DYNAMIC RESPONSES TO SOCIAL SIGNALS

Caitlin Hope Miller, Ph. D.

Cornell University 2022

Chapter 1 examines the evolution of olfactory vomeronasal receptors (V1Rs) across mouse species within the *Mus* genus. We find evidence for distinct evolutionary trajectories across receptor clades and species-specific gene expansions.

Chapter 2 utilizes thermal imaging to investigate scent mark signaling in male house mice toward variable social environments. Fight outcome and initial signal investment have profound and interactive effects on marking effort and the temporal dynamics of scent marking.

Chapter 3 inspects the role of initial signaling effort in male house mice on contest dynamics. We demonstrate clear social costs to under-signaling, as low-marking competitive males engage in higher intensity fights that take longer to resolve.

Chapter 4 explores how reproductive state shapes responses to social signals. We find that estrus and pregnant females exhibit a striking valence switch in preference toward novel male odors. We discover a state-modulated shift in decision-making and evidence for distinct processing pathways for sex and identity information.

BIOGRAPHICAL SKETCH

From the outset, my research interests have been interdisciplinary. I was set on this integrative trajectory during my first independent research project, my senior thesis at Reed College. For my thesis project, I investigated neuropeptide expression patterns underlying sexual and aggressive behaviors in cichlid fish. In the process of developing and carrying out this project, I realized the importance of understanding an organism's behavioral ecology in order to ask strong neurobiological questions. Through this experience, I acquired a passion for scientific research and realized the type of research I wanted to perform. My goal became to implement an ecological lens going into my neurobiological questions, and in doing so, provide a novel perspective towards understanding the neural basis of behavior. To achieve this goal, I sought out technical and conceptual experience in both behavioral ecology and neuroscience. I participated in two long-term field projects that examined behavior of animals in their natural ecology. In Namibia, I investigated sexual coercion and aggression in wild desert baboons, and in California I examined the reproductive ecology of Black-backed Woodpeckers. I next obtained experience in a neuroscience laboratory, working as a research technician at OHSU under Dr. Gail Mandel's mentorship. In collaboration with a postdoc, I examined the transcriptional changes in astrocytes that are crucial for the healthy maturation and development of neurons. With this diverse set of research experiences behind me, the Neurobiology and Behavior Department was an ideal fit. A key goal throughout my dissertation was to design ecologically relevant social behavior assays that are tractable in lab environments.

ACKNOWLEDGEMENTS

A massive thank you to the Sheehan Lab both past and present. Everyone in the lab has helped me in some way or another over the years. This includes some incredible undergraduate researchers who made this work possible: Klaudio, Matt, Jia, Brandon and Tess. Over the innumerable struggles of my PhD Mike has always been an incredibly supportive mentor, and from whom I've learned a great deal.

I am grateful for the Warden Lab community, which was crucial in the early years of graduate school for deepening my knowledge of systems neuroscience.

My committee members were critical for keeping my PhD grounded in reality, and provided crucial feedback over the years. The NBB administrators are truly the backbone of the department, and I am deeply thankful for all their help.

I am also honored to have worked on several DEIJ initiatives during my time in NBB, and I am grateful for the incredible team of people I worked with. I want to thank all of them for their work, time, and care. A special thank you to Bhaavya, who was on all the committees alongside me, and did an incredible job of leading the department.

I am very fortunate to have an incredible support system, including my family who has always encouraged me to be curious. Since arriving in Ithaca I've made amazing friends that made this place truly special - you know who you all are. Finally, Will and Fen have seen all the highs and lows, and deserve a special recognition for surviving the PhD process.

Thank you to everyone that has helped me get here!

TABLE OF CONTENTS

CHAPTER 1

Distinct evolutionary trajectories of V1R clades across mouse species

Caitlin H Miller[1]*, Polly Campbell[2], Michael J Sheehan[1]*

1 Neurobiology and Behavior, Cornell University

2 Evolution, Ecology and, Organismal Biology, University of California – Riverside

* authors for correspondence: chm79@cornell.edu, msheehan@cornell.edu

Abstract

Background: Many animals rely heavily on olfaction to navigate their environment. Among rodents, olfaction is crucial for a wide range of social behaviors. The vomeronasal olfactory system in particular plays an important role in mediating social communication, including the detection of pheromones and recognition signals. In this study we examine patterns of vomeronasal type-1 receptor (V1R) evolution in the house mouse and related species within the genus *Mus*. We report the extent of gene repertoire turnover and conservation among species and clades, as well as the prevalence of positive selection on gene sequences across the V1R tree. By exploring the evolution of these receptors, we provide insight into the functional roles of receptor subtypes as well as the dynamics of gene family evolution.

Results: We generated transcriptomes from the vomeronasal organs of 5 *Mus* species, and produced high quality V1R repertoires for each species. We find that V1R clades in the house mouse and relatives exhibit distinct evolutionary trajectories. We identify putative species-specific gene expansions, including a large clade D expansion in the house mouse. While gene gains are abundant, we detect very few gene losses. We describe a novel V1R clade and highlight candidate receptors for future study. We find evidence for distinct evolutionary processes across different clades, from largescale turnover to highly conserved repertoires. Patterns of positive selection are similarly variable, as some clades exhibit abundant positive selection while others display high gene sequence conservation. Based on clade-level evolutionary patterns, we identify receptor families that are strong candidates for detecting social signals and predator cues. Our results reveal clades with receptors detecting female reproductive status are among the most conserved across species,

suggesting an important role in V1R chemosensation.

Conclusion: Analysis of clade-level evolution is critical for understanding species' chemosensory adaptations. This study provides clear evidence that V1R clades are characterized by distinct evolutionary trajectories. As receptor evolution is shaped by ligand identity, these results provide a framework for examining the functional roles of receptors.

Keywords: V1R, vomeronasal, pheromone, gene family, gene expansion, clade, *Mus*, house mouse

Introduction

Olfaction involves detecting and discriminating among chemicals in the environment. Chemical compounds can vary considerably in structure, creating a highly complex chemical space in which olfactory systems evolve. In most mammals, olfaction relies on two discrete receptor systems: main olfactory receptors (ORs) and vomeronasal receptors (VRs) [1-3]. ORs detect a broad range of environmental odors [4-6], while VRs are integral to species-specific chemical detection, including pheromone detection [7, 8]. In humans, ORs are the only olfactory receptors, as the vomeronasal system is no longer functional. In other species, VRs mediate a wide range of social behaviors, including sexual, aggressive, and parental behaviors [9-18]. VRs thus provide a unique window into the chemical basis of social behaviors and the evolution of pheromone detection.

Across species, VRs exhibit striking evolutionary patterns. Whereas ORs have largely orthologous relationships among divergent species [19], VR evolution is

characterized by rapid gene turnover wherein receptors are quickly gained and lost over evolutionary time [20-22]. This pattern of gene birth-and-death results in lineage-specific receptor repertoires [19]. Consequently, there are substantial differences in receptor sequences and repertoire size across divergent species [22-29]. For example, among three mammalian species (dog, opossum, and house mouse) there are virtually no one-to-one VR orthologs [19]. This is perhaps not surprising given the broad evolutionary timescale examined. However, even among two murine rodent species (the rat and house mouse), the majority of VRs fall into lineage-specific clades with very few orthologs [21, 24]. In addition to the evolutionary changes resulting from gene turnover, selection analyses on VRs across mouse species have revealed mixed results. Some studies find evidence for positive selection and lineage-specific pseudogenization [30, 31], while another detects evidence of genetic drift and negative selection [32].

As one of the leading model organisms, further understanding the evolution of chemosensation in the house mouse will provide insight into how chemical stimuli mediate distinct behavioral and neural responses. House mice are valuable models for examining VRs as they have large VR repertoires and there exists a wealth of knowledge on their social behavior, neural activity, and genetics [14-18, 33-39]. Currently, very few VRs have known ligands, which presents a significant barrier to studying the mechanisms underlying social behavior in house mice [33, 40-42]. By examining the evolutionary trajectories of VRs, we may uncover evolutionary patterns among receptor clades, and thereby identify targets for study based on the extent of turnover or conservation observed.

Vomeronasal sensory neurons express two major gene families in a cell-specific manner: V1Rs (type-1 VRs) and V2Rs (type-2 VRs) [4, 23]. V1Rs consist primarily of

single-exon genes whereas V2Rs are multi-exonic [43]. Structurally, V1Rs have a short N-terminal extracellular region whereas V2Rs have long and highly variable N-terminal domains [4, 43]. We focus on V1Rs in this study due to the genetic tractability of their simpler gene structure for transcriptome assembly and sequence analysis. In functional terms, V1Rs primarily detect airborne volatiles [13-14, 43-46]. In house mice, V1Rs have been implicated in detecting a wide range of volatiles, including urinary steroid molecules that are crucial for gender discrimination and sexual behaviors [40, 47-51].

Here, we characterize patterns of V1R evolution among the house mouse and relatives. We take a molecular evolutionary approach and analyze V1R repertoires across six species within the genus *Mus* (**Figure 1**): *M. m. domesticus* (house mouse), *M. spicilegus*, *M. macedonicus*, *M. spretus*, *M. caroli*, and *M. pahari*. By examining the under-explored timescale of VR evolution among closely related species, this dataset offers new insight into the dynamics of VR evolution and provides a framework for understanding the selective pressures shaping V1R clades. Investigating the evolutionary history of V1R clades may in turn guide future efforts to deorphanize receptors in the house mouse, as the evolutionary trajectories of receptors are shaped by the ligands they detect. Ultimately, molecular evolutionary approaches to sensory gene repertoires seek to link function to evolutionary patterns [25, 26, 52-54]. For example, we can

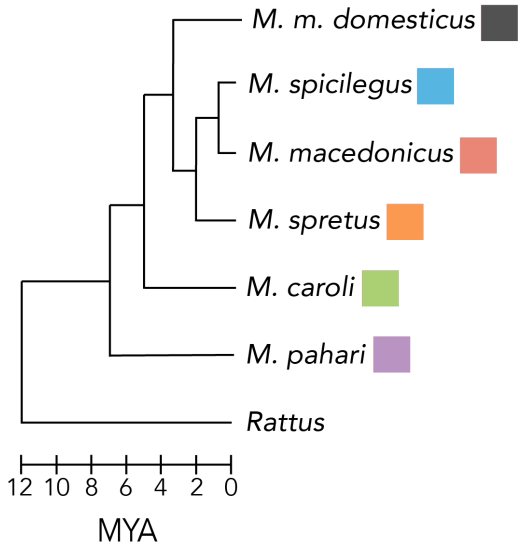

Figure 1. *Mus* species phylogeny. Includes all species in study [83, 84]. Rat (*Rattus norvegicus*) provided as outgroup. Species colors used throughout.

hypothesize that receptors detecting predator odors are highly conserved among mice due to shared or closely related predators among mouse species [55]. The present lack of resolved receptor-ligand relationships for most V1Rs precludes a comprehensive analysis of how patterns of gene turnover and selection regimes relate to ligands. The present work lays the foundation for such analyses in the future when more V1R ligands have been identified. In the present study, we provide detailed analyses of V1R clades known to detect estrus and pup cues in house mice [40, 42, 49].

Results

VNO sequencing, assembly & V1R recovery

Using wild-derived inbred mouse lines, we characterize V1R repertoires for five *Mus* species of varying evolutionary distance from the house mouse (1.5-7 mya, **Figure 1**) by sequencing their VNO transcriptomes using short-read platforms. By sequencing both males and females from inbred mouse lines our aim was to characterize the V1R gene family for each species, rather than differential gene expression or within-species variability, and subsequently compare those data to the house mouse reference genome. The final transcriptome assemblies for each species are of good quality (**Table 1**). We detect approximately twice the number of V1Rs than are currently annotated in the genomes of *M. spretus*, *M. caroli*, and *M. pahari* and provide the first *M. macedonicus* V1R dataset (**Table 1**). The number of V1Rs identified in *M. spicilegus* is in good agreement with existing genome annotations (**Table 1**). For one species (*M. spretus*), the short-read sequencing was performed at greater depth, and an additional round of long-read sequencing was done. This allows us to examine the effectiveness of short versus long-read sequencing for

assembling large and highly duplicated gene families such as V1Rs. The total number of assembled transcripts is greater for the *M. spretus* short-read dataset, as expected from greater sequencing depth (**Table 1**).

Table 1. VNO transcriptome assembly statistics, V1R transcript recovery and genome annotations.

Species	Total Transcripts	Mean Length (bp)	N50	% with ORF[f]	Total V1R Transcripts	V1Rs With Unique Annotations	V1R Genes Detected (With Duplicates)	Genome Annotated V1Rs
***M. m. domesticus*[a]**	---	---	---	---	263	---	208	208
***M. spicilegus*[b]**	228,809	664	1632	43	122	105	119	120
M. macedonicus	255,395	649	1630	42	129	117	126	---
***M. spretus*[c]**	1,181,673	688	1587	31	134 **(253)**	108 **(146)**	120 **(180)**	85
***M. caroli*[d]**	384,865	460	1919	42	131	110	126	50
***M. pahari*[e]**	450,181	305	3107	45	117	93	113	45

The mouse reference genome is shown for comparison (*M. m. domesticus*, top)[a]. Recovery estimates combining short and long-read datasets for *M. spretus* are indicated in bold. [a]GRCm38.p6, [b]GenBank accession#: QGOO00000000, [c]SPRET_EIJ_v1.1, [d]CAROLI_EIJ_v1.1, [e]PAHARI_EIJ_v1.1, [f]ORF: open reading frame

On average, 126 V1R transcripts are recovered from each species' short-read assembly (**Table 1**). A subset are transcript variants or gene duplicates, with homology to the same gene in the mouse reference genome (GRCm38.p6). The majority of V1Rs are single-exon genes, however, a substantial number contain introns and express transcript variants (**Table 1 & Figure 2**) [38]. For a conservative estimate of V1R genes, only unique transcript annotations are included (**Table 1**). When putative gene duplicates are added, the number of V1R genes increases markedly (**Table 1**). Compared to the house mouse the 5 sequenced *Mus* species have smaller V1R repertoires, consistent with V1R gene expansion in the house mouse (**Table 1**). However, the addition of long-read sequencing for *M. spretus* increases the number of V1Rs genes detected, resulting in a repertoire size similar to the house mouse (**Table 1**). Therefore, whereas the *M. spretus* V1R repertoire is likely close to complete, long-read sequencing may detect additional V1Rs in *M.*

spicilegus, M. macedonicus, M. caroli and *M. pahari*. Importantly, our analysis of V1R evolution in *Mus* is based on (1) a well-annotated mouse reference genome, (2) a comprehensive *M. spretus* V1R dataset, and (3) >100 V1Rs for all 6 *Mus* species. Therefore, small gaps in detection across the entire V1R family should not bias the broad patterns of V1R evolution reported here. Furthermore, the discrepancy in repertoire size between the house mouse and other species appears largely accounted for by a putative house mouse specific gene expansion, discussed in further detail below.

V1R evolution across *Mus* species

To explore V1R evolution, we characterize which receptors share a common ancestor (i.e. are orthologous) by examining relationships within a V1R gene tree containing six *Mus* species (the 5 sequenced species and the house mouse reference, **Additional File 1**). A subset of receptors does not exhibit a clear orthologous relationship to any V1R annotated in the mouse reference genome and are classified as non-orthologous genes, indicating either gene loss in the house mouse lineage or lineage-specific expansions in other species (**Figure 2**). Similarly, a set of receptors annotated in the mouse reference genome are not detected in any other species, suggesting recent expansion in the house mouse lineage (**Figure 2**).

We classify V1Rs into three broad categories based on their orthologous relationships: (1) V1Rs present only in the mouse reference genome, (2) non-orthologous V1Rs found in species other than the house mouse, and (3) V1Rs with orthology across multiple species. V1Rs with orthology across multiple species are further categorized based on the number of species represented in each orthologous receptor group (orthogroup). Orthogroups with 2-3 species are classified as “low

orthology," and orthogroups with 4-6 species as "high orthology" (**Figure 2A**). The majority of transcripts have some evidence for orthology (88.5%, **Figure 2A**). Furthermore, most transcripts are highly orthologous (75.1%, **Figure 2A**), indicating that missing V1Rs are unlikely to bias broad patterns identified here. Although many receptors are shared across species, approximately 25% of all V1R transcripts, and 59% of all unique V1R annotations, are either low orthology, non-orthologous, or present only in the mouse reference genome (**Figure 2A**). This indicates that the dramatic V1R gene turnover observed among more divergent mammalian species, such as across tetrapods or between rodent species [19, 21, 23], is replicated within the genus *Mus* albeit on a more limited scale. We further find a little over 5% of total V1Rs are present in only the house mouse reference genome. Nearly all of these reference-only receptors are located in a single clade and are tandemly arrayed on a single chromosome, suggesting a potential house mouse specific expansion.

A

ORTHOLOGY CATEGORY	% UNIQUE V1Rs	% TOTAL V1Rs
Reference Only	20.5	5.2
Non-Orthologous	24.4	6.2
Low Orthology *(2-3 species)*	14.0	13.4
High Orthology *(4-6 species)*	41.1	75.1
Any Orthology *(2-6 species)*	55.0	88.5

B

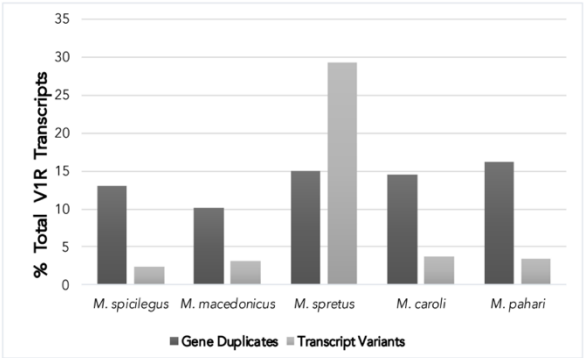

Figure 2. V1R orthology, gene duplicates, and transcript variants across *Mus* species. (A) The percent of unique and total V1Rs in each orthology category. **(B)** The percent of V1R transcripts that are either putative gene duplicates or transcript variants, for each species sequenced.

We next examine the presence of gene duplicates and transcriptional variation across species (**Additional File 2**). A similar proportion of V1R gene duplicates are identified across all 5 species (10-16%, **Figure 2B**). The proportion of V1R transcript

variants detected is also comparable across species, with the clear exception of *M. spretus* (**Figure 2B**). As expected, the addition of long-read (*M. spretus*) sequencing data recovers many more transcript variants than short-read sequencing datasets (**Figure 2B**). Interestingly, the same number of V1R genes expressing distinct coding transcript variants are detected in *M. spretus* as in the house mouse (43 V1R genes, **Additional File 3: Figure S1**). However, the identity of V1Rs exhibiting alternative spliceforms, and the clades they belong to, vary between the two species (**Additional File 3: Figure S1**). In contrast, the proportion of gene duplicates detected is similar between *M. spretus* and the other species. This indicates that, for gene families such as V1Rs, short-read datasets are sufficient for identifying gene duplicates.

Our characterization of V1R repertoires across *Mus* species allows for a reliable estimate of V1R gene loss in the house mouse. We detect evidence for 10 such gene losses, distributed across six clades (**Table 2** & **Figure 3A**: indicated in red text). All V1R genes lost in the house mouse are present in at least 3 of the 5 sequenced *Mus* species, including close relatives (**Table 2**). Most gene losses have corresponding pseudogenes in the house mouse (**Table 2**). It appears gene losses are relatively uncommon compared to the abundant gene gains, at least within the house mouse lineage.

Novel V1R clade: clade "N"

In addition to the house mouse gene losses observed in clades E, C, H, I and G, we identify a novel V1R clade (**Table 2, Figure 3A**). This novel clade "N" has been lost in the house mouse and consists of two receptor orthogroups. Both clade N receptors (*Vmn1r248* and *Vmn1r249*) are expressed in at least three *Mus* species (**Additional**

File 3: Figure S2) and have corresponding pseudogenes in both the house mouse (*M. m. domesticus*) and the rat (*Rattus norvegicus*).

Table 2. V1R gene losses in the house mouse.

Gene ID	Clade	House Mouse Pseudogene	Sequenced Species Expression
Vmn1r240	E	---	
Vmn1r241	E	Vmn1r-ps144	
Vmn1r242	G	---	
Vmn1r243	C	Vmn1r-ps15	
Vmn1r244	C	---	
Vmn1r245	I	Vmn1r-ps126	
Vmn1r246	I	Vmn1r-ps132	
Vmn1r247	H	Vmn1r-ps103	
Vmn1r248	N	Vmn1r-ps139	
Vmn1r249	N	Vmn1r-ps140	

Species with receptor expression are indicated with different colors: *M. spicilegus* (blue), *M. macedonicus* (red), *M. spretus* (orange), *M. caroli* (green), and *M. pahari* (purple).

Variable patterns of evolution across V1R clades

Gene Turnover: Orthology, Duplication & Repertoire Size

The maintenance or loss of gene orthologs is a major mode of chemosensory evolution [19, 21, 23, 27]. If different clades exhibit either high degrees of gene orthology or lineage-specific gene expansions, this suggests distinct evolutionary trajectories. Patterns of V1R gene orthology and duplication vary across clades. Four clades are very orthologous (E, F, J/K and L: >80% of receptors are high-orthology), with clade G trailing behind with more non-orthologous receptors (**Figure 3A, B**). Each of these clades has 5 or fewer gene duplicates, however, the proportion of

duplicates is variable (**Figure 3C, D**). Clades E, F and G have very low proportions of gene duplicates, while clade J/K has among the highest (**Figure 3C**).

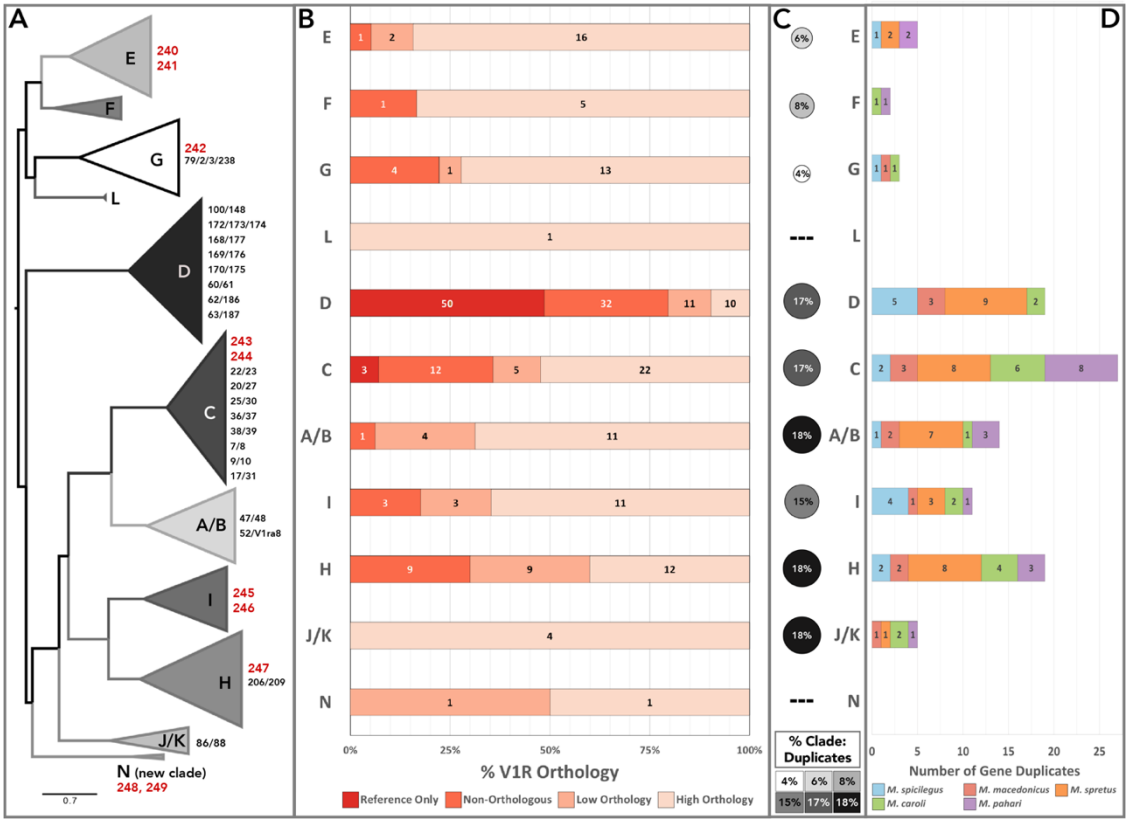

Figure 3. Patterns of orthology and gene duplication across V1R clades. (A) Phylogeny of all 11 V1R clades. Scale bar indicates 0.7 amino acid substitution per site. Shown to the right of each clade: V1R gene losses in the house mouse (red), and orthogroups with multiple reference annotations (combination-IDs, black). **(B)** Percent of V1Rs by clade that fall into each orthology category: present only in the reference-only, non-orthologous, low orthology and high orthology. **(C)** Percentage of total of (sequenced) transcripts in each clade composed of gene duplicates (reference not included). The size and color of each circle corresponds to the calculated percentage. **(D)** Total number of V1R gene duplicates detected in each clade for each species.

Clades C, D and H have abundant low-orthology and non-orthologous receptors (**Figure 3B**), indicating greater evolutionary lability. While most orthologous relationships are straightforward, some orthogroups contain multiple house mouse receptors, and are annotated with combination-IDs to indicate the relationship to multiple genes (e.g. *Vmn1r25/30*). These receptor groups are the result of one or more duplication events within the *Mus* lineage, and are unequally distributed across clades, with 76% located in clades C and D (**Figure 3A**). In addition, all reference-only V1Rs are located in these same two clades (**Figure 3B**). Not surprisingly, clades

C, D and H have the highest number of detected gene duplicates (19 or more) and have similarly high proportions of duplicates by clade size (**Figure 3C, D**). Thus, all three clades have evidence for substantial gene expansions, particularly clade D within the house mouse lineage.

We examine V1R clade sizes across all 6 species. With the striking exception of clade D, the house mouse clade sizes are very similar to the 5 other species, (**Figure 4**). This general pattern provides further evidence that receptor recovery is high and species' repertoires are near complete. Interestingly, the *M. spretus* repertoire is largest for several clades (A/B, C, E, H and I; **Figure 4**), indicative of *M. spretus*-specific gene expansions.

The size ranges of two clades (A/B and D) are skewed by the house mouse and *M. spretus* datasets. Both species have much larger clade D repertoires than the other 4 species, exposing this clade as a potential hotspot for recent gene duplications (**Figure 4**). On the other hand, the discrepancy in clade D repertoire size may be the result of poor receptor recovery for this clade, such that additional long-read sequencing may reveal comparable patterns in other species. An existing VR expression dataset sheds some light on this, as it finds clade

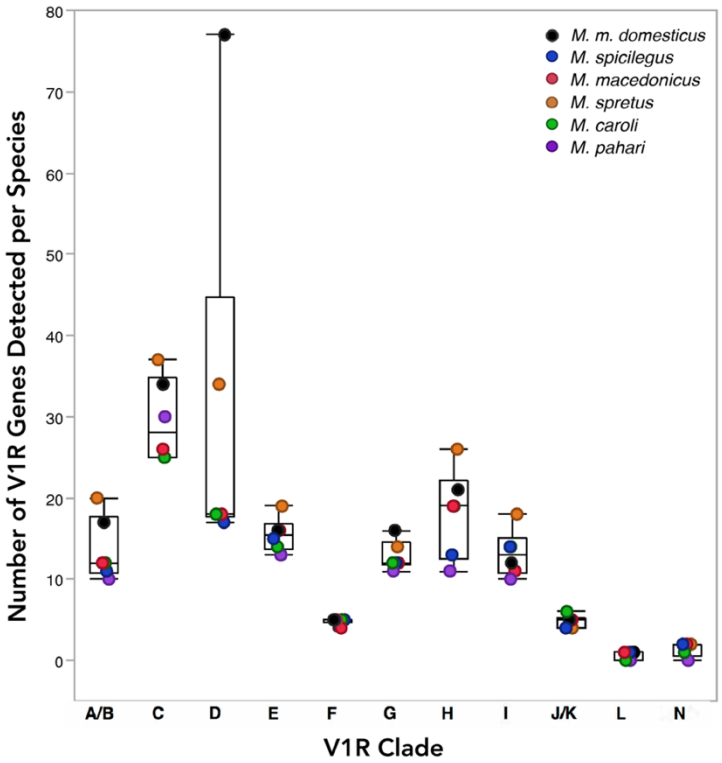

Figure 4. V1R clade receptor repertoire sizes across *Mus* species. *Mus* species are indicated with different colors.

D receptors in house mice are more lowly expressed than other clades [38]. However, while the *M. spretus* clade D is larger than the other sequenced mouse species, it is still considerably smaller than the house mouse (43 fewer receptors**, Figure 4**). Therefore, despite potential low clade D receptor recovery, our data still suggest a large house mouse specific clade D expansion. In contrast, there are several other clades which exhibit low variation in repertoire size across all species' datasets (E, F, G, J/K, L, N). Furthermore, clades C and H display variation in repertoire size across all 6 species, providing evidence for species-specific V1R gains and losses in multiple lineages (**Figure 4**).

Table 3. V1R branches under positive selection across clades.

CLADE	TERMINAL Branches[a]	INTERNAL Branches[b]	TOTAL Branches	TESTED Branches	% Branches[c]	TESTED Orthogroups	% Orthogroups[d]	Orthogroup IDs[e]
A/B	3	2	5	**119**	4.20	**11**	27.27	Vmn1r45, Vmn1r47/48, Vmn1r52
C	3	2	5	**235**	2.13	**35**	11.43	Vmn1r11, Vmn1r21, Vmn1r25/30, Vmn1r38/39
D	5	0	5	**119**	4.20	**13**	30.77	Vmn1r60/61, Vmn1r172/173/174, Vmn1r183, V1rd19
E	0	1	1	**122**	0.82	**16**	6.25	Vmn1r241
F	2	0	2	**45**	4.44	**5**	20.00	Vmn1r235
G	6	2	8	**101**	7.92	**13**	38.46	Vmn1r74, Vmn1r76, Vmn1r81, Vmn1r83, Vmn1r242
H	3	0	3	**125**	2.40	**15**	20.00	Vmn1r205, Vmn1r206/209, Vmn1r247
I	2	0	2	**100**	2.00	**13**	15.38	Vmn1r192, Vmn1r193
J/K	0	1	1	**57**	1.79	**4**	25.00	Vmn1r85
L	0	0	0	**7**	0.00	**1**	0.00	---
N	0	0	0	**5**	0.00	**1**	0.00	---
Total	**24**	**8**	**32**	**1034**	**3.09**	**127**	**19.05**	**NA**

The total number of tested branches and orthogroups are bolded, all other data columns correspond to branches under positive selection (P≤0.05). All branches, including counts and percentages, are after 5% FDR correction. [a]Terminal branches correspond to genes. [b]Internal branches correspond to deeper branches in the orthogroup. [c]Percentage of total branches tested in a given clade under positive selection. [d]Percentage of the total number of orthogroups tested in a given clade with evidence for positive selection. [e]Orthogroup gene IDs that contain at least one branch under positive selection.

Patterns of Positive Selection

To further examine the selective pressures shaping V1R clade evolution, we tested orthogroups (with at least four orthologs and/or paralogs) for the presence of episodic positive selection using an adaptive branch-site random effects model based on dN/dS estimates [56]. A total of 127 orthogroups containing 685 V1Rs genes

(including putative gene duplicates) were tested across all 11 clades (**Table 3**). We find evidence for 24 V1R genes under positive selection (3.5% of genes tested), as well as 8 deeper branches (2.3% of deeper branches tested) under a 5% false discovery rate (FDR) (**Table 3**). There are no noticeable differences in the number of branches under positive selection across species (**Additional File 3: Table S1**), however, some striking differences exist across clades (**Table 3**). Interestingly, the stark patterns of gene turnover evidenced by gene orthology and duplication, do not always align with positive selection trends. This may be due to the fact that high gene turnover makes detecting positive selection more challenging. However, it may also suggest that different clades are experiencing distinct diversifying selective pressures, ranging from large-scale gene gains and losses, to small-scale receptor sequence divergence. The most striking example is clade G, which is very orthologous with extremely low rates of gene duplication (**Figure 3)**, but simultaneously sports almost double the percentage of branches under positive selection compared to other clades (**Table 3**). In contrast, clade D shows pronounced patterns of rapid evolutionary change, with evidence for gene turnover (particularly gene gains in the house mouse lineage) as well as a large number of genes under positive selection (**Table 3**). Similarly, clade E demonstrates a consistent pattern of conservation with minimal gene turnover, and the lowest proportion of branches under positive selection (**Table 3**).

Guided by the evolutionary patterns observed across clades, we identify and categorize receptors as interesting candidates for further functional work based on striking patterns of conservation or divergence (**Additional File 3: Table S2**). We hope this list will help guide future efforts to deorphanize V1Rs.

Fast-evolving clades

Clade H

Clade H appears to be a mouse-specific V1R expansion, as it is absent in the rat genome [21]. The clade is characterized by low orthology, abundant gene duplicates, and variable repertoire size across species (**Figures 3 & 4**). In contrast to the patterns of high gene turnover, relatively few clade H branches have evidence for positive selection (**Table 3**). A sub-region of clade H containing *Vmn1r217*, *219* and *220* receptors exemplifies this pattern of low orthology, while the receptor orthogroup *Vmn1r206/209* is representative of the abundant gene duplicates (**Figure 5A**). Intriguingly, the *Vmn1r206/209* orthogroup also has evidence for positive selection, pointing to strong diversifying selection within this receptor group (**Table 3**). A striking exception to the evolutionary lability of clade H is the highly conserved *Vmn1r197* receptor group (**Figure 5A**). The general pattern of rapid species-specific gene gains and losses suggests clade H receptors may play an important role in detecting complex species-specific signals.

Clade C

Clade C is the largest V1R clade across species with the exception of the house mouse. Clade C also exhibits variable repertoire sizes across species, indicative of lineage-specific evolution (**Figure 4**). This inference is supported by the large numbers of combination-ID orthogroups, gene duplicates, non-orthologous receptors, and house mouse-specific gene gains (**Figure 3**). In contrast to the high levels of gene turnover, relatively few clade C branches have evidence of positive selection (**Table 3**). The phylogenetic structure of clade C comprises three sub-clades, one of which is quite orthologous (**Figure 5B**). Interestingly, the non-orthologous receptors

are largely clustered in one sub-clade (57%, **Figure 5B**), while the majority of receptors under positive selection are located in another (21% orthology**, Figure 5B**). Together, this suggests these subclades may be experiencing distinct forms and rates of receptor evolution. Two clade C receptors, *Vmn1r9* and *Vmn1r10*, have been implicated in pup odor detection in house mice [42]. However, these receptors also respond to female odors, and may detect chemosensory components of the nest environment [42]. These two receptors are part of a single receptor orthogroup (*Vmn1r9/10*) that is both orthologous and highly duplicated (**Figure 5B**). The sister group *Vmn1r7/8* exhibits a similar pattern of high orthology and abundant duplication (**Figure 5B**). Given the potential role of *Vmn1r9/10* receptors in pup odor detection, and the lineage-specific evolutionary patterns observed in *Vmn1r7/8* and *Vmn1r9/10,* these receptor groups are interesting candidates for future functional tests of their role in conspecific chemosignaling.

Clade D

Clade D exhibits a large skew in repertoire size within the house mouse (**Figure 4**), and has the most dramatic pattern of non-orthology across all V1R clades (**Figure 3B**). Nearly all reference-only V1Rs (50/53: 94%) are located in clade D, providing further support for a large recent gene expansion in the house mouse, despite the potentially low receptor recovery of other species in this clade (**Figure 3B**). These receptors are similar in sequence and cluster together on chromosome 7, consistent with recent tandem gene duplication. While we do not find evidence for a comparably large expansion in the other mouse species, we recover approximately twice as many clade D receptors in *M. spretus* relative to the other four species (**Figure 4**). It is possible that similar expansions exist in the other species that are not detected here,

particularly given prior evidence that clade D receptors are lowly expressed in the house mouse [38]. Clade D has a high proportion of non-orthologous receptors and gene duplicates, as well as a large percentage of orthogroups under positive selection (30.77% of tested orthogroups, **Table 3**). Given the evolutionary lability of clade D, there are a few receptors that stand out as highly orthologous (*V1rd19*, *Vmn1r179* and *Vmn1r172/173/174,* **Figure 5C**), two of which have evidence for positive selection (**Table 3**). Clade D appears to be experiencing lineage-specific evolution at the scale of both gene gains and losses, as well as sequence divergence.

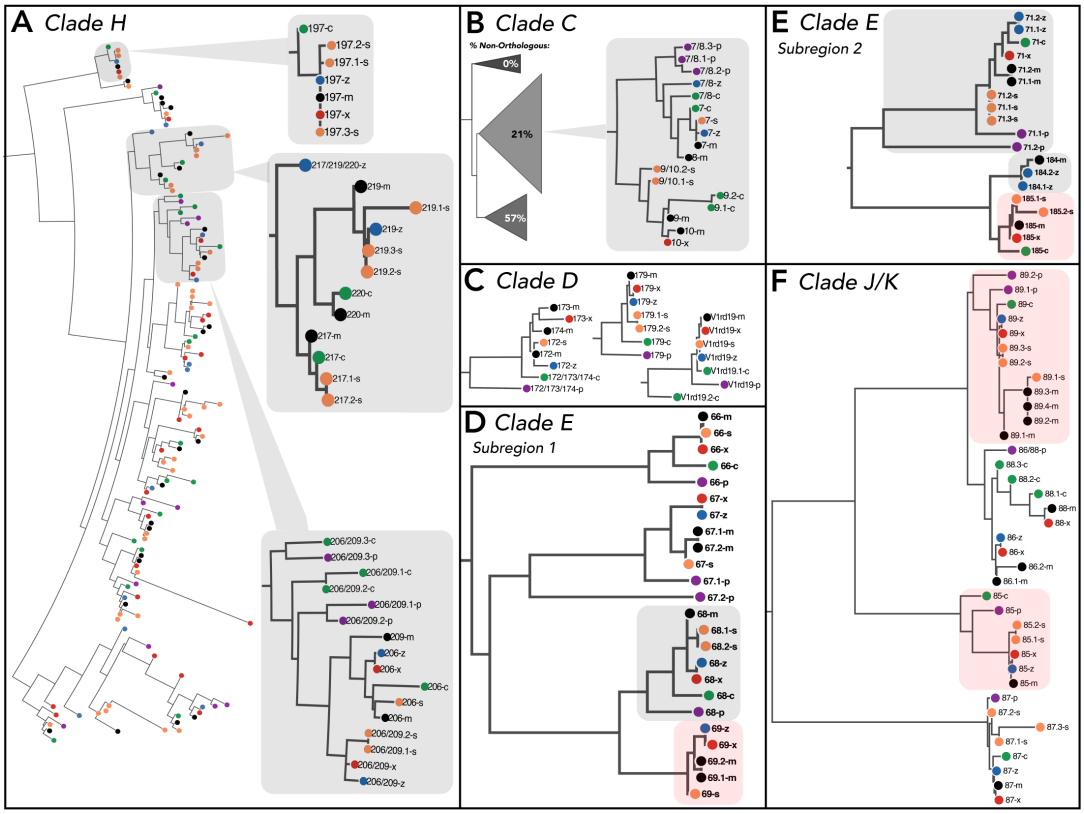

Figure 5. Example receptor groups depicting patterns of lineage-specific evolution and conservation across clades. V1R annotations are abbreviated (e.g. *Vmn1r137* as 137). Species transcripts annotated with the same reference gene have unique transcript IDs (e.g. 217.1 and 217.2). *Mus* species are indicated with colors and letters (*M. m. domesticus*: "m" and black; *M. spicilegus*: "z" and blue; *M. macedonics*: "x" and red; *M. spretus*: "s" and orange; *M. caroli*: "c" and green; *M. pahari*: "p" and purple). **(A) Clade H**: entire clade depicted, highlighting receptor groups that depict patterns of conservation and divergence. **(B) Clade C:** sub-clades shown with percentages of non-orthologous receptors. *Vmn1r7/8* and *Vmn1r9/10* are shown in detail. **(C) Clade D:** specific clade D receptor groups uniquely conserved across species. **(D-E) Clade E:** Specific receptor subregions of clade E. Highlighted receptors have some functional evidence (grey) or are deorphanized with strong evidence (red). **(F) Clade J/K:** entire clade depicted, highlighting specific deorphanized receptor groups that detect estrus cues (sulfated estrogens) in female urine.

Conserved clades & female conspecific detection: *Clades E & F*

A subset of V1R clades are highly conserved, and thus good targets for uncovering receptors with conserved olfactory functions. Clades E and F are characterized by high orthology (**Figure 3B**), long internal branch lengths and short terminal branch lengths, suggestive of old gene duplications maintained within the *Mus* lineage (**Additional File 3: Figure S3**). In contrast, very few recent gene duplications are detected (**Figure 3C, D**). In addition, clade E has the lowest proportion of branches under positive selection of any clade (**Table 3**). Clade F, on the other hand, has a single receptor (*Vmn1r235*) with evidence for positive selection in two species (**Table 3, Additional File 3: Table S1**). A subset of 5 clade E receptors is important for the detection of female-specific urine odors in house mice (*Vmn1r68, Vmn1r69, Vmn1r71, Vmn1r184, Vmn1r185*) [40]. Two clade E sub-regions containing these same 5 receptor groups are shown in **Figure 5D, E**; those with the strongest support for female odor detection are highlighted in red (*Vmn1r69* and *Vmn1r185*) [40]. *Vmn1r68* and *Vmn1r69* are sister to each other in the gene tree and are highly orthologous, however, *Vmn1r69* has no orthologs detected among the more basal species (*M. caroli* and *M. pahari*; **Figure 5D**). It is plausible that *Vmn1r69* is the result of a gene duplication event preceding the divergence of the four more derived species (**Figure 5D**), providing enhanced specificity or sensitivity toward female-specific urine odors. The second clade E sub-region contains receptors: *Vmn1r184*, *Vmn1r185,* and *Vmn1r71*. *Vmn1r184* and *Vmn1r185* are sister receptor groups, in which *Vmn1r185* is highly orthologous and *Vmn1r184* appears to be the result of a recent duplication event (**Figure 5E**). Interestingly, *Vmn1r184* is detected in only the house mouse and *M. spicilegus* (**Figure 5E**). Furthermore, *M. spicilegus* has evidence for a species-specific *Vmn1r184* duplicate, and has an absence of

Vmn1r185 expression (**Figure 5E**). The distinct expression pattern of *Vmn1r184* in *M. spicilegus* is noteworthy given this species' unique social structure, which includes cooperative behaviors and social monogamy [57]. In comparison, *Vmn1r71* is highly orthologous (**Figure 5E**), but displays remarkable transcriptional variability, most of which is located at either the C-terminus or N-terminus regions of the protein (**Additional File 3: Figure S3**). Broadly, clades E and F display patterns of conservation, with some evidence of positive selection in clade F, and potential lineage-specific gains in clade E among receptors involved in detecting female cues.

Clade J/K evolution & the detection of estrus cues

Clade J/K is a small clade of only 4 receptor groups that is highly orthologous and boasts one of the highest proportions of gene duplicates (**Figure 3**). This clade thus encompasses a unique mixture of conservation and expansion, in which there is very little gene loss but gene gains are abundant (**Figures 3 & 5F**). Clade J/K is also the only clade for which half of the receptors have known ligands [40, 49]. In the house mouse, two of the four J/K receptors have been shown to detect estrus cues (i.e. sulfated estrogens) in female urine [40, 49]. Given the unique features of this clade, we examined in greater detail the amino acid changes across species within the two deorphanized receptors (*Vmn1r85* and *Vmn1r89*). The *Vmn1r89* receptor group has evidence for short and long transcript types across *Mus* species (**Additional File 3: Figure S4**). Many species have only one form detected. However, the house mouse and *M. spretus* express both forms as transcript variants, while *M. pahari* appears to have distinct genes generating these two forms (**Additional File 3: Figure S4**). The widespread detection of both transcript types suggests they may facilitate the detection of distinct ligand (i.e. sulfated estrogen) features. This is particularly

compelling given that in the house mouse, *Vmn1r89*-expressing VSNs detect multiple sulfated estrogen molecules and are more broadly tuned than *Vmn1r85*-expressing VSNs [40]. In comparison, the *Vmn1r85* receptor group is highly conserved among the 3 *Mus* species most closely related to the house mouse (**Figure 5F**), with the majority of substitutions concentrated in *M. caroli* and *M. pahari* (**Additional File 3: Figure S5**). For both *Vmn1r85* and *Vmn1r89,* the highest proportion of amino acid site changes detected across species occurs in extracellular regions (**Additional File 3: Figure S6)**. The trend towards greater extracellular substitutions is consistent with a prior analysis of molecular evolution in 22 V1Rs, demonstrating that most sites with evidence for positive selection are located in extracellular motifs [30]. Moreover, positive selection is detected in *Vmn1r85* (**Table 3**) at an internal branch containing the house mouse and close relatives (*M. spicilegus, M. macedonicus* and *M. spretus,* **Additional File 3: Table S1**).

Discussion

V1R clades are characterized by distinct evolutionary trajectories

The complexity of the chemical environment presents unique evolutionary challenges. In addition to detecting a vast range of chemical stimuli, olfactory systems must flexibly adapt to novel environments and social contexts. One of the primary mechanisms of chemoreceptor evolution is through gene birth-and-death, mediated by duplication events and pseudogenization [21, 23, 27]. Across divergent mammalian species, VRs have been shown to be fast-evolving with high gene turnover and lineage-specific clades, compared to the more conserved and largely orthologous ORs [19]. This has led to the hypothesis that ORs are broadly-tuned generalists, and VRs are more narrowly-tuned specialists [19]. Furthermore, olfactory

specialization is hypothesized to occur through selection on distinct receptor subfamilies [23]. In this manner, receptor families may expand or contract in a lineage-specific fashion, and receptors in each family may become more diverse or conserved. Here, we identify distinct patterns of evolution among *Mus* V1R clades, consistent with a model of subfamily-specific selection. Some V1R clades have evidence of high gene turnover, while others are highly orthologous across species. We similarly detect variable patterns of positive selection across clades. Thus, the evolutionary patterns of gene turnover and positive selection are not always coincident, suggesting different evolutionary forces may act on clades in a distinct fashion. Furthermore, the evolutionary trajectories of clades could be driven by genomic processes such as variation in recombination rates across the genome. Future work examining V1R evolution in relation to additional features of the genome will be informative. Prior research has generated controversy over what evolutionary forces mediate V1R evolution. Some studies detect evidence of positive selection and lineage-specific pseudogenization, while another study finds evidence for genetic drift and negative selection [30-32]. Our data suggest that these seemingly contradictory results are not mutually exclusive. Depending on the subfamily of receptors examined, one could detect very different evolutionary patterns. This creates a functional framework in which to examine subsets of V1Rs, as receptor evolution is sculpted by the identity of their ligands.

V1R gene gains and losses

Our results support the gene birth-and-death model of V1R evolution, exemplified by the variable patterns of orthology, gene duplicates, and sequence diversity observed across clades. However, while gene gains appear abundant across *Mus* species,

clear evidence of gene losses are infrequent. A reliable estimate of V1R gene loss is restricted to the house mouse, due to constraints of V1R recovery among the other *Mus* species sequenced. Nevertheless, across all V1R clades only 10 gene losses are detected in the house mouse. We also identify a novel clade of two receptor groups, which appears to have undergone pseudogenization in house mice and in rats. This stands in contrast to a previous study examining the microevolution of V1Rs among *Mus musculus* subspecies, which detected a high frequency of null alleles [32]. On the other hand, functional gene duplicates appear plentiful. The most striking example is in the house mouse, in which clade D appears to have undergone a large species-specific gene expansion. As house mice successfully inhabit both commensal and non-commensal environments, it is tempting to posit that the clade D expansion may reflect a chemosensory adaptation to accommodate their expanded chemical environment [58, 59]. Commensal behavior would have originated (at the earliest) in conjunction with agriculture and permanent human settlements roughly 10,000 years ago. Thus, gene expansions likely predate commensal behavior and could plausibly facilitate the invasion of novel niches rather than an adaptation to it [68]. Overall, the abundant gene gains suggest that in the *Mus* genus, or at the very least within *Mus musculus* subspecies, expansion of the V1R family is ongoing.

Patterns of receptor evolution and function

Only a handful of V1Rs have known ligands. However, it has become increasingly clear that a critical function of the VNO involves detecting heterospecific odors, such as predator cues [49, 55, 60, 61]. V1Rs tuned to detecting broad classes of predator cues (e.g. birds of prey, snakes or mammals) may be conserved across mouse species. In particular, clade F has been implicated in detecting mammalian predator

cues [49]. The broad-scale patterns of conservation observed in clade F are consistent with the maintenance of a similar key function, such as the detection of predator odor cues with shared ligands [55]. Given the possible role of clade F in predator detection, further investigation of the sole receptor group (*Vmn1r235*) with evidence of positive selection warrants further investigation.

Chemical signaling is critical to social and reproductive interactions across a wide variety of mammalian species, including mice. One of the best described olfactory communication systems exists in house mouse urine scent marks [62]. House mice secrete proteins in their urine (major urinary proteins, MUPs) that facilitate pheromonal communication and individual recognition [17, 63-68]. MUPs act as transport vessels for the slow-release of volatile compounds detected by V1Rs [8, 51, 63, 67]. As these protein ligands vary considerably across *Mus* species, their corresponding volatiles likely shift as well [63, 67]. As a result, clades such as C, D and H, exhibiting highly species-specific evolution may be good targets for the detection of social cues.

Mounting evidence suggests that V1Rs are crucial for detecting sex-specific cues and the physiological status of conspecifics [40, 48, 49, 69]. A subset of clade E receptors respond to female-specific urine ligands, as such, clade E conservation may be tied to detecting conspecific sex cues [40]. Clade D has also been implicated in detecting female odors [49]. However, the activation of clade D is quite specific to *Vmn1r167* [49]. Interestingly, *Vmn1r167* contains one of the largest species-specific (*M. spicilegus*) gene duplications, and is only detected in *M. spicilegus* and the house mouse. *Vmn1r167* may thus play an important derived role in female odor detection.

Previous work demonstrates that V1Rs are strongly activated by sulfated steroids, and up to 80% of ligands detected in female urine may be sulfated steroids [48].

Clade J/K has been shown to play an important role in detecting sulfated estrogen molecules [40]. As such, the pattern of conserved orthology in clade J/K may reflect a crucial role for these receptors in discerning information about the internal state of conspecifics, particularly female reproductive state. Furthermore, the proportionally high levels of positive selection and gene duplication suggests lineage-specific evolution is occurring, though maintaining receptor functionality is important.

Conclusions

Understanding the evolutionary dynamics of the vomeronasal system reveals important properties of chemosensory evolution, as well as the functional roles of different receptors. In generating near-complete V1R repertoires for 5 *Mus* species, we find evidence for previously described patterns of high gene turnover observed among divergent species. However, by examining the evolutionary relationships of V1Rs across the *Mus* genus, we find that distinct receptor lineages have experienced different evolutionary trajectories both at the level of gene gains and losses as well as sequence divergence. Thus, clade-level evolution is critical to understanding the chemosensory adaptions of species to their diverse chemical environments. Furthermore, the evolutionary patterns of V1Rs observed supports the proposition that the detection of physiological status and female-specific cues may be an important role of V1R chemosensation [40, 48, 49, 69]. Ultimately, these results provide a key foundation for future functional studies of V1Rs.

Methods

Animal strains and tissues

All mice sequenced in this study are from wild-derived inbred lines. Mouse strains for *M. caroli* (CAR: RBRC00823) and *M. spicilegus* (ZBN/Ms: RBRC00661) were obtained from RIKEN BioResource Center (Japan). *M. pahari* (PAH/EiJ) was obtained from The Jackson Laboratory (Bar Harbor, ME). All strains were maintained in an Animal Care facility at Cornell University with a 14:10 shifted light:dark cycle, and provided food and water *ad libitum*. Experimental protocols were approved by the Institutional Animal Care and Use Committee (IACUC: Protocol #2015-0060), and were in compliance with the NIH Guide for Care and Use of Animals. All experimental mice were sacrificed by cervical dislocation, and the VNOs subsequently dissected. VNOs (stored in RNALater) for *M. macedonicus* (XBS) and *M. spretus* (SFM) were obtained from the Campbell Lab at Oklahoma State University (OSU). Mice at OSU were maintained on a 12:12 light:dark cycle and provided with food and water *ad libitum*. Live animal work at OSU was approved by the IACUC under protocol # AS-1-41.

Illumina RNA library preparation & sequencing

VNO epithelia were dissected from at least one male and one female from each inbred wild-derived species line and subsequently pooled to obtain V1R repertoires unbiased to a particular sex, except for the HiSeq dataset (ZRU: 2 males, 2 females; XBS: 1 male, 1 female; CAR: 2 males, 2 females; PAH 1 male, 1 female; SFM short-read HiSeq: 0 males, 15 females; SFM long-read Isoseq: 1 male, 1 female). Variation in the number of individuals samples per species was due to sample and data availability as well as dissection quality. This negligibly impacts our results as we are

examining V1R repertoires not expression levels. Total RNA was extracted from VNO tissues using the Qiagen RNeasy kit, and subsequently quantified using QuBit Fluorometric Quantitation. RNA sequencing libraries were generated using the NEBNext Ultra RNA Library Prep Kit for Illumina (NEB #E7530). NEBNext Poly(A) mRNA Magnetic Isolation Module (NEB #E7490) was used for RNA Isolation. Sequences were indexed using the NEBNext Multiplex Oligos for Illumina (Dual Index Primers Set 1, NEB #E7600). A series of sequencing runs were performed on Illumina and Pacific Biosciences platforms. The VNO libraries for strains ZRU, XBS and CAR were sequenced as 300 bp paired-end reads on Illumina MiSeq platform through the Biotechnology Resource Center (Institute of Biotechnology) at Cornell University. Additional VNO RNA libraries for strains ZRU, XBS, CAR and PAH were sequenced as 150 bp paired-end reads on Illumina NextSeq 500 platform through the Biotechnology Resource Center (Institute of Biotechnology) at Cornell University. A series of 15 SFM female VNO samples were sequenced as 125 bp paired-end reads on Illumina HiSeq 2500 platform at Novogene (Sacramento, CA). Pacific Biosciences (PacBio) Isoseq libraries were also generated and sequenced from pooled SFM male and female VNOs. This additional long-read dataset ensured the *M. spretus* (SFM) species-wide V1R repertoire was captured, and allowed for insight into the effectiveness of short and long-read datasets for V1R detection.

Transcript processing and assembly

FastQC reports were generated for each sample to ensure sequencing quality [70]. Trimmomatic was used to clean the raw reads [71]. The trimmed read files were concatenated for each species across the different Illumina sequencing runs. rnaSPAdes was used to generate *de novo* transcriptome assemblies for each

species' concatenated RNA sequencing dataset [72]. Transrate and rnaQUAST were used for assembly quality assessment [73, 74]. Other assemblers were tested (e.g. Trinity), however rnaSPAdes consistently assembled longer reads and more VRs were recovered from these assemblies.

Isoseq library preparation and consensus assemblies

Pacific Biosciences Isoseq was used to generate long-read sequences for the VNO from *Mus spretus* at the Arizona Genome Institute. We sequenced 4 different library sizes 0.8-1.6kb (x3 smartcells), 1.3-2.6kb (x2 smartcells), 2.2-3.7kb (x2 smartcells) and >3.0 kb (x2 smartcells) generating a total of 19GB of raw data. These data were run through the PacBio smrtpipe version 2.3 by the Arizona Genome Institute, generating polished high consensus sequences, which we analyzed further for V1R genes.

Identification of V1R sequences

The Ensembl reference annotation (version 94) of the mouse reference genome (GRCm38.p6) was used to download all known sequences for V1Rs. These reference sequences were used in a series homology-based searches (blastn, blastx and tblastn) to identify putative V1Rs in the RNA transcript assemblies for each mouse species. GetORF [75] was then used to identify open reading frames (ORFs) among the putative V1R dataset, using a well-defined V1R gene model [38]. Dedupe was used to remove exact duplicate DNA sequences and containment DNA sequences within this refined ORF dataset. DNA sequences were translated into corresponding peptide sequences using GetORF [75]. MAFFT v. 7 was used to align the peptide V1R sequences for each species, and sequences with less than 30%

identity with the entire V1R group for a given species were eliminated from further analysis [76]. While this pipeline was designed to identify functional V1R genes, given the abundance of V1R pseudogenes and the incomplete genome annotations for many of these species, some pseudogenes may inadvertently be included in these analyses.

V1R annotation and identification of orthologous receptors

Putative V1Rs were first annotated based on homology to the mouse reference genome. If multiple transcripts were *most similar* to a specific reference V1R gene (e.g., *Vmn1r30*), these transcripts were annotated with this same gene ID, and distinguished with unique numbers following the gene ID (e.g., *Vmn1r30.1* and *Vmn1r30.2*). Some annotations based on homology and their orientation within the gene tree did not always perfectly match due to the effects of gene duplications and losses at varying points in the *Mus* phylogeny. As such, some V1R annotations were adjusted upon analysis of the phylogenetic relationships of receptor sequences within the maximum-likelihood gene tree. The most important criteria for determining orthologous receptor groups was the relative orientation of all 6 species, under the general rule that the receptor phylogeny should recapitulate the species phylogeny. Using the annotation system of the reference genome meant that some gene duplications with distinct reference annotations were included in the same receptor ortholog group. Thus, some orthologous receptor groups were annotated with combination-IDs (e.g. *Vmn1r25/30*). Furthermore, a proportion of receptors from each of the five sequenced non-reference species were non-orthologous in that they did not fall into any particular ortholog group, but were basal to multiple groups or to several reference genes. These non-orthologous receptors were annotated based on

the genes they were basal to, either as a combination-ID (e.g. *Vmn1r90/168/177*) or in the format “basalgeneID” if the number of gene IDs exceeded three (the lowest gene ID number was used). Thus V1R orthologs were identified using both sequence homology and phylogenetic relationships among receptors for all 6 species. Additionally, V1Rs that have evidence for gene losses in the house mouse (and corresponding pseudogenes) could not be annotated with the pseudogene ID, as often there are functional V1Rs with the same ID number. As a result, all gene losses in the house mouse detected in multiple sequenced mouse species are provided a new gene ID that does not overlap with any existing gene numbers. The annotated V1R coding sequences for all 5 sequenced *Mus* species sequenced are provided in **Additional Files 4-8**.

Phylogenetic analysis

All V1R peptide sequences for all 6 *Mus* species were aligned in MAFFT v. 7 (**Additional File 9**) [76]. Phylogenetic relationships were inferred using RAxML v. 8 to generate a maximum likelihood gene trees (based on peptide sequences) with 1000 replicates of bootstrapping (**Additional File 1**) [77]. Trees were visualized in FigTree v1.4.3 [78]. A few traditionally separated clades were combined due to a lack of clear clade separation when viewed across all 6 *Mus* species (clades: A/B and J/K) [79].

Estimating gene duplicates

The well-characterized V1R repertoire of the reference genome was used to make estimates about which sequenced V1R transcripts are putative transcript variants or gene duplications within a given ortholog group (**Additional File 2**). Out of all the V1R transcripts in the reference, 55% code for the same peptide sequence, while 9.4%

encode different peptides. Among the transcript variants encoding different peptides, sequence variation consists of either shorter sequences (i.e. only one exon is present) or variation at the ends of the transcript surrounding regions with gaps in pairwise alignments. We classified any V1R transcripts that (1) code for the same peptide, (2) whose variation consists of shortened coding sequences (i.e. only one exon is present), (3) whose variation falls at the ends of the transcript, or (4) whose variation falls near gaps in pairwise alignments, as putative transcript variants. Transcripts classified as putative gene duplicates were only those transcripts with at least one amino acid change central to the transcript, and not surrounded by gaps in pairwise alignments. This was only observed among different genes in the reference, never among transcript variants. Pairwise alignments were performed using EMBOSS Needle [80]. Due to the dynamic nature of V1R evolution and the incomplete V1R repertoires recovered for each species, duplications aren't examined based on whether they are shared among species or are species-specific. Rather, duplications within ortholog groups are treated independently for each species.

Positive selection analysis

We performed selection analyses on orthogroups containing at least 4 orthologs and/or paralogs. To test for whether genes were under positive selection we used the adaptive branch-site relative effects-likelihood (aBSREL) model based on dN/dS estimates as implemented in the software HyPhy [56, 81]. aBSREL was run on each orthogroup of sufficient size to identify branches with evidence of positive selection. P values from each aBSREL run were corrected for multiple testing using a false-discovery rate of 5%. After correction P values ≤0.05 were considered evidence for positive selection.

Transmembrane helix prediction and mutation analysis

We focused on a two clade J/K receptors (*Vmn1r85* and *Vmn1r89*) for a more detailed examination of the amino acid changes across species, as clade J/K is a small highly orthologous clade, in which 2/4 receptor groups have the most well-supported evidence for de-orphanization [40, 49]. MAFFT v. 7 was used to align the orthologous receptor sequences [76]. TMHMM v. 2.0 was used to predict the locations of transmembrane helices [82], and which V1R protein regions are intracellular versus extracellular. For both *Vmn1r85* and *Vmn1r89* receptor groups, transcripts were aligned, transmembrane regions predicted, and sites with amino acid differences were identified across species (**Figures S4 & S5**). These amino acid differences are shown in protein schematics for each receptor (**Figure S6**). Four types of amino acid sites were characterized: (1) sites with an amino acid difference present in a single species, (2) sites with distinct amino acid differences in two different species, (3) sites with an amino acid difference shared between two to three species, (4) highly variable sites, in which amino acid differences suggest dynamism across the phylogenetic history of the genus (**Figure S6**). To examine *Vmn1r89* amino acid differences across species, the short transcriptional variants were excluded (**Figure S4**).

List of Abbreviations

OR: main olfactory receptor; VR: vomeronasal receptor; V1R: vomeronasal type 1 receptor; V2R: vomeronasal type 2 receptor; VNO: vomeronasal organ; Orthogroup: orthologous receptor group.

Declarations

Ethics approval and consent to participate. All experimental protocols conducted at Cornell University were approved by the Institutional Animal Care and Use Committee (IACUC: Protocol #2015-0060), and were in compliance with the NIH Guide for Care and Use of Animals. All experimental protocols performed at Oklahoma State University were approved by the IACUC under protocol #AS-1-41.

Availability of Data and Materials . All transcriptome sequencing data generated in this study are available in the NCBI Short Read Archive under BioProject PRJNA596328. The sequences and datasets used in this study are included in the manuscript and its additional files.

Funding. Funding for this research was provided by Cornell University and NIH DP2 – GM128202 to M.J.S. and by NSF IOS 1558109 to P.C.

Authors' Contributions. C.H.M. generated samples and sequence data, analyzed the data, and wrote the initial manuscript. M.J.S. and C.H.M. conceived and designed the experiment. P.C. contributed samples and sequencing data. All authors contributed to the editing of the manuscript.

Acknowledgements. The *M. macedonicus* (XBS), *M. spicilegus* (ZRU), and *M. spretus* (SFM) strains were originally developed by the Wild Mouse Genetic Repository (University of Montpellier). We thank Sara Miller for assistance with bioinformatic analyses.

Additional Files

Additional File 1: Maximum likelihood gene tree of 6 *Mus* species V1R peptide sequences.

Additional File 2: Categorization of V1R transcripts as either putative transcript variants or gene duplicates for the 5 non-commensal *Mus* species sequenced. (xlsx)

Additional File 3: Table S1. V1R orthogroup branches under positive selection across clades indicated by species. **Table S2.** V1Rs with evidence for positive selection, conservation (orthology and sequence identity) or gene expansions (across or within species). **Figure S1.** Number of V1R genes with splice variants in *M. m. domesticus* and *M. spretus*. **Figure S2**. Novel clade "N": *Vmn1r248* and *Vmn1r249.* **Figure S3. Left:** V1R gene tree clades E and F, displaying long internal branch lengths and short terminal branch lengths. ***Right***: Multiple alignments of *Vmn1r69* and *Vmn1r71* peptide sequences. **Figure S4.** Alignment and pairwise comparisons of *Vmn1r89* peptide sequences. **Figure S5.** Alignment and pairwise comparisons of *Vmn1r85* peptide sequences. **Figure S6.** Amino acid site changes in clade J/K receptors: *Vmn1r89* and *Vmn1r85*. (docx)

Additional File 4: *M. spicilegus* coding sequences of *V1r* genes expressed in the VNO. Gene annotations are abbreviated and contain species identifier "z": *Vmn1r137* as 137-z. (fasta)

Additional File 5: *M. macedonicus* coding sequences of *V1r* genes expressed in the VNO. Gene annotations are abbreviated and contain species identifier "x": *Vmn1r137* as 137-x. (fasta)

Additional File 6: *M. spretus* coding sequences of *V1r* genes expressed in the VNO. Gene annotations are abbreviated and contain species identifier "s": *Vmn1r137* as 137-s. (fasta)

Additional File 7: *M. caroli* coding sequences of *V1r* genes expressed in the VNO. Gene annotations are abbreviated and contain species identifier “c”: *Vmn1r137* as 137-c. (fasta)

Additional File 8: *M. pahari* coding sequences of *V1r* genes expressed in the VNO. Gene annotations are abbreviated and contain species identifier “p”: *Vmn1r137* as 137-p. (fasta)

Additional File 9: Multiple sequence alignment of all 6 *Mus* species’ V1R peptide sequences. (fasta)

REFERENCES

1. Meisami E, Bhatnagar KP. Structure and diversity in mammalian accessory olfactory bulb. Microsc. Res. Tech. 1998;43:476–499.
2. Restrepo D, Arellano J, Oliva AM, Schaefer ML, Lin W. Emerging views on the distinct but related roles of the main and accessory olfactory systems in responsiveness to chemosensory signals in mice. Horm. Behav. 2004;46: 247–256.
3. Dulac C, Torello AT. Molecular detection of pheromone signals in mammals: from genes to behavior. Nat. Rev. Neurosci. 2003;4:551–562.
4. Mombaerts P. Genes and ligands for odorant, vomeronasal and taste receptors. Nat. Rev. Neurosci. 2004;5:263–278.
5. Nara K, Saraiva LR, Ye X, Buck LB. A large-scale analysis of odor coding in the olfactory epithelium. J. Neurosci. 2011;31:9179–9191.
6. Liberles SD. Mammalian pheromones. Annu. Rev. Physiol. 2014;76:151–175.
7. Dulac C, Axel R. A novel family of genes encoding putative pheromone receptors in mammals. Cell. 1995;83:195–206.
8. Boschat C, Pélofi C, Randin O, Roppolo D, Lüscher C, Broillet M, Rodriguez I. Pheromone detection mediated by a V1r vomeronasal receptor. Nat. Neurosci. 2002;5:1261–1262.
9. Powers JB, Winans SS. Vomeronasal organ: critical role in mediating sexual behavior of the male hamster. Science. 1975;187:961–964.
10. He J, Ma L, Kim S, Nakai J, Yu CR. Encoding gender and individual Information in the mouse vomeronasal organ. Science. 2008;320:535–538.

11. Stowers L, Holy TE, Meister M, Dulac C, Koentges G. Loss of sex discrimination and male-male aggression in mice deficient for TRP2. Science. 2002;295:1493–1500.
12. Leypold BG, Yu CR, Leinders-Zufall T, Kim MM, Zufall F, Axel R. Altered sexual and social behaviors in trp2 mutant mice. Proc. Natl. Acad. Sci. 2002;99:6376–6381.
13. Kimoto H, Haga S, Sato K, Touhara K. Sex-specific peptides from exocrine glands stimulate mouse vomeronasal sensory neurons. Nature. 2005;437:898–901.
14. Chamero P, Marton TF, Logan DW, Flanagan K, Cruz JR, Saghatelian A, Cravatt BF, Stowers L. Identification of protein pheromones that promote aggressive behaviour. Nature. 2007;450:899–902.
15. Ferrero DM, Moeller LM, Osakada T, Horio N, Li Q, Roy DS, Cichy A, Spehr M, Touhara K, Liberles SD. A juvenile mouse pheromone inhibits sexual behaviour through the vomeronasal system. Nature. 2013;502:368–371.
16. Tachikawa KS, Yoshihara Y, Kuroda KO. Behavioral transition from attack to parenting in male mice: A crucial role of the vomeronasal system. J. Neurosci. 2013;158:5120–5126.
17. Kaur AW, Ackels T, Kuo T-H, Cichy A, Dey S, Hays C, Kateri M, Logan DW, Marton TF, Spehr M, Stowers L. Murine pheromone proteins constitute a context-dependent combinatorial code governing multiple social behaviors. Cell. 2014;157:676–688.
18. Orikasa C, Kondo Y, Katsumata H, Terada M, Akimoto T, Sakuma Y, Minami S. Vomeronasal signal deficiency enhances parental behavior in socially isolated male mice. Physiol. Behav. 2017;168:98–102.

19. Grus WE, Zhang J. Distinct evolutionary patterns between chemoreceptors of 2 vertebrate olfactory systems and the differential tuning hypothesis. Mol. Biol. Evol. 2008;25:1593–1601.
20. Lane RP, Young J, Newman T, Trask BJ. Species specificity in rodent pheromone receptor repertoires. Genome Res. 2004;14:603–608.
21. Grus WE, Zhang J. Rapid turnover and species-specificity of vomeronasal pheromone receptor genes in mice and rats. Gene. 2004;340:303–312.
22. Jiao H, Hong W, Nevo E, Li K, Zhao H. Convergent reduction of V1R genes in subterranean rodents. BMC Evol. Biol. 2019;19:1–9.
23. Silva L, Antunes A. Vomeronasal receptors in vertebrates and the evolution of pheromone detection. Annu. Rev. Anim. Biosci. 2017; 5:353–370.
24. Yang H, Shi P, Zhang YP, Zhang J. Composition and evolution of the V2r vomeronasal receptor gene repertoire in mice and rats. Genomics. 2005;86:306–315.
25. Shi P, Bielawski JP, Yang H, Zhang YP. Adaptive diversification of vomeronasal receptor 1 genes in rodents. J. Mol. Evol. 2005;60:566–576.
26. Young JM, Massa HF, Hsu L, Trask BJ. Extreme variability among mammalian V1R gene families. Genome Res. 2010;20:10–18.
27. Grus WE, Shi P, Zhang Y, Zhang J. Dramatic variation of the vomeronasal pheromone receptor gene repertoire among five orders of placental and marsupial mammals. Proc. Natl. Acad. Sci. 2005;102:5767–5772.
28. Hunnicutt KE, Tiley GP, Williams RC, Larsen PA, Blanco MB, Rasoloarison RM, Campbell CR, Zhu K, Weisrock DW, Matsunami H, Yoder AD. Comparative genomic analysis of the pheromone receptor class 1 family (V1R) reveals extreme

complexity in mouse lemurs (genus, microcebus) and a chromosomal hotspot across mammals. Genome Biology and Evolution. 2020;12:3562-3579.

29. Yohe LR, Davies KTJ, Rossiter SJ, Dávalos LM. Expressed vomeronasal type-1 receptors (V1rs) in bats uncover conserved sequences underlying social chemical signaling. Genome Biology and Evolution. 2020; 11:2741-2749.
30. Emes RD, Beatson SA, Ponting CP, Goodstadt L. Evolution and comparative genomics of odorant-and pheromone- associated genes in rodents. Genome Res. 2004;14:591–602.
31. Kurzweil VC, Getman M, Green ED, Lane RP. Dynamic evolution of V1R putative pheromone receptors between Mus musculus and Mus spretus. BMC Genomics. 2009;10: 1–11.
32. Park SH, Podlaha O, Grus WE, Zhang J. The microevolution of V1r vomeronasal receptor genes in mice. Genome Biol. Evol. 2011;3:401–412.
33. Fu X, Yan Y, Xu PS. Geerlof-Vidavsky I, Chong W, Gross ML, Holy TE. A molecular code for identity in the vomeronasal system. Cell. 2015;163:313-323.
34. Wagner S, Gresser AL, Torello AT, Dulac C. A multireceptor genetic approach uncovers an ordered integration of VNO sensory inputs in the accessory olfactory bulb. Neuron. 2006;50:697–709.
35. Dulac C, Wagner S. Genetic analysis of brain circuits underlying pheromone signaling. Annu. Rev. Genet. 2006;40:449–467.
36. Brignall AC, Cloutier JF. Neural map formation and sensory coding in the vomeronasal system. Cell. Mol. Life Sci. 2015;72:4697–4709.
37. Wynn EH, Sánchez-Andrade G, Carss KJ, Logan DW. Genomic variation in the vomeronasal receptor gene repertoires of inbred mice. BMC Genomics. 2012;13:19–23.

38. Ibarra-Soria X, Levitin MO, Saraiva LR, Logan DW. The olfactory transcriptomes of mice. PLoS Genet. 2014;10:9.

39. Duyck K, DuTell V, Paulson A, Ma L, Yu CR. Pronounced strain-specific chemosensory receptor gene expression in the mouse vomeronasal organ. BMC Genomics. 2017;18:965.

40. Haga-Yamanaka S, Ma L, He J, Qiu Q, Lavis LD, Looger LL, Yu CR. Integrated action of pheromone signals in promoting courtship behavior in male mice. Elife. 2014; 3:e03025.

41. Haga S, Hattori T, Sato T, Sato K, Matsuda S, Kobayakawa R, Sakano H, Yoshihara Y, Kikusui T, Touhara K. The male mouse pheromone ESP1 enhances female sexual receptive behaviour through a specific vomeronasal receptor. Nature. 2010;466:118–122.

42. Isogai Y, Wu Z, Love MI, Ahn MH-Y, Bambah-Mukku D, Hua V, Farrell K, Dulac C. Multisensory logic of infant-directed aggression by males. Cell. 2018;175:1827-1841.

43. Rodriguez I. Vomeronasal Receptors: V1Rs, V2Rs, and FPRs. In: Zufall F, Munger SD, eds. Chemosensory Transduction: The Detection of Odors, Tastes, and Other Chemostimuli. Academic Press; 2016. p. 175-185.

44. Leinders-Zufall T, Brennan P, Widmayer P. MHC class I peptides as chemosensory signals in the vomeronasal organ. Science. 2004;306:1033–1038.

45. Leinders-Zufall T. Ultrasensitive pheromone detection by mammalian vomeronasal neurons. Lett. to Nat. 2000;405:251–260.

46. Meeks JP, Arnson HA, Holy TE. Representation and transformation of sensory information in the mouse accessory olfactory system. Nat. Neurosci. 2010;13:723–730.

47. Del Punta K, Leinders-Zufall T, Rodriguez I, Jukam D, Wysocki CJ, Ogawa S, Zufall F, Mombaerts P. Deficient pheromone responses in mice lacking a cluster of vomeronasal receptor genes. Nature. 2002;419:70–74.
48. Nodari F, Hsu F-F, Fy X, Holekamp TF, Kao L-F, Turk J, Holy TE. Sulfated steroids as natural ligands of mouse pheromone-sensing neurons. J. Neurosci. 2008;28:6407–6418.
49. Isogai Y, Si S, Pont-Lezica L, Tan T, Kapoor V, Murthy VN, Dulac C. Molecular organization of vomeronasal chemoreception. Nature. 2011;478:241–245.
50. Novotny M, Jemiolo B, Harvey S, Wiesler D, Marchlewska-Koj A. Adrenal-mediated endogenous metabolites inhibit puberty in female mice. Science. 1986;231:722–725.
51. Novotny MV, Ma W, Wiesler D, Zídek L. Positive identification of the puberty-accelerating pheromone of the house mouse: the volatile ligands associating with the major urinary protein. Proc. R. Soc. Lond. B. 1999;266:2017–2022.
52. Niimura Y, Matsui A, Touhara K. Extreme expansion of the olfactory gene repertoire in African elephants and evolutionary dynamics of orthologous gene groups in 13 placental mammals. Genome Research. 214;24:1485-1496.
53. Saraiva LR, Riveros-McKay F, Mezzavilla M, Abou-Moussa EH, Arayata CJ, Makhlouf M, Trimmer C, Ibarra-Soria X, Khan M, Van Gerven L, Jorissen M, Gibbs M, O'Flynn C, McGrane S, Mombaerts P, Marioni JC, Mainland JD, Logan DW. A transcriptomic atlas of mammalian olfactory muscosae reveals an evolutionary influence on food odor detection in humans. Science Advances. 2019;5:eaax0396.

54. Vallender EJ, Xie Z, Westmoreland SV, Miller GM. Functional evolution of the trace amine associated receptors in mammals and the loss of TAAR1 in dogs. BMC Evolutionary Biology. 2010; 10:1-9.

55. Ferrero DM, Lemon JK, Fluegge D, Pashkovski SL, Korzan WJ, Datta SR, Spehr M, Fendt M, Liberles SD. Detection and avoidance of a carnivore odor by prey. PNAS. 2011;108(27):11235-11240.

56. Smith MD, Wertheim JO, Weaver S, Murrell B, Scheffler K, Kosakovsky Pond SL. Less Is More: An Adaptive Branch-Site Random Effects Model for Efficient Detection of Episodic Diversifying Selection. Molecular Biology and Evolution. 2015;32:1342-1353.

57. Tong W, Hoekstra H. Mus spicilegus. Curr. Biol. 2012;22:858–859.

58. Pocock MJO, Searle JB, White PCL. Adaptations of animals to commensal habitats: population dynamics of house mice Mus musculus domesticus on farms. J. Anim. Ecol. 2004;73:878–888.

59. Suzuki H, Nunome M, Kinoshita G, Aplin KP, Vogel O, Kryukov AP, Jin M-L, Han S-H, Maryanto I, Tsuchiya K, Ikeda H, Shiroishi T, Yonekawa H, Moriwaki K. Evolutionary and dispersal history of Eurasian house mice Mus musculus clarified by more extensive geographic sampling of mitochondrial DNA. Heredity (Edinb). 2013;111(5):375–390.

60. Papes F, Logan DW, Stowers L. The vomeronasal organ mediates interspecies defensive behaviors through detection of protein pheromone homologs. Cell. 2010;141:692–703.

61. Ben-Shaul Y, Katz LC, Mooney R, Dulac C. In vivo vomeronasal stimulation reveals sensory encoding of conspecific and allospecific cues by the mouse accessory olfactory bulb. Proc. Natl. Acad. Sci. 2010;107:5172–5177.

62. Hurst JL, Beynon RJ. Scent wars: the chemobiology of competitive signaling in mice. BioEssays. 2004;26:1288-1298.

63. Roberts SA, Prescott MC, Davidson AJ, McLean L, Berynon RJ, Hurst JL. Individual odour signatures that mice learn are shaped by involatile major urinary proteins (MUPs). BMC Biol. 2018;16:1–19.

64. Sheehan MJ, Lee V, Corbett-Detig R, Bi K, Berynon RJ, Hurst JL, Nachmann MW. Selection on coding and regulatory variation maintains individuality in major urinary protein scent marks in wild mice. PLoS Genet. 2016;12:1–33.

65. Hurst JL, Payne CE, Nevison CM, Marie AM, Humphries RE, Roberston DHL, Cavaggioni A, Beynon RJ. Individual recognition in mice mediated by major urinary proteins. Nature. 2001;414:631–634.

66. Roberts SA, Davidson AJ, McLean L, Beynon RJ, Hurst JL. Pheromonal induction of spatial learning in mice. Science. 2012;338:1462–1465.

67. Bacchini A, Gaetani E, Cavaggioni A. Pheromone binding proteins of the mouse, Mus musculus. Experientia. 1992;48:419–421.

68. Sheehan MJ, Campbell P, Miller CH. Evolutionary patterns of major urinary protein scent signals in house mice and relatives. Mol. Ecol. 2019;00:1–15.

69. Celsi F, D'Errico A, Menini A. Responses to sulfated steroids of female mouse vomeronasal sensory neurons. Chem. Senses. 2012;37:849–858.

70. Andrews, S. FastQC: A quality control tool for high throughput sequence data. http://www.bioinformatics.babraham.ac.uk/projects/fastqc/ (2010).

71. Bolger AM, Lohse M, Usadel B. Trimmomatic: A flexible trimmer for Illumina sequence data. Bioinformatics. 2014;30:2114–2120.

72. Bushmanova E, Antipov D, Lapidus A, Przhibelskiy AD. rnaSPAdes: a de novo transcriptome assembler and its application to RNA-Seq data. Gigascience. 2019;8(9).
73. Smith-Unna R, Boursnell C, Patro R, Hibberd JM, Kelly S. TransRate : reference-free quality assessment of de novo transcriptome assemblies. Genome Res. 2016;26:1134–1144.
74. Bushmanova E, Antipov D, Lapidus A, Suvorov V, Prjibelski AD. RnaQUAST: A quality assessment tool for de novo transcriptome assemblies. Bioinformatics. 2016;32:2210–2212.
75. Williams G. EMBOSS GetORF. http://www.bioinformatics.nl/cgi-bin/emboss/getorf/ (2002).
76. Katoh K, Standley DM. MAFFT multiple sequence alignment software version 7: Improvements in performance and usability. Mol. Biol. Evol. 2013;30:772–780. Available: https://mafft.cbrc.jp/alignment/software/.
77. Stamatakis A. RAxML version 8: A tool for phylogenetic analysis and post-analysis of large phylogenies. Bioinformatics. 2014;30:1312–1313.
78. Rambaut, A. FigTree v1.4.3. http://tree.bio.ed.ac.uk/software/ (2016).
79. Rodriguez I, Del Punta K, Rothman A, Ishii T, Mombaerts P. Multiple new and isolated families within the mouse superfamily of V1r vomeronasal receptors. Nat. Neurosci. 2002;5:134–140.
80. Needleman SB, Wunsch CD. A general method applicable to the search for similarities in the amino acid sequence of two proteins. J. Mol. Biol. 1970;48(3):443-53. EMBOSS Needle Available: https://www.ebi.ac.uk/Tools/psa/emboss_needle/.

81. Kosakovsky Pond SL, Frost SDW, Muse SV. HyPhy: hypothesis testing using phylogenies. Bioinformatics. 2005;21(5):676-679.

82. Krogh A, Larsson B, Von Heijne G, Sonnhammer ELL. Predicting transmembrane protein topology with a hidden Markov model: Application to complete genomes. J. Mol. Biol. 2001;305:567–580. Available: http://www.cbs.dtu.dk/services/TMHMM/.

83. Steppan SJ, Schenk JJ. Muroid rodent phylogenetics: 900-species tree reveals increasing diversification rates. PLoS ONE. 2017;12(8): e0183070.

84. Chevret P, Veyrunes F, Britto-Davidian J. Molecular phylogeny of the genus Mus (Rodentia Murinae) based on mitochondrial and nuclear data. Biological Journal of the Linnean Society. 2005;84:417-427.

CHAPTER 2

Dynamic changes to signal allocation rules in response to variable social environments in house mice

Caitlin H Miller*, Matthew F Hillock, Jay Yang, Brandon Carlson-Clarke, Klaudio Haxhillari, Annie Y Lee, Melissa R Warden, Michael J Sheehan*

Department of Neurobiology and Behavior, Cornell University, Ithaca, NY, USA

*Authors for Correspondence: Caitlin H Miller: chm79@cornell.edu

Michael J Sheehan: msheehan@cornell.ed

Abstract

Urine marking is central to mouse social behavior. Males use depletable and costly urine marks in intrasexual competition and mate attraction. We investigate how males alter signaling decisions across variable social landscapes using thermal imaging to capture spatiotemporal marking data. Thermal recording reveals fine-scale adjustments in urinary motor patterns toward competition and social odors. Males demonstrate striking winner-loser effects in scent mark allocation effort and timing. Competitive experience primes temporal features of marking and modulates responses to scent familiarity. Males adjust signaling effort, mark latency, and marking rhythm, depending on the scent identities in the environment. Winners increase marking effort toward unfamiliar relative to familiar male scents, consistent with a ‘dear enemy’ effect. Losers reduce marking effort to unfamiliar, but increase to familiar rival scents, consistent with a ‘nasty neighbor’ effect. In contrast to this dynamism, initial signal investment has stable and long-lasting effects on scent marking, revealing the possibility of alternative marking strategies among competitive males. These data show that mice flexibly update their signaling decisions in response to changing social landscapes.

Keywords: scent mark, signal allocation, competition, winner-loser effects, dear enemy, nasty neighbor, familiarity, territory, decision-making, thermal recording

Introduction

Animals adjust their signaling behavior in response to recent experience and social context. Signalers may change not only the frequency of signaling behavior, but also when, where, and how they signal in response to changing social and physical environments [1–4]. In house mice (*Mus musculus domesticus*), males use metabolically costly urine marks to mediate intrasexual competition and mate attraction. The abundance, spatial distribution, and chemical composition of urine marks contain information about a male's competitive status and identity [5–14]. While urine marks convey rich social information, they are also directly depletable. Just as a car runs out of fuel, animals have a limited supply of urine to allocate at any given moment. As a result, the timing of urine deposition is likely a crucial feature of scent mark signaling. Here, we explore the flexibility of signal allocation decisions, both on a moment-to-moment timescale as well as over the course of days.

Male social relationships are shaped by competition and familiarity with conspecifics in house mice [5,15–21]. Urine marking mediates some of these relationships by allowing assessment and recognition of individuals [6,10,11,14,22]. Both stimulus familiarity and aggressive contests independently have strong effects on male urine marking [5,6,23–25], however it remains poorly understood how the two interact. In many territorial species, familiar neighbors reduce aggressive behaviors and signaling effort toward each other known as the "dear enemy" effect [26–30] to lessen the costs of territorial defense [26–28,30,31]. Given the high costs and depletable nature of urine marks, males should dynamically modulate signal allocation as the landscape is updated with new social information. The present study aims to shed light on these decision rules by exploring how established competitive relationships and familiarity influence male signal allocation decisions across social

and scent-marked environments. The ability to keep track of experiences with specific individuals and respond to unfamiliar competitors is likely highly adaptive.

We investigate how males shift their signal allocation after an aggressive contest in response to the presence of a familiar male competitor, as well as to the presence of urine scent-marks of differing male identities. The objectives of this study were to: (1) implement thermal recording as a method for the measuring scent marking in social contexts, (2) examine how competitive experience alters marking behavior, and (3) test the hypothesis that familiarity is important for signal allocation decisions. To do this, we developed a 4-day trial design in which 31 pairs of age and weight-matched breeding male house mice of distinct wild-derived strains were paired as competitors and presented a series of social and scent-marked trials (**Figure 1A**). On the first day, paired males were placed in an arena separated by a mesh barrier (**Figure 1A**). Paired males could see, hear, and smell each other but were limited to minimal physical contact through the mesh. The mesh barrier was subsequently removed, and males engaged in an aggressive contest or “fight trial” (**Figure 1A**). Based on the total aggressive behaviors performed by each male, males were unambiguously classified as winners or losers (**Figure S1 & Table S1**). On the second day, each male was placed in an empty arena (**Figure 1A**). On the third day, males were placed back into the mesh arena with the same male competitor they encountered on the first day (**Figure 1A**). Finally, on the fourth day, each male was exposed to one of four urine-marked treatments. Each treatment contained aliquoted male urine of three possible identities (self, familiar male, or unfamiliar male) in two spatially distinct scent-marked zones (**Figure 1A**). The four treatment types span a range of scent mark combinations (self-self, self-familiar, self-unfamiliar, familiar-unfamiliar), in which the familiar stimulus is the urine of a male’s paired competitor

and the unfamiliar stimulus is novel male urine (**Figure 1A**). Urine marking and space use data were collected for each male across urine marking assays while aggression was scored in the fight trials (**Figure 1B-C; Figure S1**).

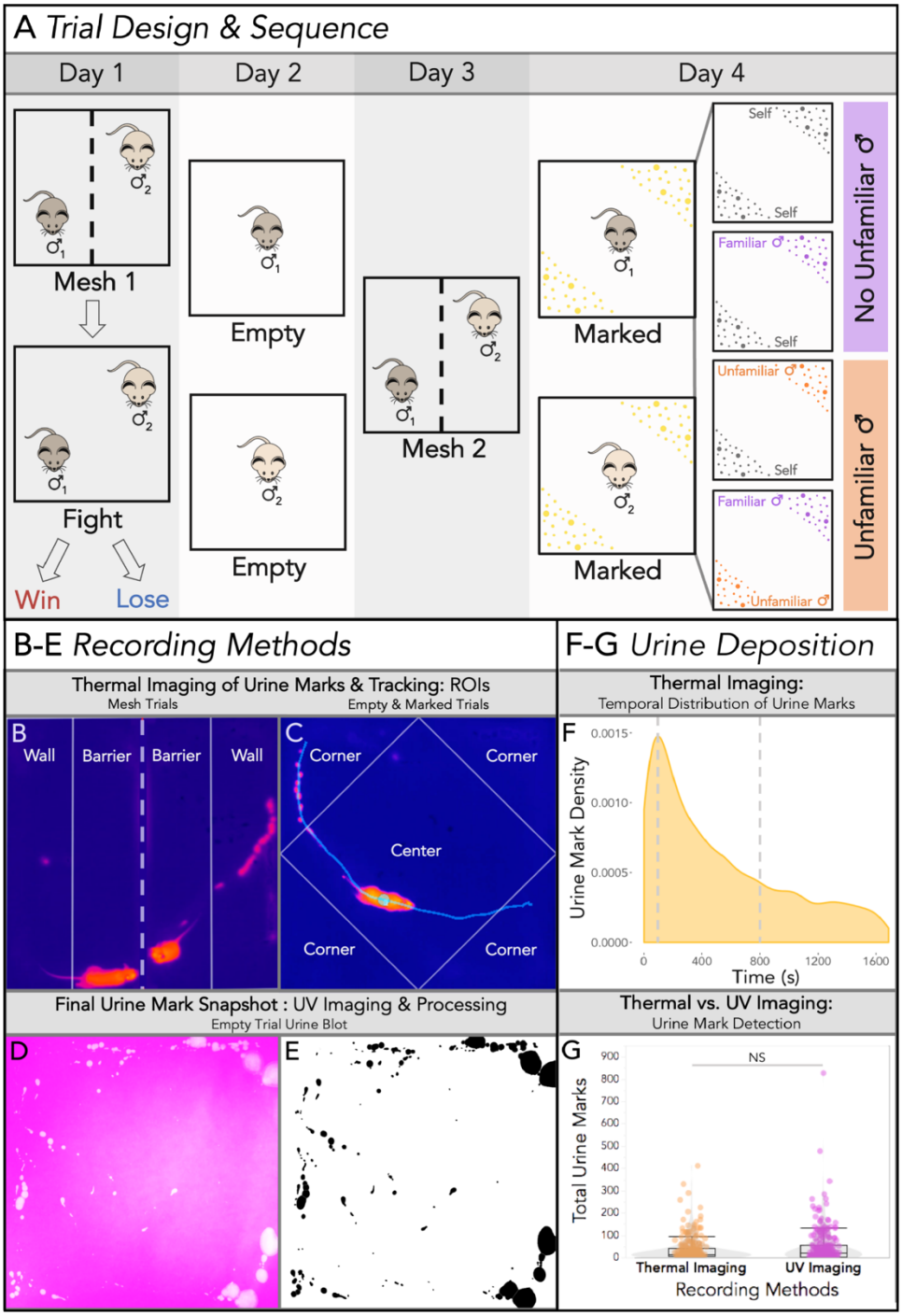

(Figure legend on the next page).

Figure 1. Experimental design and recording methods. (A) Trial design. Day 1: males were paired as competitors and placed into an arena separated by a mesh barrier indicated by a dashed line (Mesh 1). The mesh barrier was removed and males entered into an aggressive contest (Fight) concluding in winning or losing males. Day 2: each male was placed into an empty arena (Empty). Day 3: males were placed back into the mesh arena with the same (familiar) male competitor from the first trial (Mesh 2). Day 4: each male was exposed to one of 4 possible treatments of aliquoted male urine of 3 possible identities (self, familiar and unfamiliar) into two urine-marked zones. The 4 treatment groups: self-self, self-familiar male, self-unfamiliar male, familiar male-unfamiliar male. The familiar male stimulus is the urine of a male's paired competitor. **(B)** A thermal snapshot of a Mesh trial and the regions of interest (ROIs: Wall vs. Barrier) used to score urine mark depositions and track space use. The dashed line indicates the mesh barrier separating the two males. The solid lines depict ROIs males can traverse through on their side of the barrier. Urine marks are hot (orange-pink: close to the body temperature) on a cool (dark blue) ambient substrate (filter paper) temperature. **(C)** A thermal snapshot of an Empty trial (Day 2) with the ROIs used for scoring (Corners vs. Center) indicated with solid lines. The same ROIs were to score Empty (Day 2) and Marked (Day 4) trials. An example track of the mouse's trajectory two seconds before and after its current location is shown (light turquoise). **(D-E)** An example urine blot of an Empty trial imaged under UV light (D), and the processed inverted urine blot image (E: black spots: urine marks). **(F)** Density plot depicting the temporal distribution of all thermally detected urine marks across all trials. **(G)** The total number of urine marks detected across trials using thermal imaging and UV blot imaging recording methods. A linear mixed model was used to model the relationship between recording method and the total urine marks detected (M2: **Table S1**). An analysis of variance was used to test for the overall effect of recording method (significance code: NS $p>0.05$).

Results

Thermal imaging reveals spatiotemporal dynamics of scent marking in real time

To fully understand urine allocation decisions in mice, we need to measure real-time spatial and temporal patterns of scent mark deposition events. Mouse urine marking has previously been studied by capturing snapshots of marking patterns [5,11,32,33]. More recently, thermal recording has been used to detect the voiding of urine in non-social contexts [34,35]. Urine leaves the body hot (close to body temperature) and quickly cools to below the ambient substrate temperature, providing a distinctive thermal signature. Here, we used thermal imaging as an unobtrusive method for capturing the spatial and temporal allocation of urine marks by male house mice across social contexts (**Figure 1**). Trials were performed on filter paper to present urine stimuli and to generate images of urine blots under UV light (**Figure 1D-E**). This allowed us to compare thermal recording with a traditional urine detection method.

Using thermal imaging we recorded a total of 9,314 urine deposition events across trials, and explored the temporal distribution of these depositions. We observed an initial spike in urine deposition with a peak of activity at ~100s, followed by an exponential decline (**Figure 1F**). The majority (77%) of marks are deposited

within the first 15 minutes (800s), suggesting males rapidly scent mark upon entering an environment **(Figure 1F**). Thermal imaging focuses on urine deposition, as marks are scored by the distinct thermal profile of urine as it is deposited. UV light imaging cannot distinguish between deposition and distribution events, as urine is further distributed by males tracking urine with their paws and tail. Alternatively, urine deposited in close spatial proximity to existing marks can appear as a single mark under UV light at the end of a trial. The number of marks detected by thermal imaging and UV imaging did not differ (M2: $F_{1,430} = 0.0034$, $p = 0.95$; **Figure 1G & Table S1**). The two detection methods are also highly correlated (**Figure S2**), justifying the use of thermal imaging to examine how temporal urine allocation varies across social contexts. The implementation of thermal recording in social assays opens new investigative avenues within social neuroscience, as well as insights into the neurophysiological basis of voluntary urinary control.

Competitive experience and initial signal investment shape urine mark allocation

Competitive social encounters can have a range of important consequences on the behavior and physiology of individuals. How individuals respond to contest outcomes is often dependent on the assessment of their resource holding potential [36–38]. Signals play a key role in such encounters as they can convey information about the competitive ability of individuals [39–41]. In house mice, the initial marking levels of males have been shown to contain information about their competitive ability [6]. We predicted that (1) higher-marking males would be more likely to win aggressive contests, (2) winners would increase while losers would decrease in signaling effort after a fight, and (3) that the temporal marking dynamics would be shaped by recent

social experience. We compared urine marks in the presence of a competitor before (Mesh 1) and after (Mesh 2) a fight (Figure 1A). Fight outcome has a strong effect on the total number of urine marks (M3: $F_{1,68} = 10$, $p = 0.002$; Table S2), and there is a significant interaction between fight outcome and trial number (M3: $F_{1,60} = 12$, $p = 0.001$; Table S2). Before the fight (Mesh 1), the to-be winners include slightly more high-marking individuals than the to-be losers, however, the two groups did not differ significantly (M3: $t_{1,112} = -0.69$, $p = 0.88$; **Figure 2A & Table S2**). Post-fight, the total urine marks deposited by winners is significantly higher than losers (M3: $t_{1,112} = -4.6$, $p = 0.0001$; **Figure 2A & Table S2**). Similar to previous studies [5,6,23,24], this relationship appears driven in part by a decrease in marking among losing males (M3: $t_{1,61} = 3.3$, $p = 0.006$), though post-fight winners also trend towards being higher-marking (**Figure 2A,B & Table S2**).

We next assessed the role of initial signal investment (# Mesh 1 marks) and fight outcome on subsequent allocation patterns (**Figure 2C**). Given prior research, we expected some males would mark highly, lose the fight, and then suppress their marking [5]. Instead, we found that how much an individual marked pre-fight has a strong effect on the urine mark allocation post-fight (M4: $F_{1,59} = 9.2$, $p = 0.004$; **Figure 2C & Table S2**). In other words, if you start off a low-marking individual you remain relatively low-marking, regardless of the fight outcome. Accordingly, both high-marking losers and low-marking winners are observed (e.g., Pair 3 in **Figure 2B**). The pronounced winner-loser effects on urine allocation are therefore strongly modulated by initial signal investment.

Losing has a notable effect not only the on number of marks, but also where individuals place those marks in the arena (**Figure S3**). In post-fight mesh trial, losers allocate their marks differently in space (at the wall vs. barrier) depending on whether

they started off as high or low-marking (**Figure S3A-B**), suggesting losers may alter signaling strategies in addition to signaling effort. Space use, on the other hand, does not differ (**Figure S3C**). All individuals spend more time in the social region of the arena (barrier) regardless of fight outcome (**Figure S3C**). Surprisingly, where males spend time does not correlate with where they mark (**Figure S3D**), indicating males are not simply marking where they spend time but are specifically allocating their urine marks.

Social experience influences the temporal dynamics of scent mark allocation

In addition to the total number of urine marks, mice may alter the relative timing of urine mark deposition, such that marks are more temporally clustered or more evenly distributed. The relative timing of urine deposition provides novel information on the instantaneous rates of signaling, revealing how mice choose to spend their urine reserves. A slow and regular mark deposition strategy is distinct from marking in rapid bursts.

We inspected the distribution of urine deposition for winners and losers across mesh trials (**Figure 2D**). Pre-fight, winners and losers display an initial peak at ~100 seconds (**Figure 2D**). Post-fight the effects of fight outcome are clear, with winners marking more and losers less (**Figure 2D**). The density curves, however, reveal that both winners and losers allocate more of their marks earlier post-fight (**Figure 2D**). The shift to mark more rapidly regardless of fight outcome suggests a general priming effect of social competition on the temporal allocation of urine marks. This is evidenced by a diminished statistical difference between the winner and loser urine

deposition distributions in the post-fight mesh trial compared to the pre-fight trial (**Figure S4B**).

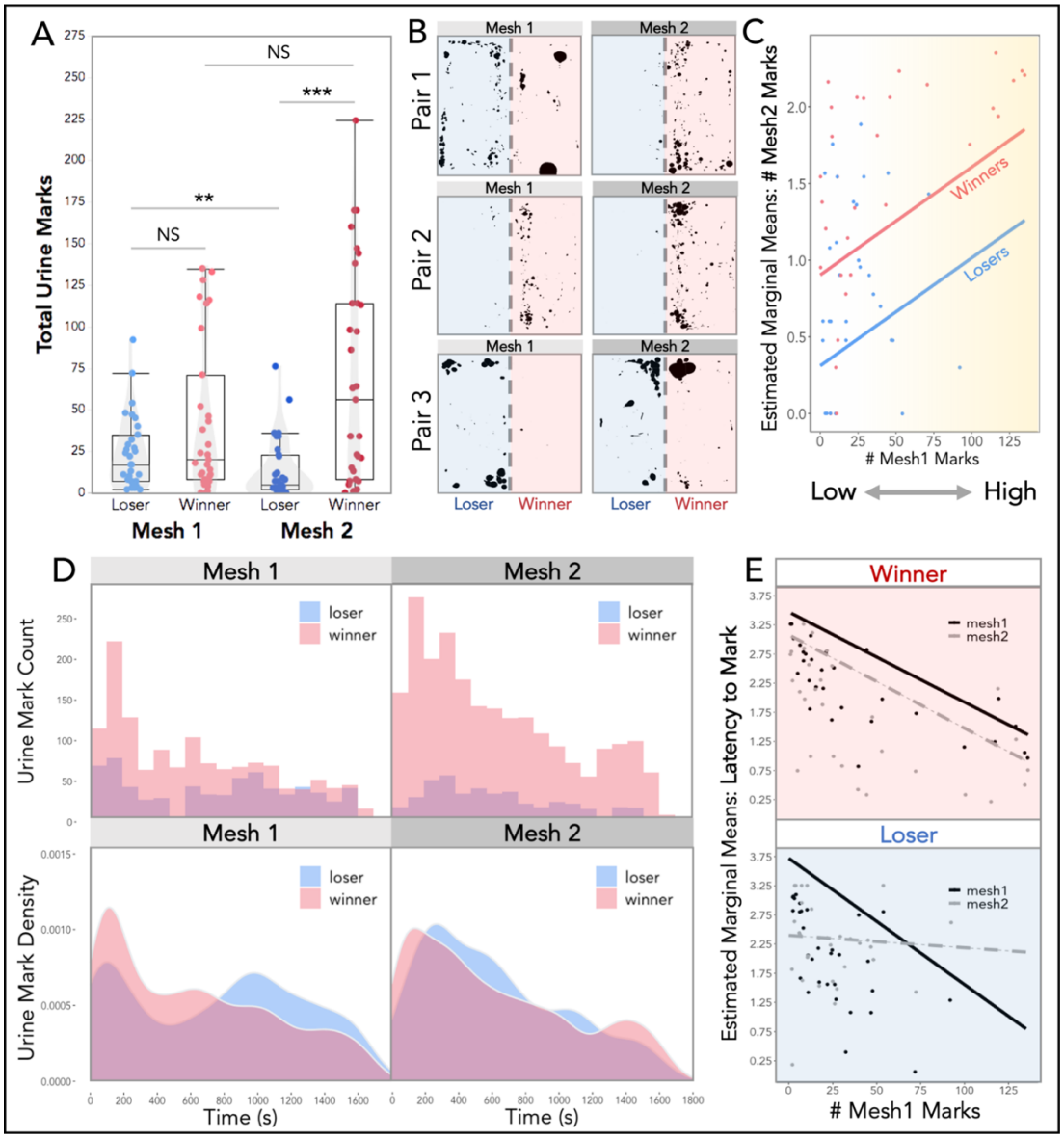

Figure 2. Male urine mark allocation in response to social competition across mesh trials. (A) Total urine marks deposited in Mesh 1 (pre-fight) and Mesh 2 (post-fight) by losers and winners. **(B)** Example mesh trial urine blots of three paired male competitors (winner and loser) pre- and post-fight. **(C)** Estimated marginal means of the total number of Mesh 2 marks (log-transformed) given fight outcome (winner: red, loser: blue) and initial signal investment (# Mesh 1 marks). **(D)** Histograms (top) of the temporal distribution of urine marks deposited by winners and losers in Mesh 1 (pre-fight) and Mesh 2 (post-fight) trials. Density plots (bottom) depict the density of urine mark deposition events over both 30-minute mesh trials, distinguished by fight outcome. **(E)** Estimated marginal means of mark latency (log-transformed) in both mesh trials given the fight outcome and initial signal investment (# Mesh 1 marks). **(A,C,E)** Linear mixed models were used to model relationships (M3-M5: **Table S2**), analyses of variance were used to test for overall effects, and post hoc pairwise comparisons were performed using the *emmeans* package (significance codes: NS p>0.05, ** p<0.01, *** p<0.001). Dependent variables were logarithmically transformed to meet assumptions for model residuals.

The timing of a male's first scent mark is strongly influenced by how highly or lowly that male marked initially (M5: $F_{1,59}$ = 37, p = 9e-08; **Table S2**). Similarly, trial order has a clear effect on the latency to mark (M5: $F_{1,58}$ = 10, p = 0.002; **Table S2**), while fight outcome does not (M5: $F_{1,57}$ = 0.26 p = 0.61; **Table S2**). The three-way interaction between trial order, fight outcome, and initial mark investment significantly effects mark latency (M5: $F_{1,58}$ =12, p = 0.001; **Figure 2E & Table S2**). For both winners and losers, low-marking males are slower to mark than high-marking males, characterizing a low and slow pattern on the first day. Conversely, high-marking individuals typically mark rapidly upon entering the arena on the first day, representing a high and fast pattern. Across the two trials, winners mark more quickly, though this effect is scaled to their initial mark investment (**Figure 2E**). Initially high-marking losers are slower to mark after losing, but individuals who initially marked infrequently speed up (**Figure 2E**). Therefore, the initial peak in marking activity observed among losers pre-fight (**Figure 2D**) is primarily due to high-marking males (**Figure S4C**). Together this demonstrates that complex changes in signaling behaviors are dependent on the initial signaling state of individuals.

We next examined the temporal rhythm of urine marking across mesh trials, which revealed unanticipated patterns. The intervals between marks differ noticeably in the pre- and post-fight, particularly when marks are made in close sequence to each other (**Figure 3A**). Pre-fight, mark sequences have larger intervals, producing chains of marking events (**Figure 3A & S5**). Whereas post-fight the mark sequences are compressed into shorter intervals, creating bursts of marking events (**Figure 3A**). To examine this relationship further, we inspected the distribution of inter-mark intervals (IMIs) among winners and losers for both trials (**Figure 3B**). Pre-fight, the most frequent IMIs are less than 3 seconds for winners and losers, though winners

have a lower median mark value. (**Figure 3B & S5**). Post-fight, there is a clear peak of IMIs of less than 1 second for both winners and losers (**Figure 3B**). Therefore, both winners and losers are producing mark "chains" per-fight, and "bursts" of marks post-fight. The overall median IMI interval is unchanged for winners but increases notably in losers.

To explore this shift in temporal dynamics within urine mark sequences, we classified marks that occur in IMIs of less than 3 seconds as marking bouts (**Figure S5**). Bouts can thus consist of a single mark or a series of marks. We then examined the variation in IMIs within urine mark bouts (i.e. IMIs for bouts with 2+ marks, **Figure 3C**). Trial has a strong effect on within-bout IMIs (M6: $F_{1,428}$ =304, p = 2.0e-16; **Table S3**), while fight outcome does not (M6: $F_{1,46}$ = 0.079, p = 0.78; **Figure 3C & Table S3**). Thus, marking events within bouts are more rapid post-fight for winners and losers, indicating competitive experience primes particular marking motor patterns, regardless of fight outcome. What is particularly striking is that the observed shift chain-like to burst-like mark motor patterning occurred as a result of a single competitive encounter.

We further investigated whether marking bouts are composed of 1 mark, 2 marks or 3+ marks (**Figure 3D**). Pre-fight losers have more single-mark bouts and winners have more multi-mark bouts (**Figure 3D**). This relationship becomes even more stark post-fight. Losers decrease the overall number of marks across mesh trials, but the bout composition remains similar (**Figure 3D**). Winners, on the other hand, increase the number of marks and alter their bout composition to include more multi-mark bouts (**Figure 3D**). We compared the average number of marks per bout by fight outcome and trial (**Figure 3E**). Bout composition is strongly affected by fight outcome (M7: $F_{1,58}$ = 10, p = 0.002; **Figure 3E & Table S3**). Post-fight, winners have a

significantly higher average number of marks per bout than losers (M7: $t_{1,111} = -3.0$, p

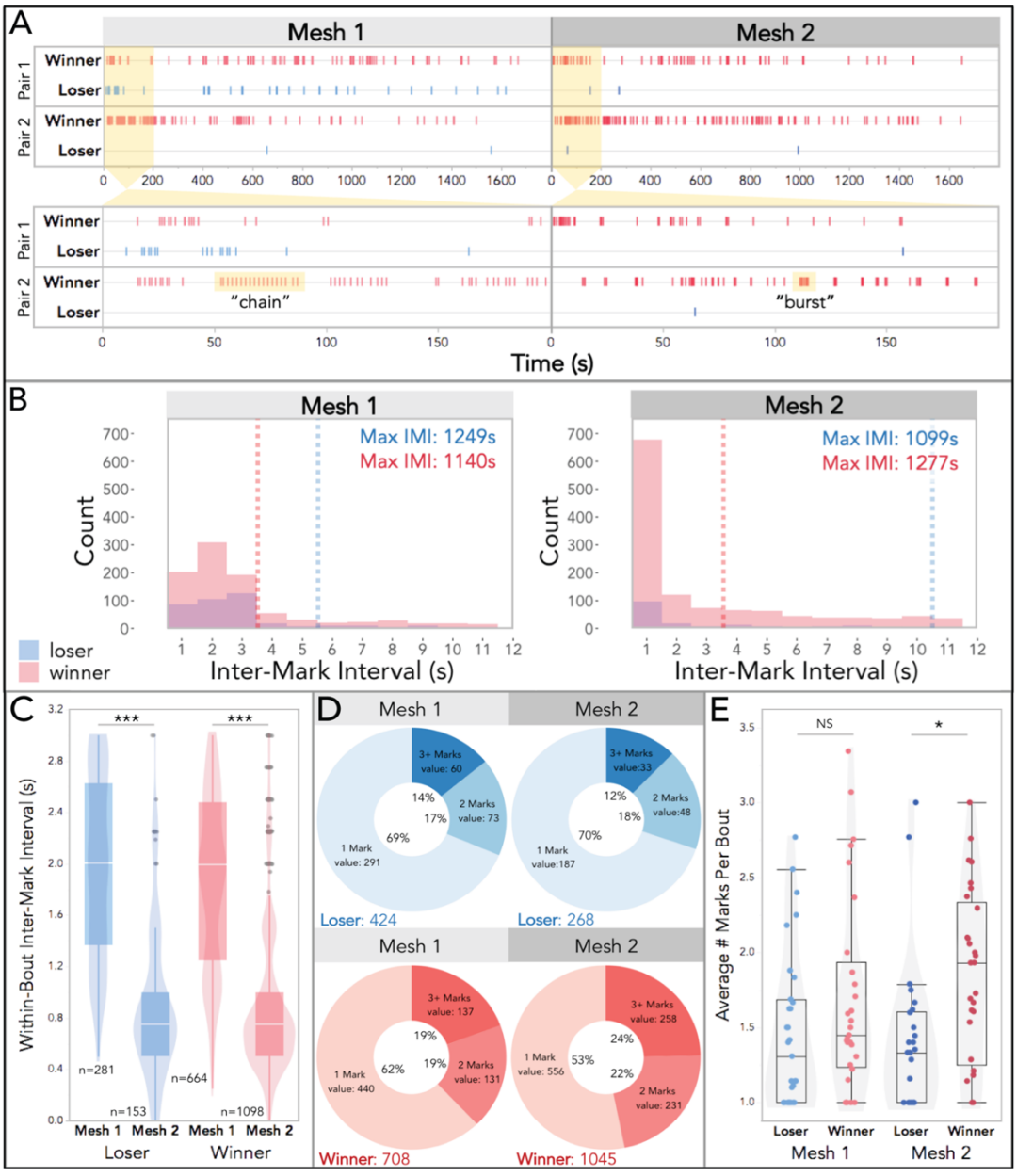

Figure 3. Temporal dynamics of urine mark allocation across mesh trials. (A) Example event plots depicting urine marking of two pairs of male competitors over the course of both mesh trials for the trial duration (top) and a zoomed-in view of the first 200s (bottom). "Chain"-like and "burst"-like marking bout examples are highlighted in yellow **(B)** Histograms of the inter-mark intervals (IMIs) for winners and losers in both mesh trials. Median values are indicated with dashed lines. The range of IMIs extends to nearly the full trial length (only the first 12s is shown). The maximum values are reported in the top right corner. Mesh 1: 65% of all IMIs are shown (< 12s), 57% of loser IMIs and 69% of winner IMIs. Mesh 2: 68% of all IMIs are shown (< 12s), 51% of loser IMIs and 72% of winner IMIs. **(C)** Box and violin plots of within-bout IMIs by fight outcome and mesh trial. **(D)** Donut plots by fight outcome and mesh trial depicting the proportions of bouts composed of: 1 mark, 2 marks, or 3+ marks. Mark totals are indicated (bottom left). **(E)** Boxplot of the average number of marks per bout by fight outcome and mesh trial. **(D,E)** Linear mixed models were used to model relationships (M6-M7: **Table S3**), analyses of variance were used to test for overall effects, and post hoc pairwise comparisons were performed using the *emmeans* package (significance codes: NS p>0.05, * p<0.05, ** p<0.01, *** p<0.001). Dependent variables were logarithmically transformed to meet assumptions for model residuals.

= 0.01; **Figure 3E & Table S3**). This dataset reveals striking patterns of signaling behavior in male house mice that would have otherwise gone undetected without the use of thermal imaging.

Dominance and familiarity interact to shape countermarking dynamics

Given that males dynamically adjust marking behavior in response to social competition, we next explored allocation decisions toward the scent marks of other males. We were especially interested in whether males use knowledge of a recent competitor's identity in their signaling decisions, as males will competitively counter-mark to (i.e. mark over) the urine marks of other males [11,42]. While it is well-established that males alter marking behavior in response to fight outcome [5,6,9] and can finely discriminate urine identities [10,11], we have a limited understanding of how males implement this information in a competitive marking context. Do males adjust their scent marking behavior depending on their relationship to a male competitor? What role does familiarity play in signal allocation dynamics? We hypothesized that fight outcome would shape urine marking, and that familiarity would strongly govern signal allocation decisions.

To address these questions, we compared two trial types within the trial series in which no conspecifics were present: empty arena trials and urine-marked trials (**Figure 1A**). The "Empty" trials contained no stimuli, and the "Marked" trials each contained two spatially distinct urine-marked zones of specific identities: their own urine (self: S), familiar male (FM) competitor urine, and/or unfamiliar male (UM) urine (**Figure 4B**). FM urine was collected from their paired male competitor, and UM urine was collected from novel adult males that had a different genotype and thus produce distinct major urinary protein profiles from the experimental males. We examined

responses to an empty arena and to the four different urine stimulus sets: S-S, S-FM, S-UM and FM-UM (**Figure 1A**) by fight outcome and initial signal investment. Trial type (M8: $F_{4,76} = 5.2$, $p = 0.0009$), fight outcome (M8: $F_{1,83} = 27$, $p = 2e\text{-}06$), and initial signal investment (M8: $F_{1,58} = 32$, $p = 4e\text{-}07$), all significantly affect the marking behavior of males (**Figure 4A & Table S4**). As does the two-way interaction between trial type and fight outcome (M8: $F_{4,77} = 5.8$, $p = 0.0004$; **Table S4**). Winners tend to mark more, and losers mark relatively lowly across treatment types. This pattern is observed in the responses to an empty arena (M8: $t_{1,100} = -3.9$, $p = 0.003$; **Figure 4A & Table S4**). Notably, winners and losers show opposite responses towards familiar versus unfamiliar urine. Treatments without unfamiliar urine (**Figure 4A-B**, purple: S-S and S-FM) exhibit comparable marking responses in winners and losers (**Figure 4A**). While it's perhaps less surprising that winners and losers mark comparably lowly to their own urine (S-S; M8: $t_{1,99} = -0.83$, $p = 1.0$), it is truly striking that winners and losers do not differ in their response to the S-FM treatment (M8: $t_{1,105} = -0.44$, $p = 1.0$; **Figure 4A & Table S4**). Particularly for winners, as these males are not marking highly to the presence to another male's urine in the environment. The opposite pattern is observed in the presence of unfamiliar urine. Winners mark significantly more than losers to S-UM (M8: $t_{1,108} = -3.6$, $p = 0.009$) and FM-UM (M8: $t_{1,109} = -6.0$, $p < 0.0001$) treatments (**Figure 4A & Table S4**).

We originally anticipated that in trials with two different urine identities males would differentially allocate urine towards each marked corner, we did not however detect any differences (**Figure S6A**). It became clear while scoring trials that the space was too small to delineate corner-based stimuli, as males frequently deposit scent marks in sequence across multiple regions. Our results also suggest that males mark in response to the most 'extreme' social odor in the environment (**Figures 4 &**

5). As a result, we consider each urine-marked treatment (**Figure 4B**) as an entire scent environment, rather than as discrete subregions. Interestingly, while we did not detect spatial differences in signaling within these spatial confines, we did detect region-specific differences in space use (**Figure S6B**). Losers spend less time in the center ROI compared to winners ($t_{1,230}$ = -3.7, p = 0.007), and spend less time in UM-marked corners relative to empty ones ($t_{1,199}$ = -3.5, p = 0.001) (**Figures 1C & S6B**).

Given that we observed very similar responses in the two treatments with unfamiliar urine present (S-UM and FM-UM) as well as the two treatments without unfamiliar urine (S-S and S-FM), we collapsed these similar treatments (purple: no unfamiliar male, orange: familiar male) to further explore the role of familiarity and fight outcome on signal allocation (**Figures 4B-E**). We standardized the marking behavior of males by calculating the difference in marks made in an empty arena relative to a scent-marked environment (**Figure 4C**). The interaction between fight outcome and familiarity strongly shapes marking behavior in scent-marked contexts (M9: $F_{1,58}$ = 13, p = 0.0005; **Figure 4C & Table S5**). Winners increase the number of marks significantly more than losers in trials when unfamiliar urine is present (M9: $t_{1,58}$ = -3.0, p = 0.007), whereas winners and losers do not differ when familiar-only scent marks are present (M9: $t_{1,58}$ = 2.0, p = 0.17; **Figure 4C & Table S5**).

We therefore find an inverse response among winners and losers toward familiarity (**Figure 4C**). Winners mark highly to unfamiliar urine and lowly to familiar-only urine (M9: $t_{1,58}$ = -3.0, p = 0.01), while losers mark lowly to unfamiliar urine and more to familiar-only urine (M9: $t_{1,58}$ = 2.2, p = 0.12; **Figure 4C & Table S5**). Notably, losers in the familiar-only treatment ($t_{1,14}$ = 4.5, p = 0.0005) and winners in the unfamiliar treatments ($t_{1,16}$ = 4.4, p = 0.0004) deviate significantly from zero, while their opposing treatments do not (shown in green: **Figure 4C**).

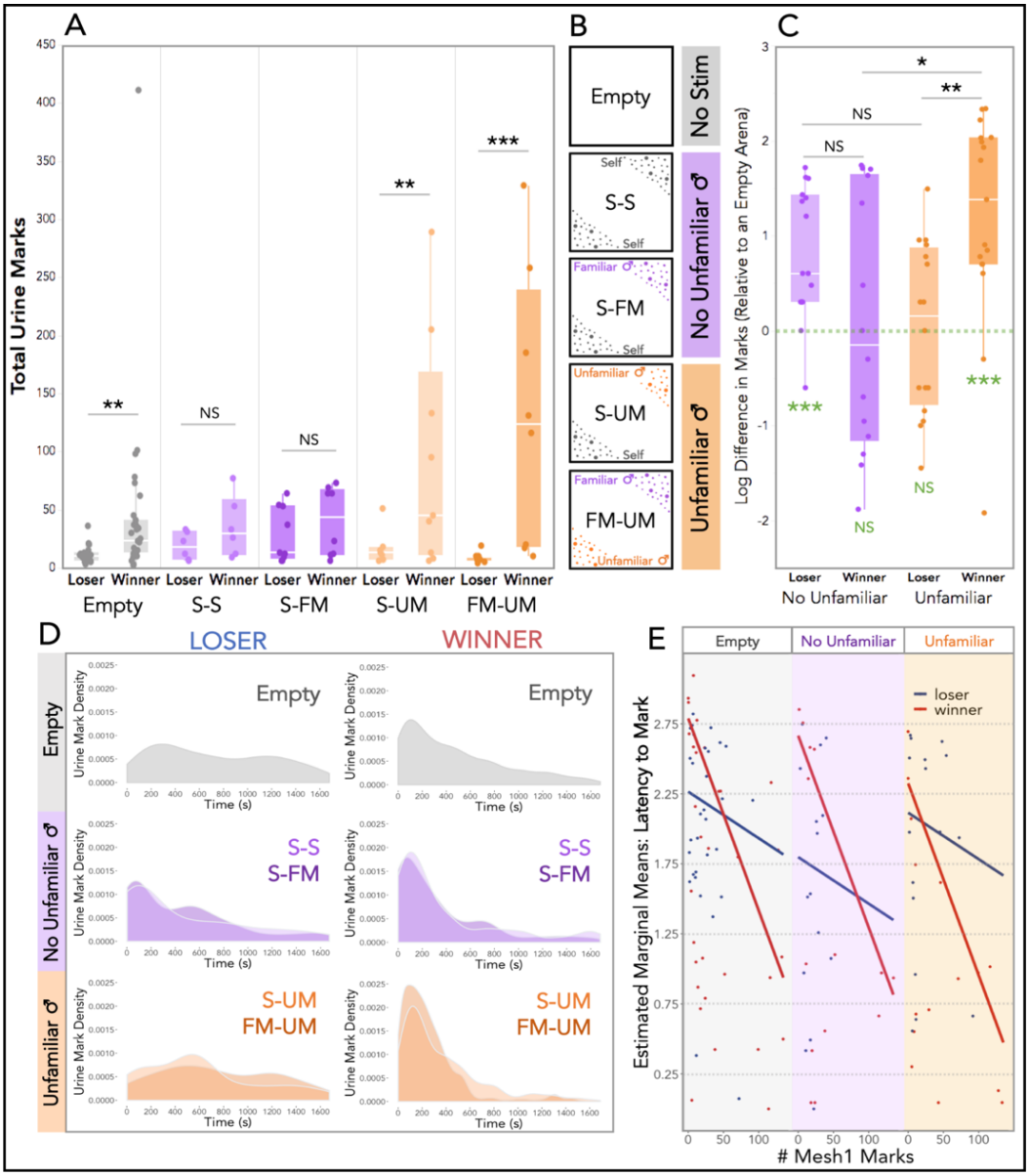

Figure 4. Urine mark allocation across scent-marked contexts. **(A)** Total urine marks deposited by winning and losing males in an empty arena and the four urine-marked treatments: self-self (S-S), self-familiar male (S-FM), self-unfamiliar male (S-UM) and familiar male-unfamiliar male (FM-UM). All males experienced an empty arena, as well as one of the 4 urine-marked treatments. **(B)** Schematic of the urine stimulus components. Empty trials have "no stimulus" (gray), S-S and S-FM have "no unfamiliar male" urine present (purple), and S-UM and FM-UM trials have "unfamiliar male" urine present (orange). **(C)** The difference in total marks deposited by males in the urine-marked trials relative to the empty trials (log-transformed). Urine-marked treatments are grouped as "no unfamiliar male" urine (purple: S-S and S-FM) and "unfamiliar male" urine (orange: S-UM and FM-UM). Post hoc pairwise comparison significance values are indicated at the top of boxplots. One-sample t-tests (deviation from 0) significance values are indicated on the bottom of the boxplots (green) **(D)** Urine mark density plots of losing and winning males toward an empty arena, and to trials with no unfamiliar male urine: S-S (light purple) and S-FM (dark purple), and to trials with unfamiliar male urine: S-UM (light orange) and FM-UM (dark orange). **(E)** Estimated marginal means plot of mark latency in the empty trials (gray), urine-marked trials with "No Unfamiliar" male urine (purple), and "Unfamiliar" male urine (orange), given fight outcome and initial signal investment (# Mesh1 marks). **(A,C,E)** Linear mixed models were used to model relationships (M8-M10: **Tables S4 & S5**), analyses of variance were used to test for overall effects, and post hoc pairwise comparisons were performed using the *emmeans* package (significance codes: NS p>0.05, * p<0.05, ** p<0.01, *** p<0.001). Dependent variables were logarithmically transformed to meet assumptions for model residuals.

Temporal variation in signal allocation during countermarking

The timing of signal allocation in scent-marked environments was also examined (**Figure 4D**). In trials with no urine stimulus (Empty), winners allocate marks early in the trial (peak density ~100s), while losers mark less with a later peak at ~250s (**Figure 4D**). In contrast, though the distributions are statistically distinct, winners and losers have quite similar density curves in familiar-only trials in terms of the timing of the initial peak (purple: S-S and S-FM) (**Figure 4D & Figure S6D**). What is also striking, is that the distributions of the S-S and S-FM trials are completely overlapping for losing males (D = 0.23, p = 1.0), and only moderately different for winning males (D = 0.13, p = 0.04; **Figure S6D**). Whereas in trials with unfamiliar urine, winners and losers differ dramatically (D = 0.48, p = 2e-16; **Figure S6D**). Winners quickly deposit large amounts of urine, creating a large initial spike in the density curves in S-UM (light orange) and FM-UM (dark orange) treatments (**Figure 4D**). Losing males drop off and slow down their urine mark deposition, generating density curves with small and delayed peaks (**Figure 4D**). The temporal distribution of urine marks is therefore modulated by fight outcome and familiarity in scent-marked environments.

As the temporal dynamics of scent-marks were overlapping in trials with or without unfamiliar male urine, we collapsed these into treatment groups (**Figure 4E**). We further modeled the effects of treatment group, fight outcome, and initial signal investment, on the latency to mark (**Figure 4E**). Mark latency is significantly predicted by the number of marks made in the first mesh trial, i.e. the initial investment recorded 3 days earlier (M10: $F_{1,57} = 10$, $p = 0.002$; **Figure 4E & Table S5**). For winners and losers, initially low-marking individuals are slower to mark, and initially high-marking individuals are faster to mark (**Figure 4E**). This relationship is most stark among winners, which exhibit steep slopes across treatment groups, while losers display

more modest slopes (**Figure 4E**). The interaction between fight outcome and initial signal investment, however, is moderate (M10: $F_{1,57} = 3.7$, $p = 0.06$; **Figure 4E & Table S5**). The effect of fight outcome on mark latency is not significant (M10: $F_{1,56} = 1.3$, $p = 0.25$; **Figure 4E & Table S5**). Treatment group on the other hand, significantly effects the speed of marking response (M10: $F_{1,75} = 3.2$, $p = 0.048$; **Figure 4E & Table S5**). Losers mark most rapidly in familiar-only trials, and winners mark most rapidly in trials with unfamiliar urine (**Figure 4E**). The intersection points of the linear models for winners and losers reveal additional insights. Winners transition to a more rapid marking response relative to losers differently across treatments groups depending on initial signal investment. In familiar-only trials, only the initially very high-marking (>85 marks) winners mark more rapidly than losers, other winners

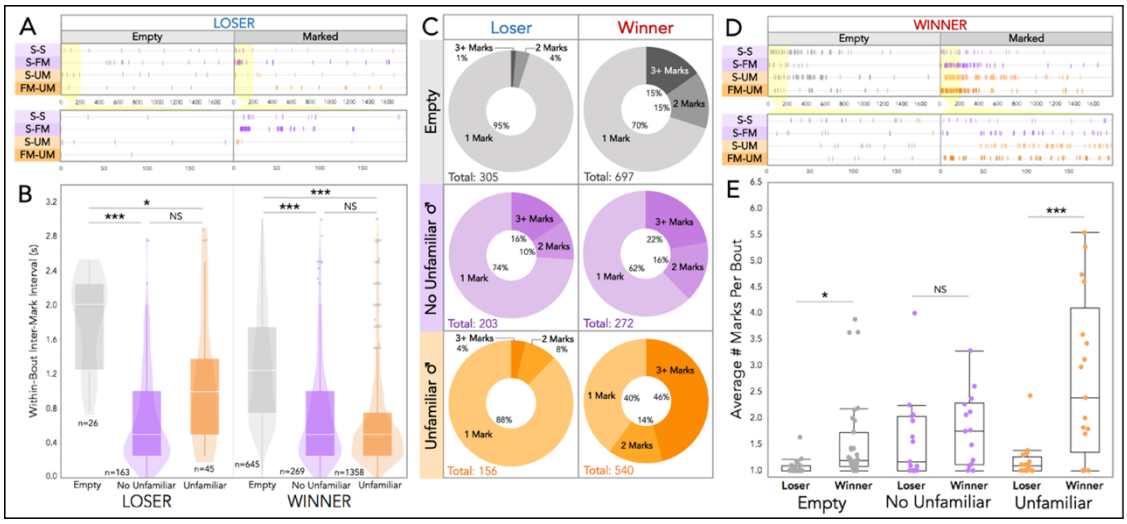

Figure 5. Temporal dynamics of urine signal allocation across scent-marked contexts. **(A)** Example event plots depicting urine marking in Empty and Marked trials of four losing males, each exposed to one of the four different urine-marked treatments: self-self (S-S), self-familiar male (S-FM), self-unfamiliar male (S-UM), and familiar male-unfamiliar male (FM-UM). The event plot for the entire trial duration is shown on top and a zoomed-in view of the first 200s is shown below. **(B,C,D)** Urine-marked treatments are grouped as "no unfamiliar male" urine (purple: S-S and S-FM) and "unfamiliar male" urine (orange: S-UM and FM-UM). **(B)** Box and violin plots of within-bout IMIs by fight outcome and trial group: Empty, No Unfamiliar (S-S & S-FM), and Unfamiliar (S-UM & FM-UM). **(C)** Donut plots by trial group and fight outcome depicting the proportion of bouts composed of: 1 mark, 2 marks or 3+ marks. Mark totals are indicated in the bottom left-hand corner. **(D)** Example event plots depicting urine marking in Empty and Marked trials of four winning males, each exposed to one of the four different scent-marked treatments: S-S, S-FM, S-UM, FM-UM. The event plot for the entire trial duration is shown on top and a zoomed-in view of the first 200s is shown below. **(E)** Boxplot of the average number of marks per bout by fight outcome and trial group. **(B,E)** Linear mixed models were used to model relationships (M11-M12: **Table S6**), analyses of variance were used to test for overall effects, and post hoc pairwise comparisons were performed using the *emmeans* package (significance codes: NS p>0.05, * p<0.05, ** p<0.01, *** p<0.001). Dependent variables were logarithmically transformed to meet assumptions for model residuals.

are slower to mark. The opposite is true in trials with unfamiliar urine, in which even initially low-marking (>20 marks) winners mark more rapidly than losers (**Figure 4E**). This demonstrates that initial signal investment has long-term power for predicting marking behavior, including the temporal allocation of urine marks.

We next examined the timing and composition of marking bouts (**Figure 5**). More chain-like bouts are observed in no-stimulus empty trials, whereas more rapid bursts of urine marking are produced in scent-marked trials (**Figures 5A, 5D & S6C**). Therefore, over the 4-day trial series males mark increasingly in bursts, suggesting competitive experience shapes temporal features of signal allocation. To explore this further we looked at within-bout IMIs (**Figure 5B**). Both fight outcome (M11: $F_{1,64}$ = 6.2, p = 0.02) and treatment group (M11: $F_{1,152}$ = 40, p = 1e-14) significantly effect within-bout IMIs, with a modest interaction (M11: $F_{1,154}$ = 2.5, p = 0.08; **Figure 5B & Table S6**). As expected, the within-bout IMIs are significantly longer in empty arena trials than either scent-marked treatment groups among winners or losers (**Figure 5B**). Winners, however, marked with similar rapid bursts (short IMIs) regardless of familiarity with the urine stimulus (**Figure 5B**). Conversely, losers tend to mark in bursts specifically during familiar-only trials (**Figure 5B**). This bout timing is most prominent in the S-FM trials (**Figure 5A & S6C**), which reveals losers distinctly allocate their urine marks based on the identity of urine marks in the environment. It is striking that, again, losers signal most conspicuously toward males who recently defeated them in a competitive contest.

The number of marks per bout changes with social outcome and scent-mark type (**Figure 5C**). The average number of marks deposited per bout is significantly shaped by scent-mark familiarity (M12: $F_{1,76}$ = 13, p = 1e-05) and fight outcome (M12: $F_{1,66}$ = 22, p = 2e-05), with a strong two-way interaction (M12: $F_{1,76}$ = 6.3, p = 0.003; **Figure**

5E & Table S6). Fight outcome and familiarity both influence the composition of marking bouts (**Figures 5C & 5E**). In an environment empty of scent marks, winners allocate considerably more multi-mark bouts than losers (30% vs 5%; **Figure 5C**), and the average number of marks per bout is significantly higher among winners (M12: $t_{1,105} = -3.0$, $p = 0.03$; **Figure 5E & Table S6**). Interestingly, the differences in bout composition narrows in scent-marked trials with familiar-only urine (**Figure 5C**). In these trials, winners deposit slightly more multi-mark bouts (38%), while losers dramatically shift the amount of multi-mark bouts (26%; **Figure 5C**). The average number of marks per bout does not differ between winners and losers in familiar-only trials (M12: $t_{1,117} = -1.0$, $p = 0.87$; **Figure 5E & Table S6**). The reverse is true for trials with unfamiliar male urine present (**Figure 5C**). Here, losers produce bouts with similar bout compositions to the empty arena trials (**Figure 5C**). Winners double the proportion of multi-mark bouts compared to empty arena trials (60%), and many bouts contain at least 3 marks (46%; **Figure 5C**). The average number of marks per bout is significantly higher among winners when unfamiliar urine is present (M12: $t_{1,117} = -5.6$, $p = <0.0001$; **Figure 5E & Table S6**). Thus, the temporal rhythm and composition of urine allocation patterns change in response to the presence of different urine identities in the environment.

Discussion

Using a thermal imaging approach, we discovered context-dependent dynamic and static responses in urine mark allocation, latency, and rhythm, toward competition and variable social environments (**Figures 2 & 3**). Collectively, these data provide strong evidence that male mice remember their experiences with other individuals, and update their decisions based on this information. Winning or losing has strong and

long-lasting effects on signaling decisions (**Figures 4 & 5**), most prominently on total allocation effort and marking bout composition. As described in the literature, we find males quickly downregulate urine allocation after losing a competitive contest [5,23,24]. However, we also find that initial signal investment has stable and robust effects on marking behavior. In other words, where males start off influences their signaling decisions days later. Low-marking individuals remain relatively low-marking, and high-marking individuals remain relatively high-marking. The magnitude of the observed winner-loser effects is therefore contingent on the initial investment decisions of males.

Our data demonstrate that male house mice dynamically adjust their signal allocation and timing depending on the social scent landscape. Prior studies have shown that male mice finely distinguish self from non-self urine [11,42], and that females recognize specific males based on their urine marks [10,22]. However, it has been less clear whether males use such information in territorial contexts. Here we find that signaling decisions are profoundly shaped by contest outcomes and familiarity with male competitors. Surprisingly, losers tend to increase mark allocation effort and display more frequent bursts of multi-mark bouts toward familiar male urine marks. In contrast, winners downregulate their marking efforts toward familiar urine. The responses toward familiar males are even more stark when compared to how males respond to unfamiliar male urine. A key component of our design was that a single standardized male urine stimulus was used across all trials as the unfamiliar male, so the differences in responses to the unfamiliar male must be attributed to shifts in mouse behavior in response to recent experiences rather than any variation in scents they were presented. Winners dramatically upregulate all competitive marking efforts and losers go scent “silent.” Under the dear enemy model, territorial

males should remain vigilant toward unfamiliar males, as they threaten their current dominance status [26–31]. In our study, winners adhere to these expectations by aggressively signaling toward novel male urine. Losers on the other hand are at risk of further aggression. By staying “silent” losers may avoid conflict with a new territorial contender, potentially in a “wait-and-see” strategy [43]. However, when presented with urine of the male that recently defeated them, losers actually upregulate marking efforts. This response may be a “nasty neighbor” effect, in which the threat of familiar territorial males exceeds that of strangers [28]. Alternatively, this increased marking response could be a form of subordinate marking. We thus find evidence for the dear enemy effect in winners and the nasty neighbor effect in losers, suggesting recent social experiences modulate how animals invest in territorial advertisement and signaling.

Competitive experience also has strong priming effects on temporal features of scent marking. Mice mark more rapidly after a contest, regardless of outcome (**Figure 2**). Similarly, the time between deposition events shrinks, such that marking bouts transition from chain-line sequences to rapid bursts. Aggressive contests likely shift males into a competitive state, driving changes in urinary motor patterns. Strikingly this occurs after just a single aggressive contest. Voluntary, involuntary, and context-dependent urination are all mediated by neuronal subpopulations in the Barrington’s nucleus in the brainstem [32–34]. The fine-scale adjustments in urinary motor control we observe reveals additional complexity to this underlying circuitry, opening avenues for future research to examine how competitive interactions and social signals modulate motor outputs.

We unexpectedly detected a cohort of “silent” low-marking winners, for which we could find no prior description of in the literature, suggesting several possible

hypotheses. First, the result may be driven in part by our trial design. By pairing evenly-matched males, we may have observed more instances of low-marking males winning. Furthermore, better-than-expected outcomes could give rise to slower response times than worse-than-expected outcomes, in which high-marking losers rapidly downregulate signal allocation [5,23,24]. Second, low-marking males may differ in some aspect of hydration physiology. Species and strains of mice vary in water intake and urination levels [44–46], though we observed low marking winners in both strains used in this study. Third, “silent” yet competitive males might represent a distinct signaling strategy in house mice. Given the high metabolic costs of signaling, it’s plausible that some males might withhold signal investment to continue investing in body mass or to avoid detection by other males. Male house mice therefore may pursue diverse signaling strategies, including the classically described “territorial males” that invest highly in urine marking as well as scent-silent “sneaker males” [47–49]. While our data does not directly test this relationship, the frequency of low-marking winners warrants further investigation. Certainly, the simple correlation between marking and dominance is considerably more complex than previously described.

This work emphasizes the importance of examining signaling behaviors across variable social contexts in order to examine the decision rules underlying costly and complex behaviors. Furthermore, the implementation of thermal recording in social behavior assays has the potential to reveal important features underlying the neurophysiological basis of socially-modulated and voluntary urination behaviors.

Methods

Experimental animals

All experimental subjects in this study were males (n=62) from two wild-derived inbred strains (NY2 and NY3) of house mice (*Mus musculus domesticus*). The progenitors of these strains were captured near Saratoga Springs, NY in 2013 by MJS [50] and are related to the SarA/NachJ, SarB/NachJ and SarC/NachJ strains now available from the Jackson Lab. Wild-derived strains were used because naturalistic competitive behaviors are less pronounced in highly inbred and domesticated laboratory strains [51,52] and inbred strains tend to share identical urinary protein profiles [53]. Individual wild house mice have distinct blends of urinary proteins that are used to each other [10,54,55]. We therefore wanted to ensure that all interacting males smelled distinct in an ecologically relevant manner. In other words, that they assessed and interacted with genotypically distinct individuals. At weaning age (3-4 weeks) males were placed into a holding cage alone for 1-2 weeks, and were subsequently paired with a female to allow for sexual experience, as sexually naïve mice are known to exhibit different social behaviors [56]. All males were allowed to reach adulthood (3-5 months old by the time of experimental testing), and had the opportunity to produce one or more litters. All holding and breeding cages contained corn cob bedding, cardboard huts, and cotton nestlets. Mice were maintained in an Animal Care facility at Cornell University with a 14:10 shifted light:dark cycle (lights went out at 10 PM and on at 12 PM) and were provided food and water *ad libitum*. Mice were handled minimally and with transfer cups whenever possible to reduce stressful handling. All experimental protocols conducted at Cornell University were approved by the Institutional Animal Care and Use Committee

(IACUC: Protocol #2015-0060) and were in compliance with the NIH Guide for Care and Use of Animals.

Behavioral experiments

One day prior to experimentation, we recorded subject male body weights to size-match individuals as closely as possible (average weight difference: 2.4g). All males were in breeding cages at the time of the experiment and most successfully reproduced (84%) prior to start of the trial series. As house mice are nocturnal, all experiments were conducted in the dark during the dark cycle [57]. All experimentation occurred between 12 PM - 5 PM to minimize circadian variation. Trial series were performed in sets of between 2-5 male pairs.

Behavioral trials consisted of a 4-day trial design, in which age and weight-matched adult breeding males of distinct wild-derived strains (NY2 and NY3) were paired as competitors and presented a series of social and scent-marked trials (**Figure 1A**). We pair-matched each NY2 mouse with a NY3 mouse to ensure that no two paired mice were genotypically identical and that their scent marks were perceptibly different (unique major urinary protein profiles) [11,53–55], resulting in a total of 31 pairs (n=62). All inbred strains of house mice have identical major urinary proteins (as a result of inbreeding)[53–55]. Because major urinary proteins are used in recognizing individuals [10,11,42,54], we wanted to ensure paired males had distinct urine profiles.

To guarantee identification of males within a pair (NY2 and NY3 strains are visibly indistinguishable), we ear-clipped and bleached a patch of rump fur of one male in each pair a week prior to experimentation. Mice were anesthetized with isoflurane (5%). A heating pad was used to maintain a stable body temperature. Isoflurane was

delivered at 1-3% throughout the bleaching procedure. L'Oreal Colo Rista Bleach Ombre (salon bleach) was mixed as per the manufacturer's instructions and dabbed onto the top layer of fur using a sterile cotton swab. Care was taken to prevent bleach from contacting the skin. Twenty minutes after application, sterile cotton tipped swabs dipped in water were used to rinse the bleach from the fur. The fur was then dabbed dry with paper towels. Mice were placed under a heat lamp for 5 minutes or until they were fully recovered from anesthesia before being transferred back to their home cage.

All trials were performed in one of two trial chambers that were sound proofed and fitted with recording systems. For all trials large sheets of Whatman filter paper lined the floor of each trial to collect urine blots and to present urine stimuli. The same size PVC arenas were used throughout (50 cm x 50 cm), though split in half with the mesh barrier for the Mesh trials (**Figure 1A**). At the end of each trial, males were placed back into their breeding cages. On Day 1 of the trial series, paired males were placed on either side of a wire mesh barrier in an arena for 30 minutes (Mesh 1, **Figure 1A**). At the end of the 30 minutes, males were briefly removed from the arena into large transfer cups, the filter paper was labeled and removed, a fresh filter paper was placed in the arena, and the mesh barrier was removed. Males were placed back into the arena for a 30-minute aggressive contest (Fight, **Figure 1A**). On Day 2, each male was placed alone in an stimulus-free empty arena for 30 minutes (Empty, **Figure 1A**). On Day 3, males were placed back into the mesh arena for 30 minutes with the same male competitor encountered on the first day, without the subsequent fight trial (Mesh 2 trial, **Figure 1A**). On Day 4, males were placed into the arena alone for a 30-minute urine-marked stimulus trial, consisting of one of 4 possible treatment types. Each treatment included two spatially distinct urine-marked zones placed in

opposite corners of the arena (front right – back left vs. back right – front left). Urine-marked corner zones contained aliquoted male urine of 3 possible identities: self, familiar, or unfamiliar male. Self-urine was collected from the experimental trial mouse; familiar male urine was from the paired male competitor of the experimental mouse; unfamiliar male urine was collected from novel adult males that had distinct urine profiles from experimental males. The urine stimuli were thawed, pooled and kept on ice until aliquoted for the urine-marked stimulus trial onto filter paper. Urine stimuli were placed on the filter paper directly before the trial start in standardized locations and volumes. The four treatment types span a range of scent mark combinations: self-self, self-familiar, self-unfamiliar, familiar-unfamiliar. Paired males (winner-loser pairs) received the same urine-marked stimulus treatment, with the exception of three pairs due to urine collection constraints. For all trials (Days 1-4) the first and last minute of each trial was trimmed prior to analysis. This was done to minimize detection of startle-based urination events caused by placement of mice into arenas and any jostling caused during trial set-up and take-down. The total analyzed trial length was thus 28 minutes.

Trials and treatments were randomized as follows. Male trial order and arena chamber was pseudo-randomized each day to avoid confounds in arena location and marking behavior over the course of the designated trial period. The orientation within the Mesh 1 trials was also randomized (whether males were placed near the back or front of the arena) to account for variation in sound disturbances for males closer to the chamber door; orientations were subsequently flipped for each pair in Mesh 2. Urine-marked trial treatments were pseudo-randomly assigned to each male pair, to ensure similar numbers of male pairs were exposed to the 4 treatment types across sets of trials series. The orientation of urine stimuli was randomly assigned to corner

orientations (front right – back left vs. back right – front left). Lastly, the fur bleaching for male identification was performed on one mouse strain (NY2 or NY3) for each trial set, but the bleached strain was switched between trial sets to prevent errors within a trial set and to avoid bleaching only one strain across trial sets.

Urine collection

Urine was collected from each experimental male subject to present self and familiar male (paired competitor) urine in the urine-marked zones on the final day of the trial series (**Figure 1A**). For unfamiliar male urine, we collected from a third distinct inbred mouse line (C57BL/6), to again ensure that the novel male urine presented had a distinct urinary protein profile from experimental individuals. This was necessary in order to have the urine scent marks of self, familiar male and unfamiliar male be distinguishable as different urine identities in the environment, given that mice have been shown to use major urinary proteins in this capacity [10,11,42,54].

Urine collection was performed using the single animal method: males were placed atop a metal grate (an upside down cage hopper) over a clear plastic bag for 30 minutes to 1 hour [58]. Males were subsequently taken off the plastic bag and returned to their breeding cage. The urine droplets present on the plastic bag were collected and stored at -80°C until use. Urine collected from subject males was stored individually until the day of the urine-marked trials (Day 4: **Figure 1A**). For sufficient urine volume for the urine-marked trial treatments (**Figure 1A**), between 200-400uL was collected from each NY2 and NY3 male subject. On the day of the urine-marked trials, individual aliquots for a subject male were thawed on ice and pooled together. For unfamiliar male urine we collected a large batch of urine from over 20 adult breeding C57BL/6 males. Urine was stored on the day of collection at -80°C. Once a

sufficient volume was collected to use as stimuli across all trials, individual aliquots were thawed on ice, and all C57BL/6 male urine was pooled into a single volume and subsequently aliquoted and stored at -80°C. This was done such that the identical unfamiliar C57BL/6 urine stimuli were presented to males across all trials, without any individual-specific effects of urine odors.

Recording methods

All trials were recorded with a security camera system (iDVR-PRO CMS) at 1080p and 30 frames per second to visualize the high-speed aggressive encounters and to clearly distinguish the male identities (ear-marked and bleached fur). All trials (including fight trials) were recorded thermally using an infrared camera system (PI 640; Optris Infrared Sensing). Thermal cameras were fitted with 33° x 25° lenses and mounted above the experimental arena chambers such that field-of-view for each camera covered the entire arena. The thermal detection window was set at: 61°F - 107°F. Data frames were collected at the max speed, averaging at 3 Hz. Thermal video data was saved by screen-capturing live Optris video output using OBS Studio software. Raw temperature data was also collected in semicolon-delimited CSVs, providing a readout of the temperature in each pixel for each frame.

Behavioral scoring and analysis

All videos were scored using Behavioral Observation Research Interactive Software (BORIS) [59]. For the fight trials (**Figure 1A**), we scored the following aggressive behaviors: chasing, hitting, boxing, and wrestling bouts (**Figure S1C**) using the infrared security camera video recordings. To score urine mark deposition events Optris thermal video recordings were used for all trials. Urine depositions were scored

as a clear hot spot following the focal mouse's trajectory that subsequently cooled below substrate temperature. Urine marks placed in close spatial and temporal proximity were considered separate deposition events if at the moment of deposition there was a detectable cold barrier line separating the urine marks. Fecal depositions could be eliminated as they are frequently cooler upon deposition event, cool much more slowly, have a distinct shape, and are typically moved around the arena quickly. In addition to scoring the timing of urine deposition events, the placement of urine marks was also scored. Using screen annotation software, we drew precise lines on the video observation corresponding to regions of interest for each thermally-recorded trial (**Figure 1B-C**). In the scent-marked trials with two different urine identities (**Figure 1A**), we had anticipated males would differentially allocate urine towards each marked corner. We did not detect clear effects of differential allocation to marked corners (**Figure S5A**), suggesting two non-mutually exclusive possibilities: (1) the scent of unfamiliar males may be more important in driving allocation decisions and (2) the size of the arena may be too small for delineated corner-based allocation. While scoring the trials, it became clear that the space was likely too small, as males frequently walk through corners while performing a scent-mark bout that extends across multiple ROIs. As such, subsequently analyses focused on the presence of familiar and unfamiliar urine in the entire arena environment.

Tracking

Mice were tracked using the software UMATracker (Release 12) [60]. Infrared security camera recordings were used to track focal mouse movement, as the video were recorded at a higher framerate. Filters were generated using the following modular settings (in order): output – Closing: Kernel = 6 – Opening: Kernel = 6 –

Threshold: 100 – BGRToGray – input. Videos were tracked using Group Tracker GMM algorithm. Area51 was used to generate desired regions of interest for each trial (**Figure 1B-C**) and analyze the relative space use in each of these regions. The R package *trajr* [61] was used to quantitatively characterize the following information from the tracked data frames: speed, acceleration, and trajectory length.

Urine blot imaging and processing

Trials were run on Whatman filter paper substrate. Arena edges were outlined with pencil on the filter paper at the end of each trial. We collected all sheets of filter paper used in experimentation (except for the Fight trial) and photographed them under ultraviolet (UV) light. We used three UV bulbs to evenly distribute light on the large filter paper area. Images were converted to greyscale in Adobe Photoshop and the magentas were reduced to ~20% to observe edges of urine marks clearly. Greyscale images were subsequently processed in ImageJ (Fiji). We subtracted background pixels for a cleaner image (100 px), applied image thresholding (manually adjusted when necessary), and converted images to binary in order to convert to mask, fill holes and perform watershed algorithm. This processed image was then used to analyze the number of particles, with Size (pixel^2): 100-Infinity and Circularity (0-1.00).

Urine mark bout classification

The median inter-mark interval (2.99 seconds) for all males across all trials was used to determine whether marks get clustered into a marking “bout” (**Figure S5A**). Any two marks that occur in sequence with an inter-mark interval less than 3 seconds are clustered together into a multi-mark bout, allowing us to examine within-bout

dynamics. Other clustering methods were attempted but were less successful at classifying marking bouts, when visually checked with scored videos.

Statistical analyses

We conducted all statistical analyses in R 3.6.0 (R Development Core Team 2019). We used linear mixed models (LMMs) and paired statistical tests to examine relationships between dependent and response variables. Models were fitted using the package *lme4* [62]. The *lmerTest* package was used to calculate degrees of freedom (Satterthwaite's method) and p-values [63]. Dependent variables were transformed for a subset of models to meet assumptions for model residuals after visually inspecting model residuals. We used a type 3 analysis of variance (ANOVA) to test for overall effects of fixed factors or interactions in the models. Post hoc comparisons were conducted using the *emmeans* package [64]. R script and data sheets used for all statistical analyses are provided.

Data availability

Data sheets and R code used in all analyses are available on the Dryad Digital Repository.

Declarations

Acknowledgments

We thank Kevin Besler, Kusuma Anand, Christen Rivera-Erick and Melanie Colvin for crucial technical assistance; Russell Ligon and Caleb Vogt for helping establish recording systems and tracking methods in the lab; James Tumulty and Rose Tatarsky for manuscript feedback.

Author contributions

CHM and MJS conceived the study. CHM performed trials and analyses. MFH, JY, BCC, KH and AYL collected samples, scored behavioral trials, and generated tracking data. CHM wrote the initial drafts of the paper. MJS and MRW edited the manuscript. All authors contributed to manuscript preparation.

Competing interests

The authors declare no competing interests.

Supplementary information

Table S1. Linear mixed model details (M1-M2) accompanying Figures S1 & 1F.

	M1 : # Aggressive Behav. (Figure S1B) log_{10}(#Aggressive Behaviors+1)~Fight Outcome+(1|Strain)			M2 : # Marks (Figure 1F) log_{10}(#Urine Marks+1)~Recording Method+(1|maleID)		
Coefficients	Estimates	CI	p	Estimates	CI	p
Fixed Effects						
(Intercept)	0.49	0.36 – 0.62	<0.001	1.26	1.14 – 1.39	<0.001
Fight Outcome (Win vs. Loss)	1.60	1.41 – 1.78	<0.001			
Recording Method (UV vs. Thermal)				0.00	-0.07 – 0.08	0.954
Random Effects						
σ^2	0.13			0.17		
τ_{00}	0.00_{strain}			0.21_{maleID}		
ICC				0.55		
N	2_{strain}			61_{maleID}		
Observations	62			492		
Marginal R^2 / Conditional R^2	0.833 / NA			0.000 / 0.551		

Table S2. Linear mixed model details (M3-M5) accompanying Figure 2.

	M3 : # Total Marks (Figure 2A) log_{10}(#Urine Marks+1)~Fight Outcome*Mesh Trial+(1|maleID)			M4 : # Mesh2 Marks (Figure 2C) log_{10}(#Mesh2 Marks+1)~Fight Outcome+log_{10}(#Mesh1 Marks+1)+(1|strain)			M5 : Mark Latency (Figure 2E) log_{10}(Mark Latency+0.08)~Fight Outcome*Mesh Trial*log_{10}(#Mesh1 Marks+1)+(1|maleID)		
Coefficients	Estimates	CI	p	Estimates	CI	p	Estimates	CI	p
Fixed Effects									
(Intercept)	1.23	1.02 – 1.43	<0.001	0.31	-0.13 – 0.76	0.168	3.82	3.04 – 4.59	<0.001
Fight Outcome (Win vs. Loss)	0.10	-0.19 – 0.39	0.493	0.59	0.29 – 0.90	<0.001	-0.36	-1.35 – 0.62	0.465
Mesh Trial (Mesh1 vs. Mesh2)	-0.38	-0.61 – -0.15	0.001				-1.50	-2.40 – -0.60	0.001
Fight Outcome : Mesh Trial	0.56	0.24 – 0.89	0.001				1.14	-0.00 – 2.28	0.051
Initial Investment (Mesh1 Marks)				0.44	0.15 – 0.74	0.004	-1.48	-2.07 – -0.88	<0.00
Fight Outcome : Initial Investment							0.48	-0.24 – 1.21	0.190
Mesh Trial : Initial Investment							1.40	0.70 – 2.09	<0.001
Fight Outcome : Mesh Trial : Initial Investment							-1.49	-2.34 – -0.64	0.001
Random Effects									
σ^2	0.21			0.34			0.32		
τ_{00}	0.13_{maleID}			0.01_{strain}			0.16_{maleID}		
ICC	0.37			0.03			0.32		
N	61_{maleID}			2_{strain}			61_{maleID}		
Observations	124			62			124		
Marginal R^2 / Conditional R^2	0.151 / 0.469			0.305 / 0.327			0.409 / 0.601		

Table S3. Linear mixed model details (M6-M7) accompanying Figure 3.

	M6 : Within-Bout IMIs (Figure 3C) log_{10}(Within-Bout IMI+0.0005)~ Fight Outcome*Mesh Trial+(1|boutID)+(1|maleID)			M7 : Avg. Marks per Bout (Figure 3E) log_{10}(Avg Marks per Bout)~ Fight Outcome*Mesh Trial+(1|maleID)		
Coefficients	Estimates	CI	p	Estimates	CI	p
Fixed Effects						
(Intercept)	0.29	0.22 – 0.35	**<0.001**	0.14	0.09 – 0.19	**<0.001**
Fight Outcome (Win vs. Loss)	-0.02	-0.10 – 0.07	0.702	0.06	-0.02 – 0.13	0.122
Mesh Trial (Mesh1 vs. Mesh2)	-0.45	-0.53 – -0.36	**<0.001**	-0.02	-0.09 – 0.06	0.659
Fight Outcome : Mesh Trial	0.05	-0.04 – 0.15	0.266	0.06	-0.05 – 0.16	0.266
Random Effects						
σ^2	0.10			0.02		
τ_{00}	0.00_{boutID}			0.00_{maleID}		
	0.01_{maleID}					
ICC	0.12			0.04		
N	54_{maleID}			62_{maleID}		
	81_{boutID}					
Observations	2199			115		
Marginal R^2 / Conditional R^2	0.249 / 0.341			0.095 / 0.130		

Table S4. Linear mixed model details (M8) accompanying Figure 4A.

	M8 : # Total Marks (Figure 4A) log_{10}(#Urine Marks+1)~Fight Outcome*Trial+log_{10}(#Mesh1 Marks+1)+(1|maleID)		
Coefficients	Estimates	CI	p
Fixed Effects			
(Intercept)	0.47	0.22 – 0.72	**<0.001**
Fight Outcome (Win vs. Loss)	0.84	0.57 – 1.12	**<0.001**
Trial [Empty]	0.09	-0.10 – 0.27	0.371
Trial [S-S]	0.29	0.01 – 0.57	**0.046**
Trial [S-FM]	0.38	0.12 – 0.63	**0.004**
Trial [S-UM]	0.21	-0.06 – 0.49	0.127
Fight Outcome : Trial [Empty]	-0.53	-0.81 – -0.26	**<0.001**
Fight Outcome : Trial [S-S]	-0.71	-1.12 – -0.30	**0.001**
Fight Outcome : Trial [S-FM]	-0.78	-1.15 – -0.41	**<0.001**
Fight Outcome : Trial [S-UM]	-0.32	-0.70 – 0.06	0.100
Initial Investment (Mesh1 Marks)	0.39	0.26 – 0.53	**<0.001**
Random Effects			
σ^2	0.05		
τ_{00}	0.05		
ICC	0.51		
N	61		
Observations	124		
Marginal R^2 / Conditional R^2	0.504 / 0.757		

Table S5. Linear mixed model details (M9-M10) accompanying Figure 4C & 4E.

	M9 : Log Diff. Marks (Figure 4C) log_{10}(#Marked-Empty Marks+1)~Fight Outcome*Trial Group			M10 : Mark Latency (Figure 4E) log_{10}(Mark Latency+1)~Fight Outcome+log_{10}(#Mesh1 Marks+1)+Trial Group+Fight Outcome*Trial Group+Fight Outcome*log_{10}(#Mesh1 Marks+1)+(1|maleID)		
Coefficients	Estimates	CI	p	Estimates	CI	p
Fixed Effects						
(Intercept)	0.82	0.29 – 1.36	**0.003**	2.27	1.53 – 3.00	**<0.001**
Fight Outcome (Win vs. Loss)	-0.75	-1.52 – 0.02	0.055	0.52	-0.42 – 1.46	0.273
Fight Outcome : Trial Group	1.93	0.88 – 2.98	**0.001**			
Trial Group [UM]	-0.80	-1.54 – -0.06	**0.036**	-0.15	-0.58 – 0.28	0.486
Trial Group [No UM]				-0.47	-0.90 – -0.03	**0.036**
Initial Investment (Mesh1 Marks)				-0.21	-0.76 – 0.34	0.452
Fight Outcome : Trial Group [UM]				-0.31	-0.91 – 0.28	0.298
Fight Outcome : Trial Group [No UM]				0.35	-0.28 – 0.97	0.276
Fight Outcome : Initial Investment				-0.66	-1.33 – 0.02	0.055
Random Effects						
σ^2				0.44		
τ_{00}				0.19_{maleID}		
ICC				0.29		
N				61_{maleID}		
Observations	62			124		
Marginal R^2 / Conditional R^2	0.205/0.163			0.245/0.467		

Table S6. Linear mixed model details (M11-M12) accompanying Figure 5.

	M11 : Within-Bout IMIs (Figure 5B) log_{10}(Within-Bout IMI+0.0005)~ Fight Outcome*Trial Group+(1|boutID)+(1|maleID)			M12 : Avg. Marks / Bout (Figure 5E) log_{10}(Avg Marks / Bout)~ Fight Outcome*Trial Group+(1|maleID)		
Coefficients	Estimates	CI	p	Estimates	CI	p
Fixed Effects						
(Intercept)	0.26	0.09 – 0.42	**0.002**	0.02	-0.03 – 0.08	0.422
Fight Outcome (Win vs. Loss)	-0.17	-0.34 – 0.01	0.061	0.12	0.04 – 0.21	**0.003**
Trial Group [UM]	-0.31	-0.52 – -0.11	**0.003**	0.04	-0.05 – 0.12	0.399
Trial Group [No UM]	-0.52	-0.71 – -0.34	**<0.001**	0.14	0.05 – 0.23	**0.002**
Fight Outcome : Trial Group [UM]	-0.03	-0.24 – 0.18	0.762	0.19	0.07 – 0.30	**0.002**
Fight Outcome : Trial Group [No UM]	0.16	-0.03 – 0.36	0.103	-0.06	-0.19 – 0.06	0.314
Random Effects						
σ^2	0.12			0.02		
τ_{00}	0.00_{boutID}			0.01_{maleID}		
	0.01_{maleID}					
ICC	0.09			0.35		
N	50_{maleID}			62_{maleID}		
	93_{maleID}					
Observations	2506			123		
Marginal R^2 / Conditional R^2	0.160 / 0.233			0.321 / 0.561		

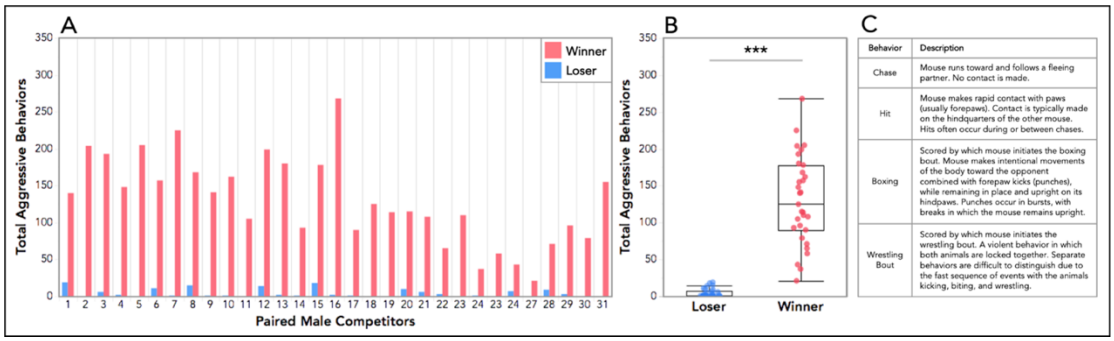

Figure S1. Male aggressive behaviors scored in contests (fight trials) between paired competitors. **(A)** Total aggressive behaviors performed by each paired male competitor. The fight outcome (the categorization of winners and losers) was determined by which male performed more aggressive behaviors within a pair. **(B)** Across all 31 pairs, winning males performed significantly more aggressive behaviors than losing males ($t_{1,31}$= -13, p = 1e-13*)*. Welch's t-test was used to compare the total aggressive behaviors performed by the two fight outcome categories (significance code: *** p<0.001). A linear mixed model was also used to model this relationship, and an analysis of variance was used to test for overall effects (M1: $F_{1,60}$= 304, p = 2e-16; **Table S1**). **(C)** Ethogram used to score aggressive behaviors. State events: chase, boxing and wrestling bouts. Points events: hits. All events were coded for a male subject if the individual initiated the behavior (i.e. wrestling bout is coded for only one participant – the initiator – of that event).

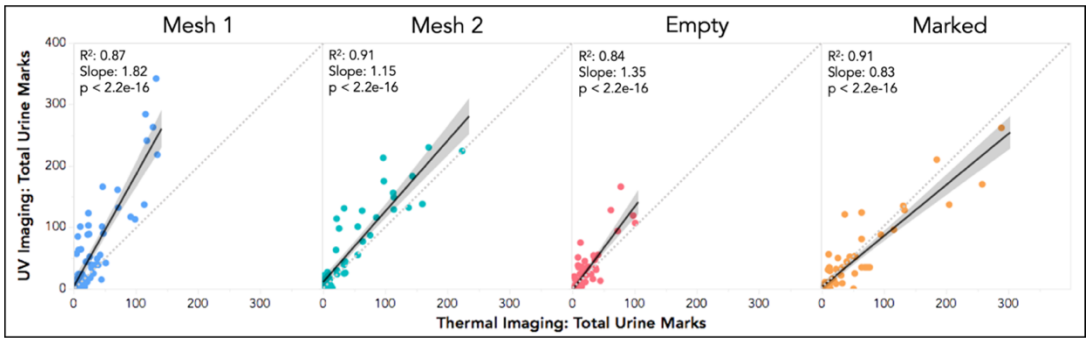

Figure S2. Comparison of urine mark detection methods across trial types: Ultraviolet light (UV) blot imaging vs. thermal imaging. The two detection methods are well-correlated with each other (R > 0.8). For both Mesh trials and the Empty trials, UV imaging consistently detected more urine marks than thermal imaging. The Marked trials revealed the opposite pattern, with thermal imagining detecting more urine marks than UV imaging. This is likely due to the challenge of detection marks placed on top of the aliquoted urine placed in the arena at the beginning of each Marked trial. Three trials were excluded from this dataset due to poor urine blot quality, and one trial was excluded as an outlier.

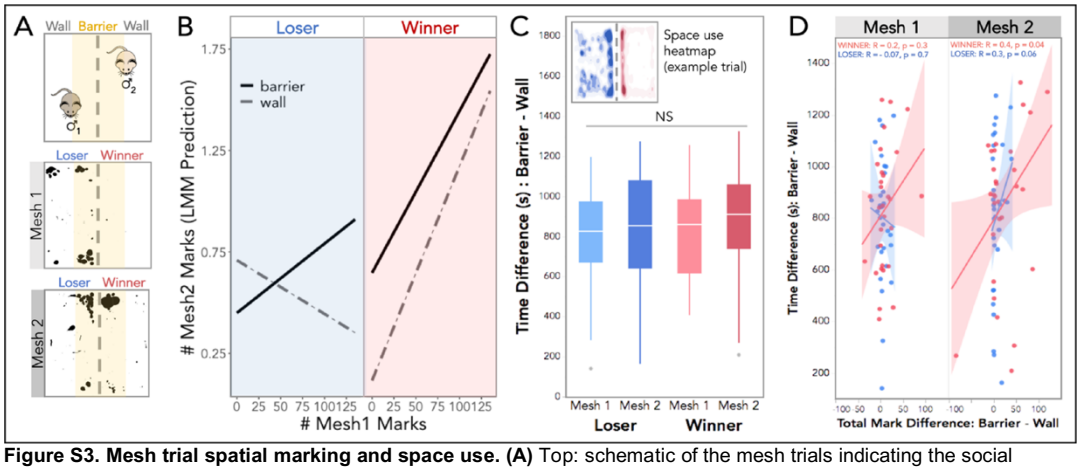

Figure S3. Mesh trial spatial marking and space use. (A) Top: schematic of the mesh trials indicating the social "Barrier" (yellow) and non-social "Wall" regions of interest (ROIs). Below: Example mesh trial urine blots of a male pair (winner and loser) pre- and post-fight demonstrating the spatial allocation of urine marks at the social boundary. **(B)** Estimated marginal means plot for the total number of marks in the post-fight mesh trial (Mesh 2) given the fight outcome (winner: red, loser: blue), initial signal investment (# Mesh 1 marks), and the ROI (Barrier: solid, Wall: dashed). **(C)** Difference in time (s) spent in the Barrier vs. Wall regions of interest (ROIs) across mesh trials by winning and losing males. Winners and losers spend more time at the social boundary (Barrier) across mesh trials. Top left corner: an example heat map of a male pair in a mesh trial (Mesh 1), depicting how all males spend more time at the social boundary (Barrier) than the non-social ROI (Wall) across mesh trials, regardless of fight outcome. **(D)** Comparison of the difference in time spent vs. the difference in total marks allocated in the ROIs (Barrier – Wall) by winners and loser across trials. In both mesh trials, space use and changes in urine allocation effort are not detectably correlated with each other among winning or losing males ($R < 0.2$). **(B-D)** Linear mixed models were used to model relationships, analyses of variance were used to test for overall effects (see Data Availability for code) and post hoc pairwise comparisons were performed using the *emmeans* package (significance code: NS $p>0.05$).

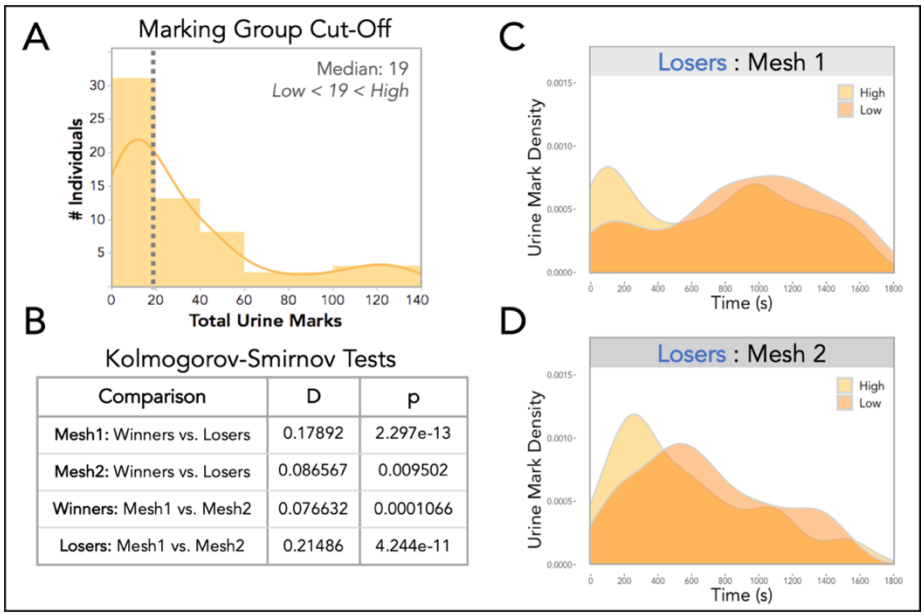

Comparison	D	p
Mesh1: Winners vs. Losers	0.17892	2.297e-13
Mesh2: Winners vs. Losers	0.086567	0.009502
Winners: Mesh1 vs. Mesh2	0.076632	0.0001066
Losers: Mesh1 vs. Mesh2	0.21486	4.244e-11

Figure S4. Comparisons of temporal distributions of urine mark deposition. (A) Males were separated into two groups (high and low-marking) based on whether the number of marks deposited pre-fight (Mesh 1) fell about or below the median number of marks (19: dashed line). Histogram of the distribution of total urine marks deposited by all males competitors in the Mesh 1 (pre-fight). This categorization was used to examine differences in mark distribution across low and high-marking losers (C-D). **(B)** Kolmogorov-Smirnov two-sample statistical tests comparing the distributions of scent marking across the trial duration depicted in **Figure 2D**. **(C-D)** Density plots depicting urine deposition events over the two 30-minute mesh trials (Mesh 1: top, Mesh 2: bottom) for losing males that were either initially high-marking (yellow) or low-marking (orange). During the first mesh trial high marking losers are contributing most to the early peak ~150s, while low-marking losers don't peak in marking activity until ~1000s. This dramatic difference diminishes by the second mesh trial.

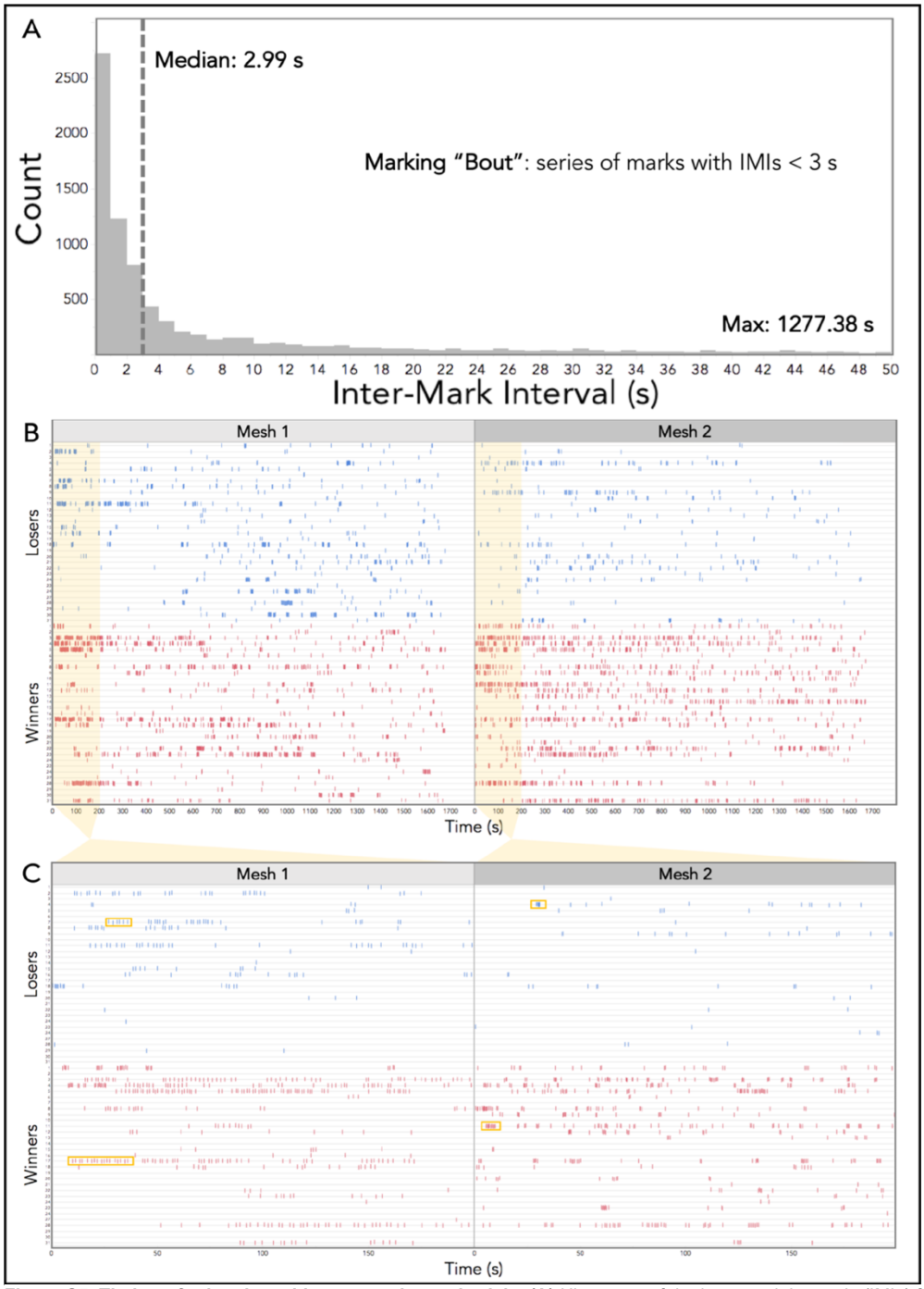

Figure S5. Timing of urine deposition events in mesh trials. (A) Histogram of the inter-mark intervals (IMIs) for all males across all trials. The median value is indicated with a dashed line (2.99 seconds). The range of IMIs extends to nearly the full trial length (only the first 50s is shown), The maximum values are reported in the bottom right corner. The median IMI value was used to define a marking "bout." Such that any two marks that occur in sequence with an IMI < 3 seconds are grouped together into a multi-mark bout. **(B)** Event plots depicting the urine marking of all male competitors over the course of both mesh trials (Mesh 1=left, Mesh 2 = right) for the entire trial duration (1800 seconds). Pair IDs are indicated on the left-hand axis. Losers depicted on top in blue, and winners on the bottom in red. **(C)** Event plots depicted for a zoomed-in view of the first 200 seconds of the trials for all individuals. Example "chain"-like bouts are outlined in the Mesh 1 panel, and example "burst"-like marking bouts are highlighted in the Mesh 2 panel (yellow boxes).

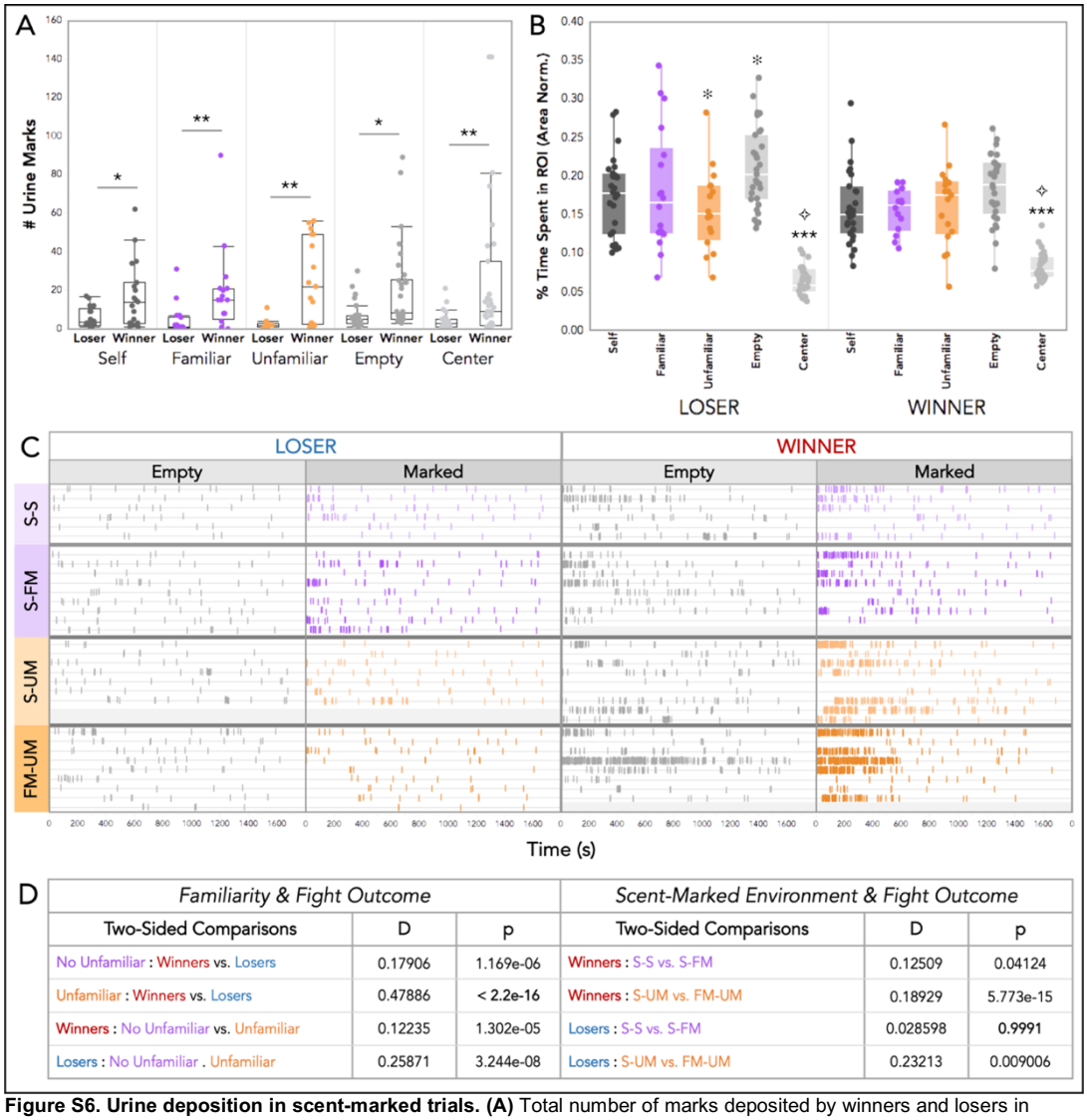

D

Familiarity & Fight Outcome			*Scent-Marked Environment & Fight Outcome*		
Two-Sided Comparisons	D	p	Two-Sided Comparisons	D	p
No Unfamiliar : Winners vs. Losers	0.17906	1.169e-06	Winners : S-S vs. S-FM	0.12509	0.04124
Unfamiliar : Winners vs. Losers	0.47886	< 2.2e-16	Winners : S-UM vs. FM-UM	0.18929	5.773e-15
Winners : No Unfamiliar vs. Unfamiliar	0.12235	1.302e-05	Losers : S-S vs. S-FM	0.028598	0.9991
Losers : No Unfamiliar . Unfamiliar	0.25871	3.244e-08	Losers : S-UM vs. FM-UM	0.23213	0.009006

Figure S6. Urine deposition in scent-marked trials. (A) Total number of marks deposited by winners and losers in scent-marked trials to specific ROIs: scent-marked corners (containing self, familiar, or unfamiliar male urine), empty corners, or the center of the arena (significance codes: * p<0.05; ** p<0.01). **(B)** The percent of time spent in specific urine-marked trial ROIs by winners and losers, normalized to the total area of each ROI (to account for the center being larger). Winners and losers spend significantly less time in the center ROI than all corner ROIs (Self, Familiar, Unfamiliar or Empty; *** p<0.001). Losers spend significantly less time in the center ROI than winners (✧ p<0.01). Losers spend significantly less time in corners with unfamiliar urine relative to empty ones (⁎ p<0.05). **(A,B)** Linear mixed models were used to model relationships, analyses of variance were used to test for overall effects, and post hoc pairwise comparisons were performed using the *emmeans* package (see Data Availability for code) **(C)** Event plots depicting the urine marking of winning and losing males to the empty trials and the urine-marked trials for the entire trial duration (1800 seconds). Males are grouped by the four different scent-marked treatments: self-self (S-S: light purple), self-familiar male (S-FM: dark purple), self-unfamiliar male (S-UM: light orange), and familiar male-unfamiliar male (FM-UM: dark orange). Almost all male pairs experienced the same treatment, three pairs received different urine-marked treatments due to urine stimuli collection constraints (hence some of the treatment groups have unequal paired number across fight outcome groupings). **(D)** Kolmogorov-Smirnov two-sample statistical tests comparing the distributions of scent marking across the trial durations depicted in **Figure 4D**. Comparisons were by trial groups (No Unfamiliar vs. Unfamiliar), as well as for specific scent-marked treatments (S-S, S-FM, S-UM & FM-UM).

REFERENCES

1. Hobson EA. Differences in social information are critical to understanding aggressive behavior in animal dominance hierarchies. Current Opinion in Psychology. 2020 Jun;33:209–15.
2. Pasch B, Tokuda IT, Riede T. Grasshopper mice employ distinct vocal production mechanisms in different social contexts. Proc R Soc B. 2017 Jul 26;284(1859):20171158.
3. Rauber R, Manser MB. Experience of the signaller explains the use of social versus personal information in the context of sentinel behaviour in meerkats. Sci Rep. 2018 Dec;8(1):11506.
4. Sullivan-Beckers L, Hebets EA. Tactical adjustment of signalling leads to increased mating success and survival. Animal Behaviour. 2014 Jul;93:111–7.
5. Desjardins C, Maruniak JA, Bronson FH. Social Rank in House Mice: Differentiation Revealed by Ultraviolet Visualization of Urinary Marking Patterns. Science. 1973 Nov 30;182(4115):939–41.
6. Drickamer LC. Urine marking and social dominance in male house mice (Mus musculus domesticus). Behavioural Processes. 2001 Mar;53(1–2):113–20.
7. Ferkin MH. Scent marks of rodents can provide information to conspecifics. Anim Cogn. 2019 May;22(3):445–52.
8. Gosling LM, Roberts SC, Thornton EA, Andrew MJ. Life history costs of olfactory status signalling in mice. Behavioral Ecology and Sociobiology. 2000 Sep 12;48(4):328–32.
9. Hurst JL. Urine marking in populations of wild house mice Mus domesticus rutty. I. Communication between males. Animal Behaviour. 1990 Aug;40(2):209–22.

10. Hurst JL, Payne CE, Nevison CM, Marie AD, Humphries RE, Robertson DHL, et al. Individual recognition in mice mediated by major urinary proteins. Nature. 2001 Dec;414(6864):631–4.
11. Kaur AW, Ackels T, Kuo TH, Cichy A, Dey S, Hays C, et al. Murine Pheromone Proteins Constitute a Context-Dependent Combinatorial Code Governing Multiple Social Behaviors. Cell. 2014 Apr;157(3):676–88.
12. Lee W, Khan A, Curley JP. Major urinary protein levels are associated with social status and context in mouse social hierarchies. Proc R Soc B. 2017 Sep 27;284(1863):20171570.
13. Nelson AC, Cunningham CB, Ruff JS, Potts WK. Protein pheromone expression levels predict and respond to the formation of social dominance networks. J Evol Biol. 2015 Jun;28(6):1213–24.
14. Nevison CM, Barnard CJ, Beynon RJ, Hurst JL. The consequences of inbreeding for recognizing competitors. Proc R Soc Lond B. 2000 Apr 7;267(1444):687–94.
15. Anderson PK, Hill JL. Mus musculus: Experimental Induction of Territory Formation. Science. 1965 Jun 25;148(3678):1753–5.
16. Crowcroft P, Rowe FP. SOCIAL ORGANIZATION AND TERRITORIAL BEHAVIOUR IN THE. Proceedings of the Zoological Society of London. 1963 May;140(3):517–31.
17. Harrington JE. Recognition of Territorial Boundaries by Olfactory Cues in Mice (Mus musculus L.). Zeitschrift für Tierpsychologie. 1976;41(3):295–306.
18. Koolhaas JM, Coppens CM, de Boer SF, Buwalda B, Meerlo P, Timmermans PJA. The Resident-intruder Paradigm: A Standardized Test for Aggression, Violence and Social Stress. JoVE. 2013 Jul 4;(77):4367.

19. Mackintosh JH. Territory formation by laboratory mice. 1970 Feb;18:177–83.
20. Poole TB, Morgan HDR. Social and territorial behaviour of laboratory mice (Mus musculus L.) in small complex areas. Animal Behaviour. 1976 May;24(2):476–80.
21. Wolff RJ. Mating behaviour and female choice: their relation to social structure in wild caught House mice (*Mus musculus*) housed in a semi-natural environment. Journal of Zoology. 1985 Sep;207(1):43–51.
22. Hurst JL, Thom MD, Nevison CM, Humphries RE, Beynon RJ. MHC odours are not required or sufficient for recognition of individual scent owners. Proc R Soc B. 2005 Apr 7;272(1564):715–24.
23. Arakawa H, Arakawa K, Blanchard DC, Blanchard RJ. A new test paradigm for social recognition evidenced by urinary scent marking behavior in C57BL/6J mice. Behavioural Brain Research. 2008 Jun;190(1):97–104.
24. Arakawa H, Blanchard DC, Arakawa K, Dunlap C, Blanchard RJ. Scent marking behavior as an odorant communication in mice. Neuroscience & Biobehavioral Reviews. 2008 Sep;32(7):1236–48.
25. Jones RB, Nowell NW. Aversive and aggression-promoting properties of urine from dominant and subordinate male mice. Animal Learning & Behavior. 1973 Sep;1(3):207–10.
26. Booksmythe I, Jennions MD, Backwell PRY. Investigating the ‘dear enemy’ phenomenon in the territory defence of the fiddler crab, Uca mjoebergi. Animal Behaviour. 2010 Feb;79(2):419–23.
27. Briefer E, Rybak F, Aubin T. When to be a dear enemy: flexible acoustic relationships of neighbouring skylarks, Alauda arvensis. Animal Behaviour. 2008 Oct;76(4):1319–25.

28. Christensen C, Radford AN. Dear enemies or nasty neighbors? Causes and consequences of variation in the responses of group-living species to territorial intrusions. Behavioral Ecology. 2018 Sep 10;29(5):1004–13.
29. Tumulty JP, Bee MA. Ecological and social drivers of neighbor recognition and the dear enemy effect in a poison frog. Ridley A, editor. Behavioral Ecology. 2021 Mar 2;32(1):138–50.
30. Zorzal G, Camarota F, Dias M, Vidal DM, Lima E, Fregonezi A, et al. The dear enemy effect drives conspecific aggressiveness in an Azteca-Cecropia system. Sci Rep. 2021 Dec;11(1):6158.
31. Tumulty JP. Dear Enemy Effect. In: Vonk J, Shackelford T, editors. Encyclopedia of Animal Cognition and Behavior [Internet]. Cham: Springer International Publishing; 2018 [cited 2022 Jan 10]. p. 1–4. Available from: http://link.springer.com/10.1007/978-3-319-47829-6_693-1
32. Hou XH, Hyun M, Taranda J, Huang KW, Todd E, Feng D, et al. Central Control Circuit for Context-Dependent Micturition. Cell. 2016 Sep;167(1):73-86.e12.
33. Keller JA, Chen J, Simpson S, Wang EHJ, Lilascharoen V, George O, et al. Voluntary urination control by brainstem neurons that relax the urethral sphincter. Nat Neurosci. 2018 Sep;21(9):1229–38.
34. Verstegen AMJ, Klymko N, Zhu L, Mathai JC, Kobayashi R, Venner A, et al. Non-Crh Glutamatergic Neurons in Barrington's Nucleus Control Micturition via Glutamatergic Afferents from the Midbrain and Hypothalamus. Current Biology. 2019 Sep;29(17):2775-2789.e7.

35. Verstegen AM, Tish MM, Szczepanik LP, Zeidel ML, Geerling JC. Micturition video thermography in awake, behaving mice. Journal of Neuroscience Methods. 2020 Feb;331:108449.
36. Arnott G, Elwood RW. Assessment of fighting ability in animal contests. Animal Behaviour. 2009 May;77(5):991–1004.
37. Enquist M, Leimar O. Evolution of fighting behaviour: Decision rules and assessment of relative strength. Journal of Theoretical Biology. 1983 Jun;102(3):387–410.
38. Humphries EL, Hebblethwaite AJ, Batchelor TP, Hardy ICW. The importance of valuing resources: host weight and contender age as determinants of parasitoid wasp contest outcomes. Animal Behaviour. 2006 Oct;72(4):891–8.
39. Kodric-Brown A, Brown JH. Truth in Advertising: The Kinds of Traits Favored by Sexual Selection. The American Naturalist. 1984 Sep;124(3):309–23.
40. Ligon RA, McGraw KJ. Social costs enforce honesty of a dynamic signal of motivation. Proc R Soc B. 2016 Oct 26;283(1841):20161873.
41. Tibbetts EA, Izzo A. Social Punishment of Dishonest Signalers Caused by Mismatch between Signal and Behavior. Current Biology. 2010 Sep;20(18):1637–40.
42. Hurst JL, Beynon RJ. Scent wars: the chemobiology of competitive signalling in mice. Bioessays. 2004 Dec;26(12):1288–98.
43. Rychlik L, Zwolak R. Behavioural mechanisms of conflict avoidance among shrews. Acta Theriol. 2005 Sep;50(3):289–308.
44. Bittner NKJ, Mack KL, Nachman MW. Gene expression plasticity and desert adaptation in house mice*. Evolution. 2021 Jun;75(6):1477–91.

45. Fertig DS, Edmonds VW. The Physiology of the House Mouse. Sci Am. 1969 Oct;221(4):103–10.
46. Moro D, Bradshaw SD. Water and sodium balances and metabolic physiology of house mice (Mus domesticus) and short-tailed mice (Leggadina lakedownensis) under laboratory conditions. Journal of Comparative Physiology B: Biochemical, Systemic, and Environmental Physiology. 1999 Dec 9;169(8):538–48.
47. Bhandiwad AA, Whitchurch EA, Colleye O, Zeddies DG, Sisneros JA. Seasonal plasticity of auditory saccular sensitivity in “sneaker” type II male plainfin midshipman fish, Porichthys notatus. J Comp Physiol A. 2017 Mar;203(3):211–22.
48. Sinervo B, Lively CM. The rock–paper–scissors game and the evolution of alternative male strategies. Nature. 1996 Mar;380(6571):240–3.
49. Zamudio KR, Sinervo B. Polygyny, mate-guarding, and posthumous fertilization as alternative male mating strategies. Proceedings of the National Academy of Sciences. 2000 Dec 19;97(26):14427–32.
50. Phifer-Rixey M, Bi K, Ferris KG, Sheehan MJ, Lin D, Mack KL, et al. The genomic basis of environmental adaptation in house mice. Payseur BA, editor. PLoS Genet. 2018 Sep 24;14(9):e1007672.
51. Chalfin L, Dayan M, Levy DR, Austad SN, Miller RA, Iraqi FA, et al. Mapping ecologically relevant social behaviours by gene knockout in wild mice. Nat Commun. 2014 Dec;5(1):4569.
52. Tuttle AH, Philip VM, Chesler EJ, Mogil JS. Comparing phenotypic variation between inbred and outbred mice. Nat Methods. 2018 Dec;15(12):994–6.

53. Cheetham SA, Smith AL, Armstrong SD, Beynon RJ, Hurst JL. Limited variation in the major urinary proteins of laboratory mice. Physiology & Behavior. 2009 Feb;96(2):253–61.
54. Cheetham SA, Thom MD, Jury F, Ollier WER, Beynon RJ, Hurst JL. The Genetic Basis of Individual-Recognition Signals in the Mouse. Current Biology. 2007 Oct;17(20):1771–7.
55. Sheehan MJ, Lee V, Corbett-Detig R, Bi K, Beynon RJ, Hurst JL, et al. Selection on Coding and Regulatory Variation Maintains Individuality in Major Urinary Protein Scent Marks in Wild Mice. Barsh GS, editor. PLoS Genet. 2016 Mar 3;12(3):e1005891.
56. Stowers L, Liberles SD. State-dependent responses to sex pheromones in mouse. Current Opinion in Neurobiology. 2016 Jun;38:74–9.
57. Peirson SN, Brown LA, Pothecary CA, Benson LA, Fisk AS. Light and the laboratory mouse. Journal of Neuroscience Methods. 2018 Apr;300:26–36.
58. Kurien BT, Scofield RH. Mouse urine collection using clear plastic wrap. Lab Anim. 1999 Jan 1;33(1):83–6.
59. Friard O, Gamba M. BORIS : a free, versatile open-source event-logging software for video/audio coding and live observations. Fitzjohn R, editor. Methods Ecol Evol. 2016 Nov;7(11):1325–30.
60. Yamanaka O, Takeuchi R. UMATracker: an intuitive image-based tracking platform. Journal of Experimental Biology. 2018 Jan 1;jeb.182469.
61. McLean DJ, Skowron Volponi MA. trajr: An R package for characterisation of animal trajectories. Tregenza T, editor. Ethology. 2018 Jun;124(6):440–8.
62. Bates D. Parsimonious Mixed Models. ArXiv. 2018 May 26;arXiv:1506.04967:21.

63. Kuznetsova A, Brockhoff PB, Christensen RHB. lmerTest Package: Tests in Linear Mixed Effects Models. J Stat Soft [Internet]. 2017 [cited 2022 Jan 10];82(13). Available from: http://www.jstatsoft.org/v82/i13/

64. Lenth RV. Least-Squares Means: The *R* Package **lsmeans**. J Stat Soft [Internet]. 2016 [cited 2022 Jan 10];69(1). Available from: http://www.jstatsoft.org/v69/i01/

CHAPTER 3

Scent mark signal investment predicts fight dynamics in house mice

Caitlin H. Miller*, Klaudio Haxhillari, Matthew F. Hillock, Tess M. Reichard, Michael J. Sheehan*

Department of Neurobiology and Behavior, Cornell University, Ithaca, NY, USA

*Authors for Correspondence: Caitlin H. Miller: chm79@cornell.edu;
Michael J. Sheehan: msheehan@cornell.edu

Abstract

Signals mediate competitive interactions by allowing rival assessment, yet are often energetically expensive to produce. Individuals face tradeoffs when deciding when and where to signal, such that over or under-investing in signaling effort can be costly. One of the key mechanisms maintaining signal reliability is via social costs. While the social costs of over-signaling are well-known, the social costs of under-signaling are underexplored, particularly for dynamic signals. In this study we investigate a dynamic and olfactory-mediated signaling system that is ubiquitous among mammals: scent marking. Male house mice territorially scent mark their environment with metabolically costly urine marks. While competitive male mice are thought to deposit abundant scent marks in the environment, we recently identified a cohort of low-marking males that win fights. Whereas there are clear energetic costs to investing in urine signals in mice, we hypothesized that there may be social costs imposed on individuals who under-invest in signaling. Here we find that scent mark investment predicts fight dynamics. Despite fight outcome being unambiguous, aggressive intensity varies considerably across trials. Males that produce fewer scent marks engage in more intense fights that take longer to resolve. This effect appears to be driven by an unwillingness among losers to acquiesce to weakly signaling winners. We therefore find evidence for rival assessment of scent marks as well as social costs to under-signaling, which supports existing hypotheses for the importance of social punishment in maintaining optimal signaling equilibria. Our results further highlight the possibility of diverse signaling strategies in house mice.

Keywords: signal investment, social costs, scent marking, strategy, house mice

Introduction

Signals of competitive ability play an important role in mediating rival assessment in aggressive contests [1–9]. However, signal production is often energetically expensive, and individuals face tradeoffs when investing in signaling effort relative to other life history traits [10–12]. For example, increased signal investment can result in reduced gamete production [13–15], immune deficits [16,17], and higher risks of parasitism or predation [18–22].

In addition to production tradeoffs, there are social costs to signaling either too much or too little. Individuals that “over-signal” their competitive ability receive heightened aggression from competitors [23–28]. Whereas individuals that “under-signal” struggle to establish dominance relationships [26,28]. Such mismatches in signaled versus actual competitive ability muddle accurate rival assessment, resulting in escalated contests [26,28]. Receiver-dependent social punishment has been hypothesized as an important mechanism in maintaining optimal signaling equilibria [23]. While the social costs of over-signaling (i.e. ‘bluffing’ or ‘cheating’) have been well-examined, the social costs of under-signaling are under-studied, particularly for dynamic signals.

Here, we explore a dynamic and olfactory-mediated signaling system that is central to mammalian communication: scent marking [29–31]. Scent marks persist in the environment for long periods of time [32–35] and provide a record of social relationships that can be assessed by receivers [33,35–37]. Scent marks have further been proposed as ‘cheat-proof’ signals of status due to the inherent metabolic and physical challenges of maintaining a scent-marked territory [35,36].

In house mice (*Mus musculus domesticus*), urine marking is arguably the most prominent signaling modality. The generally accepted canon is that competitive males

are aggressive, territorial, and mark highly [38–41]. In addition to the costs of actively re-marking and patrolling a territory, urine marks themselves are metabolically costly in house mice [36,42–44]. Urine marking has previously been shown to have important life history costs in house mice, as males that invest in marking earlier in life experience reduced body growth [42]. It is, therefore, generally assumed that urine marking is an honest indicator of a male's status and competitive ability [38–41,45–47]. Yet, we have recently tested this assumption and found it to be incomplete—urine marking prior to a contest did not predict wins or losses among size-matched rivals, in part due to the presence of low-marking competitive males [48].

This surprising result led us to ask whether and how male house mice use scent mark information in competitor assessments. The objectives of this study were to: (1) test the hypothesis that scent mark signaling prior to a fight shapes contest dynamics, and (2) examine the potential social costs of under-signaling. We predicted that high quality individuals that accurately signaled their competitive ability would beneficially engage in less intense aggressive behaviors, and more quickly resolve their fights. In contrast, individuals that under-signaled their competitive ability would face the social costs of escalated aggressive encounters, and experience delayed contest resolution.

Material & Methods

(a) Study system

To explore scent marking and aggressive behaviors we used male house mice (n=62), as males will competitively urine mark and exhibit territorial aggression [33,39–41,46,49–51]. Experimental individuals were from two wild-derived inbred strains (NY2 and NY3) of house mice [52]. The progenitors of these strains were captured near Saratoga Springs, NY in 2013 by MJS and are related to the

SarA/NachJ, SarB/NachJ and SarC/NachJ strains now available from the Jackson Lab. We used two wild-derived strains because competitive behaviors are less pronounced in highly inbred and domesticated laboratory strains [53,54], and individuals within inbred strains tend to share identical urinary protein profiles [55]. At the time of experimentation all males were adult (3-5 months old) and sexually experienced. Mice were housed in an Animal Care facility at Cornell University with a 14:10 shifted light:dark cycle (dark cycle: 12PM–10PM), with food and water provided *ad libitum.* To reduce handling stress confounds, mice were transferred between their home cage and the experimental arena using transfer cups [56].

(b) Scent mark signaling and aggressive contests

In our previous work examining signal allocation decisions, we were surprised to find that scent marking behavior did not clearly predict wins or losses during fights, and instead identified a cohort of low-signaling competitive males [48]. Together, these results led us to investigate the aggressive contests within this dataset in greater detail to better understand the relationship between signaling and competitive ability [48].

We placed males in an arena separated by a mesh barrier where they could see, hear, and smell each other but were limited to minimal physical contact (**Figure 1A**). This allowed us to measure male urine marking prior to a contest. After 30 minutes, we removed the mesh barrier and males engaged in a fight trial for an additional 30 minutes (**Figure 1A**). Trials were performed on filter paper to prevent smearing of urine marks, for easier detection of urine deposition events. One day prior to experimentation, we recorded male body weights to size-match individuals. As house mice are nocturnal, we conducted all experiments during the dark cycle between 12

PM-5 PM. Age and weight-matched adult breeding males of distinct wild-derived strains (NY2 and NY3) were paired as competitors, resulting in a total of 31 pairs (n=62). We therefore ensured that no two paired competitors were genotypically identical and that their scent marks were perceptibly different (i.e. characterized by unique major urinary protein profiles) [44,46,55,57,58]. We ear-clipped and bleached a patch of rump fur of one male in each pair a week prior to experimentation for easy identification of males within a pair (NY2 and NY3 strains are visibly indistinguishable).

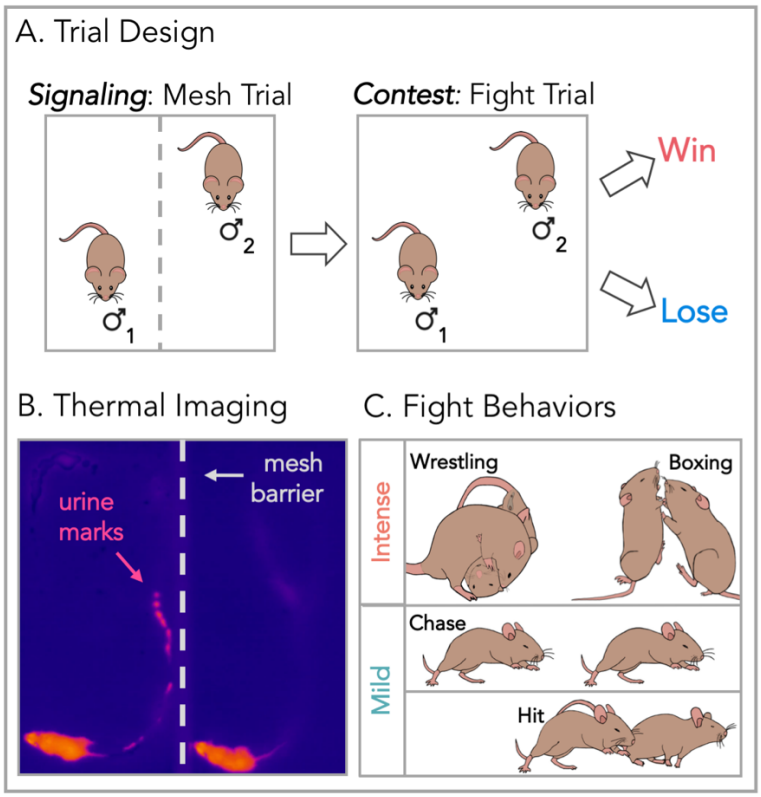

Figure 1. Trial design and recording methods. (A) Two-part trial design starting with a 30-minute signaling trial where paired competitors were separated by a mesh barrier, and urine marking was measured. The mesh barrier was removed and males entered into the contest phase of the trial (fight trial) for an additional 30 minutes. **(B)** Urine depositions were recorded using thermal imaging. Urine exits the body hot and then cools below substrate temperatures, providing a distinct thermal signature. **(C)** For each fight trial, four aggressive behaviors were scored: wrestling, boxing, chases, and hits. Wrestling and boxing were classified as intense attacks; chases and hits were classified as mild attacks.

All trials were recorded with a thermal imaging camera system (PI 640; Optris Infrared Sensing; 33° x 25° lens; ~3 Hz; thermal detection: 61°F - 107°F) and a security camera system (iDVR-PRO CMS; 1080p; 30 fps). Thermal imaging allowed for the detection of urine mark deposition events with fine spatiotemporal detail. Urine leaves the body hot (close to body temperature) and quickly cools to below the ambient substrate temperature, providing a distinctive thermal signature

(**Figure 1B**). The security camera system was used to visualize high-speed aggressive encounters. Both systems were used to cross-check for recording errors.

Videos were scored blindly using Behavioral Observation Research Interactive Software (BORIS) [59]. Urine depositions were scored as a clear hot spot in the focal mouse's trajectory that subsequently cooled below substrate temperature (**Figure 1B**). Based on the total aggressive behaviors performed by each male, males were unambiguously classified as winners or losers (**Figures 2A & S2**). Males were further categorized as low-marking or high-marking based on whether the total urine marks deposited in the "mesh trial" (pre-fight) fell below or above the median **(Figures 1A & S1A**). These classifications were used to interrogate interactions between signal investment and fight dynamics. The following behaviors were scored in "fight trials": chasing, hitting, boxing, and wrestling bouts [60–62] based on which male initiated these behaviors (**Figure 1C & S2A**). Aggressive behaviors were further categorized as mild or intense based on the risk of injury (i.e. belly exposure and likelihood of bites occurring) and the extent of physical contact. Chases and hits were classified as mild attacks, while boxing and wrestling bouts were classified as intense attacks (**Figure 1C**). Importantly, intense attacks are interactive behaviors, which require that the male receiving the attack actively defends themselves rather than fleeing from the interaction. No mice experienced sustained injury in these trials.

(c) Statistical analyses

We conducted all statistical analyses in R 3.6.0 (R Development Core Team 2019). We used linear mixed models and paired statistical tests to examine relationships between dependent and response variables (**Tables S1-S4**). Models were fitted using the package *lme4* [63]. The *lmerTest* package was used to calculate degrees of

freedom (Satterthwaite's method) and p-values [64]. Dependent variables were logarithmically transformed for a subset of models to meet assumptions for model residuals (**Tables S1-S4**). We used a type 3 analysis of variance to test for overall effects of fixed factors or interactions in the models. Post hoc comparisons were conducted using the *emmeans* package [65]. R script and data sheets used for all statistical analyses are provided (see Data Availability).

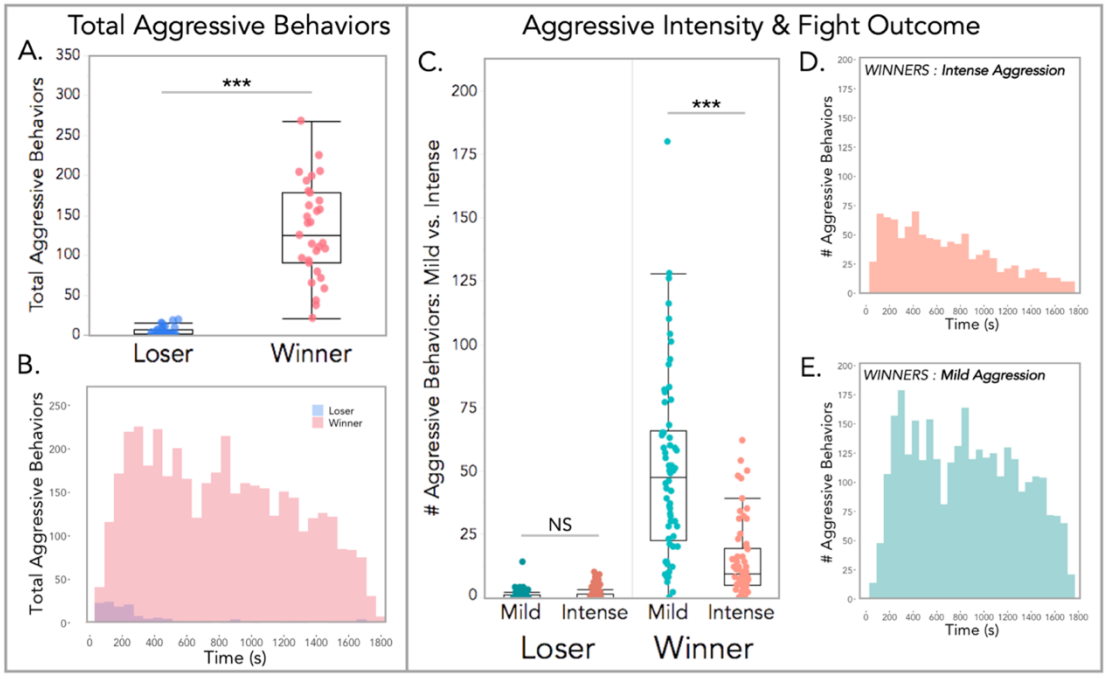

Figure 2. Winners displayed more aggressive behaviors throughout the fight trial, while losers rarely displayed any aggression after the first five minutes. (A) Total aggressive behaviors performed by males that either won or lost the fight. **(B)** Histogram of the temporal distribution of aggressive behaviors performed by winners and losers over the fight trial duration. **(C)** Total mild vs. intense aggression displayed by winners and losers. **(D,E)** Histograms of intense vs. mild aggression exhibited by winning males over the course of the fight trial. **(A,C)** Linear mixed models were used to model relationships (**Table S1)**. Analyses of variance were used to test for overall effects. Dependent variables (# aggressive behaviors) were logarithmically transformed to meet assumptions for model residuals. Significance codes: NS p>0.05, * p<0.05; ** p<0.01, *** p<0.001.

Results

(a) Contest outcomes and aggressive intensity

Fight outcome was unambiguous in all contest pairings (**Figure S2**). Winners performed significantly more aggressive behaviors than losers (M1: $F_{1,60}$= 287, p <

0.0001; **Figure 2A & Table S1**). This was true for both cumulative aggression (**Figure 2A**), as well as for specific fight behaviors (**Figure S2B**). Across all fight trials, winners performed 21-268 total attacks, while losers performed 0-19 (**Figure S2C**). Within pairs, the difference in attack count ranged from 21-266, with an average attack difference of 126+/-11 between competitors. These winner-loser relationships were typically apparent within the first 5 minutes, as losing males quickly halt aggression (**Figure 2B**). Winners on the other hand, rapidly escalated aggression with peak activity occurring at ~300 seconds, followed by a gradual decline (**Figure 2B**). Males thus performed fast competitor assessments once they physically engaged. While males were weight-matched as closely as possible, some variation in body weight was inevitable (**Figure S3A**). Body weight moderately predicted the total aggressive behaviors performed by individuals (M2: $F_{1,59}$ = 4.5, p = 0.04**; Table S1)**, however including body weight resulted in a worse model overall (M1 vs. M2: **Table S1**). Body weight also did not differ between winning and losing males across trials ($t_{1,60}$ = 0.4, p = 0.69; **Figure S3B**).

We further explored the intensity of aggressive behaviors initiated by competitors during contests and found that aggressive intensity has a significant interaction with fight outcome (M3: $F_{1,184}$ = 64, p < 0.0001; **Figure 2C & Table S1**). Losers exhibit similarly few mild and intense aggressive behaviors (M3: $t_{1,184}$ = 1.5, p = 0.39; **Figure 2C & Table S1**). In contrast, winners perform significantly more mild attacks than intense ones (M3: $t_{1,184}$ = -9.8, p < 0.0001; **Figure 2C & Table S1**). Given the low rates of aggressive attacks performed by the eventual contest losers, we focused on the dynamics of aggressive behaviors initiated by the ultimate contest winners. Among winners, the temporal dynamics reveal the number of intense attacks steadily declines over the course of the fight (**Figure 2D**). Whereas mild attacks remain

elevated for longer and decline in frequency more slowly (**Figure 2E**). These data indicate that while fight outcome is straightforward, attack frequency varies with intensity. Furthermore, there appear to be distinct temporal patterns for mild and intense fight behaviors.

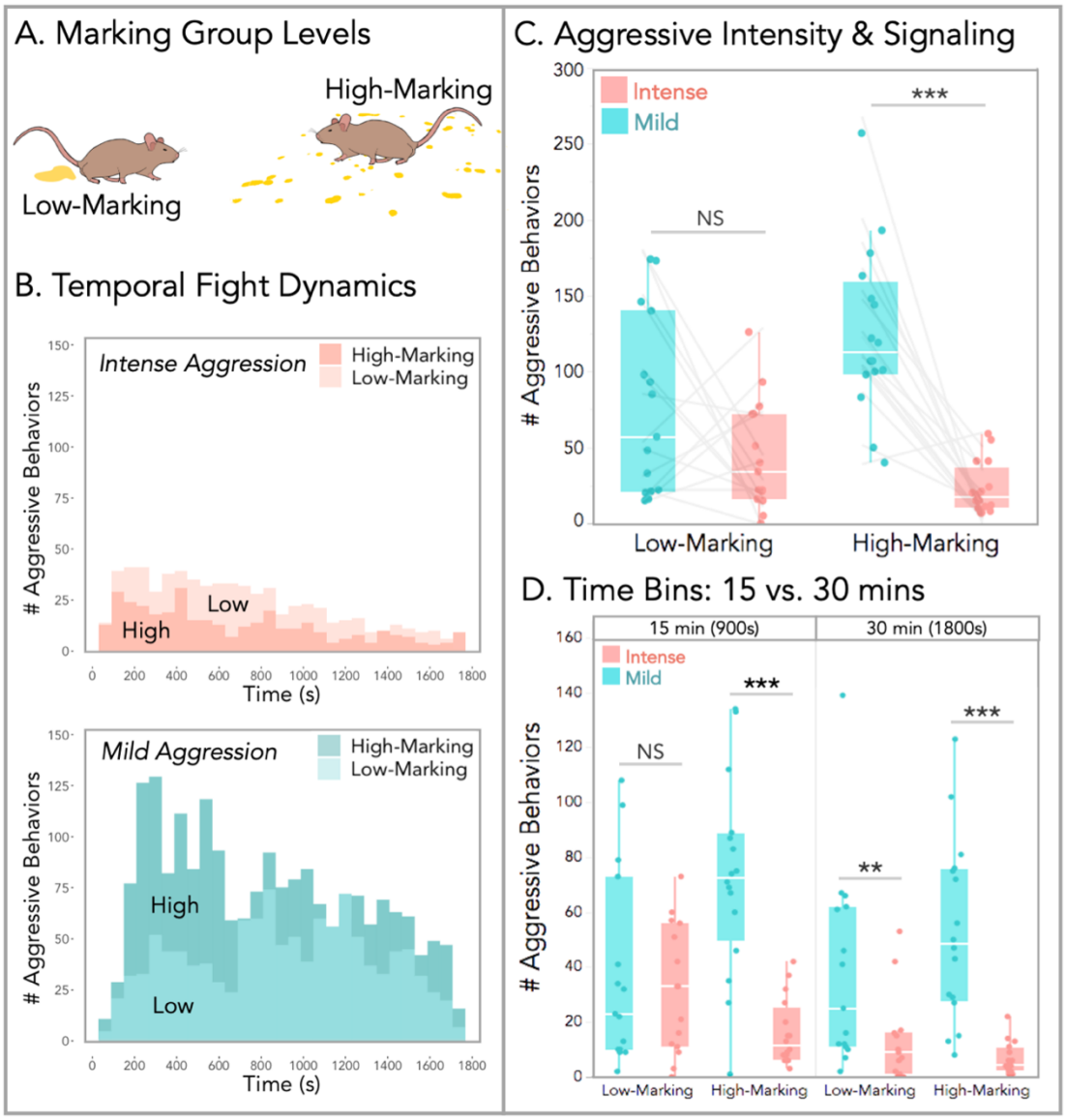

Figure 3. Temporal fight dynamics and intensity vary with initial signaling effort of winning males. (A) Males were categorized as low or high-marking individuals based on whether the total number of marks deposited prior to the fight trial fell either below or above the median (**Figure S1A**). **(B)** Histograms of the temporal distributions for intense (top) and mild (bottom) aggressive behaviors for the two marking groups (high vs. low-marking). **(C)** Boxplot of total aggressive behaviors by marking group and fight intensity. **(D)** Boxplot of total aggressive behaviors by marking group, attack intensity, and fight trial 15-minute time bins. **(C,D)** LMMs were used to model relationships, and analyses of variance were used to test for overall effects. Dependent variables were logarithmically transformed to meet assumptions for model residuals. Significance codes: NS $p>0.05$, * $p<0.05$; ** $p<0.01$, *** $p<0.001$.

(b) Scent mark signaling prior to a contest predicts fight dynamics

We next explored the relationship between scent mark signaling and fight dynamics among winning males, as these individuals initiated the vast majority of aggressive behaviors (**Figure 2**). Males were categorized as either low or high-marking individuals, based on whether their total number of urine deposition events fell below or above the median number of marks (**Figures 3A & S1A**). This categorization is supported by our prior work, which shows that initial mark investment predicts marking levels days later (**Figure S1**; 48). In other words, males that are low or high-marking adhere to their respective marking groups days after an aggressive contest [48].

The total number of attacks initiated by winners did not significantly differ between low and high-marking males (M4: $F_{1,29} = 3.3$, $p = 0.08$; **Table S2**). However, striking patterns emerged when we inspected the intensity of aggressive behaviors. We first examined the temporal distribution of mild and intense attacks for low and high-marking winners (**Figure 3B**). Low-marking winners performed more intense attacks across the fight duration (**Figure 3B**). While an inverse relationship is observed for mild aggression. High-marking winners performed dramatically more mild attacks than low-marking winners, particularly in the first 15 minutes of the fight trial (**Figure 3B**).

We further modeled the effects of fight intensity and signaling effort on contest aggression (**Figure 3C & Table S2**). The signaling effort of winners significantly predicted aggressive intensity (M5: $F_{1,58} = 32$, $p < 0.0001$; **Table S2**). Interestingly, initial marking effort did not predict aggressive behaviors in other dyadic comparisons. Initial signaling efforts of the eventual losing males did not predict loser aggression (M8: $F_{1,58} = 0.59$, $p = 0.44$; **Figure S4A & Table S4**) or winner aggression (M9: $F_{1,58} =$

1.2, p = 0.27; **Figure S4A & Table S4**). Similarly, the marking effort of winners did not predict loser aggression (M10: $F_{1,58}$ = 1.1, p = 0.29; **Figure S4B & Table S4**). Moreover, body weight did not differ across low or high-marking winners and losers (**Figure S3C**).

(c) Social costs of under-signaling

We next examined the social costs of under-signaling, and found a significant interaction between fight intensity and initial marking effort (M5: $F_{1,58}$ = 6.8, p = 0.01; **Figure 3C & Table S2**). Winning males that invest more in scent marking perform fewer intense attacks and more mild attacks (**Figure 3C**). Whereas, males that invest less in marking engage in more intense aggression (**Figure 3C**). Comparing rates of each type of aggression per winner revealed that low-marking winners do not differ in their levels of attack intensities (M5: $t_{1,29}$ = -2.1, p = 0.14; **Figure 3C & Table S2**). The opposite is true for high-marking winners, which perform significantly more mild relative to intense attacks (M5: $t_{1,29}$ = -5.9, p < 0.0001; **Figure 3C & Table S2**).

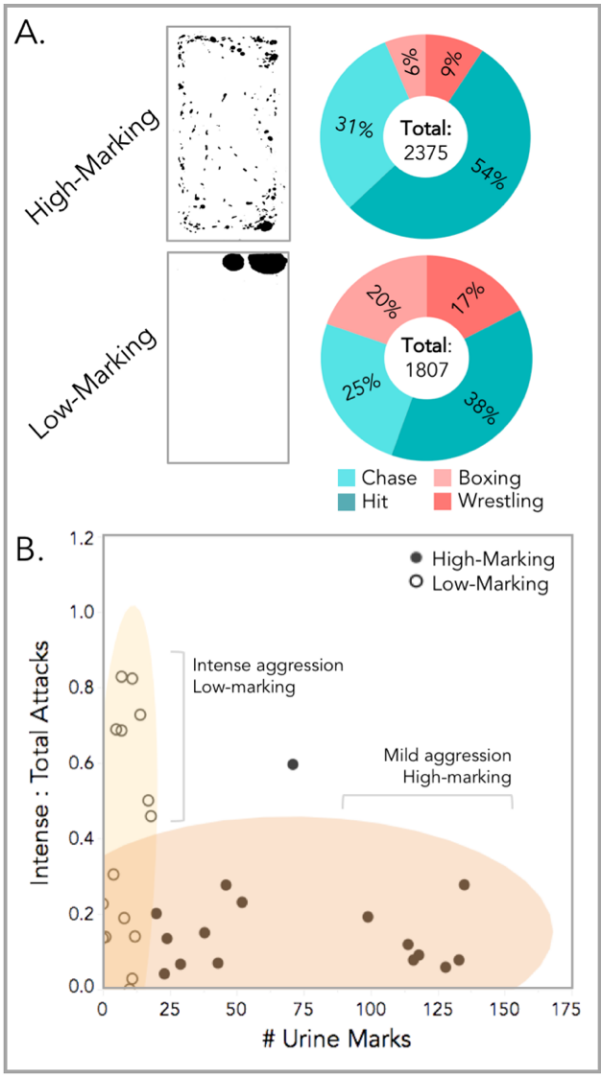

Figure 4. Proportions of mild and intense aggression. (A) Example processed urine blots of high and low-marking males (urine spots shown in black). Donut plots depict proportions of individual fight behaviors for the two marking groups **(B)** The proportion of intense : total attacks by the total number of urine marks deposited prior to the fight. Low and high-marking winners are labeled. Ellipses indicate 90% data coverage.

Given that the differences in fight intensity toward signaling effort occurred specifically among winners, we further interrogated the temporal dynamics of these behaviors. To do this we split the fight trial into two 15-minute time bins, corresponding to the first and second half of the trial (**Figure 3D**). The differences in fight dynamics are particularly stark in the first 15 minutes (**Figure 3D**). Time bin has a strong effect on contest aggression (M6: $F_{1,87}$ = 11, p = 0.002; **Table S2**), with a significant two-way interaction between fight intensity and time bin (M6: $F_{1,87}$ = 5.9, p = 0.02; **Table S2**). Comparing rates of mild and intense acts of aggression per winner revealed that in the first half of the trial, low-marking winners are performing the same levels of mild and intense attacks (M6: $t_{1,87}$ = -0.45, p = 1.0; **Figure 3D & Table S2**). While high-marking winners perform dramatically more mild attacks relative to intense attacks (M6: $t_{1,87}$ = -4.4, p = 0.0003; **Figure 3D & Table S2**). This difference in fight intensity between marking groups diminishes in the second half of the trial, such that all winners display significantly higher rates of mild compared to intense aggression (**Figure 3D**). Thus, the fights of low-signaling winners exhibit more severe escalation in the first 15 minutes, suggesting males that under-signal take longer to resolve aggressive contests than males investing more in signaling effort.

Together, these data indicate that the relative proportion of intense aggressive behaviors males perform varies with signaling effort. We assessed the proportions of specific fight behaviors executed by low and high-marking individuals (**Figure 4A**). This demonstrates that low-marking winners perform considerably more intense aggression (i.e. wrestling bouts and boxing matches; **Figure 4A**). The aggressive behaviors of high-marking individuals, however, are heavily skewed towards mild aggression (i.e. chases and hits; **Figure 4A**). We further examined the proportion of intense-to-overall attacks relative to the signaling efforts of each winning male prior to

the contest (**Figure 4B**). The proportion of intense attacks is predicted by marking group (M7: $F_{1,28}$ = 8.8, p = 0.006; **Table S3**). This illustrates a striking delineation between low and high-signaling competitive males (**Figure 4B**). Furthermore, it reveals what appear to be two distinct groups of males that each comprise a quarter of all winners: (1) intensely aggressive low-marking males and (2) mildly aggressive very high-marking males (**Figure 4B**).

Discussion

Here we have shown that despite fight outcome being overwhelmingly clear (**Figure 2**), there are stark differences in contest dynamics depending on how males signaled prior to a fight. We find evidence for social costs to under-signaling in house mice, as low-marking winners experienced more intense fights and delayed contest resolution (**Figures 3 & 4**). This suggests there are likely important tradeoffs underlying signal investment decisions in terms of competitor assessment and aggression. Particularly as in our prior work, we identified a cohort of competitive yet stably low-marking male mice [48]. Our work underlies the complex decisions animals face when determining their signal investment and willingness to engage in aggressive encounters. At any given moment, individuals confront metabolic resource limitations. Deciding when and where to invest these resources has important fitness consequences.

The observed differences in aggressive intensity in male house mice could be driven by winners, losers, or a combination of the two. A winner-driven explanation is that winners allocate more effort toward aggression rather than signaling, such that the total energy invested is constant across low-marking and high-marking winners. Alternatively, losing males may be less inclined to back down during attacks initiated by weakly signaling males. Importantly, intense aggressive behaviors (i.e. wrestling

and boxing) are highly interactive, and require that losers actively defend themselves rather than flee from the encounter (i.e. chases). This lends support for the observed differences being loser-driven, and alludes to a possible key difference between losing an encounter and submitting to a competitor.

The trial design limits males' ability to escape the interaction. In naturalistic environments males would likely avoid prolonged encounters, and dominance relationships would be established through shorter repeated interactions. Nevertheless, the sustained encounters used in this study allowed us to observe temporal shifts in fight intensity. We find that low-signaling winners don't transition to more mild aggression until midway through the fight, whereas high-signaling winners start off relatively mild. Fight resolution is therefore delayed when winners signal lowly prior to a fight. Similar to what has been observed in aggressive contests between paper wasps [26] and chameleons [28], we find that male house mice experience social costs as a result of inaccurately signaling their competitive ability. This is striking because the costs of under-signaling appear quite high. "Scent-silent" males engage in more intense fights, take longer to resolve dominance relationships, and incur greater risk of injury.

Given the potential social costs, the existence of competitive low-signaling males suggests there may be fitness benefits to remaining scent-silent, at least under some socioecological conditions. Perhaps the most obvious benefit to reduced signaling is that it may save energy. Males might withhold signal investment to build up their metabolic reserves, as urine marking is energetically expensive [42,43,47,66]. In doing so, males may gain body mass and more effectively defend territories later in the season. This is plausible given that prior work has shown males who invest early in urine marking pay the cost of reduced body size [42]. The low-signaling effort

observed among competitive males could therefore reflect important features of life history in house mice, and potentially in many other species.

Males entering into the trials had no prior competitive experience. Males may strategically hold off scent mark investment until there are rival males present, suggesting population density may have large effects on signaling strategies [67–69]. This is particularly intriguing given prior hypotheses of urine marking as 'cheat-proof' [35,36]. These hypotheses emphasize the inability to deceptively over-report (i.e. bluff) one's competitive ability but do not address the possibility of males under-reporting. Our results highlight the importance of investigating under-signaling strategies, as they may be more common than previously appreciated across taxa.

Another possibility is that male mice exhibit a spectrum of signaling strategies, including the classically described "territorial males" that invest highly in marking as well as scent-silent "satellite" males. In this scenario, low-signaling individuals might avoid detection by other males yet are competitive enough to mate, though reduced marking effort likely decreases the chances of obtaining mating opportunities [33,70,71]. Previous work described males reducing their scent marking after losing [41]. Indeed, in the trials reported here, we found that high-marking males dramatically reduce their marking efforts after losing [48]. However, this scenario does not readily explain the observed patterns among winning males that continue to mark infrequently. It may be that in time they would increase investment in scent marking, and shifting to high-marking is a slower process than downregulating after a loss [43,47]. Studies of scent marking effort in more natural contexts are sorely needed.

We find evidence for direct social costs as a result of under-signaling one's competitive ability. This supports existing theoretical frameworks underlying the

importance of social punishment in shaping patterns of signal investment [23,25,26]. Our results further provide evidence that urine marking is used in competitor assessments and appears to determine losers' willingness to submit. Furthermore, our findings highlight the possibility of diverse signaling strategies in house mice. As a dynamic signaling system, individuals may flexibly adjust scent mark investment depending on the social landscape and their energetic reserves. Diverse strategies may be more commonplace for dynamic signals across taxa than is currently recognized, and warrants further investigation.

Supplementary information

Table S2. Linear mixed model (LMM) details accompanying results section 3a (Figure 2). The response variable for all three models (M1-M3) is the number of aggressive behaviors (count), and is logarithmically transformed in all cases.

	M1 : (Figure 2A) log_{10}(Aggressive Behaviors+1)~ Fight Outcome+(1|Strain)			M2 : log_{10}(Aggressive Behaviors+1)~ Fight Outcome+Weight+(1|Strain)			M3 : (Figure 2C) log_{10}(Aggressive Behaviors+1)~ Fight Outcome*Intensity+(1|malelD)		
Coefficients	Estimates	CI	p	Estimates	CI	p	Estimates	CI	p
Fixed Effects									
(Intercept)	0.49	0.36 – 0.62	<0.001	-0.47	-1.38 – 0.44	0.308	0.23	0.13 – 0.33	<0.001
Fight Outcome (Win vs. Loss)	1.58	1.39 – 1.76	<0.001	1.59	1.40 – 1.77	<0.001	0.77	0.63 – 0.91	<0.001
Weight (g)				0.04	0.00 – 0.08	0.039			
Intensity (Mild vs. Intense)							-0.09	-0.20 – 0.03	0.136
Fight Outcome : Intensity							0.67	0.50 – 0.83	<0.001
Random Effects									
σ^2	0.13			0.13			0.11		
τ_{00}	0.00_{strain}			0.00_{strain}			0.03_{malelD}		
ICC							0.20		
N	2_{strain}			2_{strain}			62_{malelD}		
Observations	62			62			248		
Marginal R^2 / Conditional R^2	0.825 / NA			0.835 / NA			0.721 / 0.777		
AIC	64.6			68.2			220		

Table S2. Linear mixed model (LMM) details accompanying results section 3b (Figure 3). The response variable for all three models (M4-M6) is the number of aggressive behaviors (count), and is logarithmically transformed in all cases.

	M4 : log_{10}(Aggressive Behaviors+1)~ Marking Group+(1|Strain)			M5 : (Figure 3C) log_{10}(Aggressive Behaviors+1)~ Marking Group*Intensity+(1|malelD)			M6 : (Figure 3D) log_{10}(Aggressive Behaviors+1)~ Fight Outcome*Intensity*Time Bin+(1|malelD)		
Coefficients	Estimates	CI	p	Estimates	CI	p	Estimates	CI	p
Fixed Effects									
(Intercept)	2.14	2.02 – 2.26	<0.001	1.28	1.10 – 1.47	<0.001	1.13	0.92 – 1.34	<0.001
Marking Group (High vs. Low)	-0.15	-0.33 – 0.02	0.081	0.17	-0.09 – 0.44	0.200	0.20	-0.10 – 0.50	0.199
Intensity (Mild vs. Intense)				0.78	0.52 – 1.04	<0.001	0.63	0.35 – 0.91	<0.001
Marking Group : Intensity				-0.49	-0.87 – -0.11	0.012	-0.56	-0.97 – -0.16	0.007
Time Bin (15 vs. 30 min)							-0.35	-0.64 – -0.07	0.015
Marking Group : Time Bin							-0.11	-0.52 – 0.29	0.584
Intensity : Time Bin							0.23	-0.17 – 0.63	0.263
Marking Group : Intensity : Time Bin							0.25	-0.33 – 0.82	0.395
Random Effects									
σ^2	0.06			0.14			0.16		
τ_{00}	0.00_{strain}			0.00_{maleOD}			0.02_{malelD}		
ICC							0.09		
N	2_{strain}			$_{31malelD}$			$_{31malelD}$		
Observations	31			62			124		
Marginal R^2 / Conditional R^2	0.099 / NA			0.398 / NA			0.374 / 0.431		
AIC	12.2			72.5			170		

Table S3. Linear mixed model (LMM) details accompanying Figure 4. The response variable is the proportion of intense : total aggressive behaviors.

	M7 : *Proportion Attacks (Intense:Total)~Marking Group+(1|Strain)*		
Coefficients	Estimates	CI	p
Fixed Effects			
(Intercept)	0.18	-0.01 – 0.37	0.058
Marking Group (High vs. Low)	0.23	0.07 – 0.39	**0.006**
Random Effects			
σ^2	0.05		
τ_{00}	0.01		
ICC	0.19		
N	2		
Observations	31		
Marginal R^2 / Conditional R^2	0.192 / 0.344		
AIC	8.6		

Table S4. Linear mixed model (LMM) details accompanying Figure S4. The response variable for all models (M8-M10) is the number of aggressive behaviors (count) performed by losers (M8,M9) or winners (M10), and is logarithmically transformed.

	M8 : (Figure S4A) loser aggression ~ loser signaling *log_{10}(Aggressive Behaviors+1)~ Marking Group*Intensity+(1|Strain)*			M9 : (Figure S4A) loser aggression ~ winner signaling *log_{10}(Aggressive Behaviors+1)~ Marking Group*Intensity+(1|malelD)*			M10 : (Figure S4B) winner aggression ~ loser signaling *log_{10}(Aggressive Behaviors+1)~ Fight Outcome*Intensity*Time Bin+(1|malelD)*		
Coefficients	Estimates	CI	p	Estimates	CI	p	Estimates	CI	p
Fixed Effects									
(Intercept)	0.37	0.17 – 0.56	**<0.001**	0.39	0.21 – 0.58	**<0.001**	2.12	2.00 – 2.24	**<0.001**
Marking Group (High vs. Low)	0.02	-0.25 – 0.29	0.895	-0.04	-0.30 – 0.23	0.792	-0.06	-0.23 – 0.10	0.454
Intensity (Mild vs. Intense)	-0.46 – 0.09	0.191	-0.06	-0.32 – 0.21	0.672	0.00	-0.17 – 0.17	1.000	-0.46 – 0.09
Marking Group : Intensity	0.11	-0.27 – 0.49	0.562	-0.14	-0.52 – 0.24	0.463	-0.00	-0.23 – 0.23	1.000
Random Effects									
σ^2	0.14			0.14			0.05		
τ_{00}	0.00_{strain}			0.00_{strain}			0.00_{strain}		
N	2_{strain}			2_{strain}			2_{strain}		
Observations	62			62			62		
Marginal R^2 / Conditional R^2	0.041 / NA			0.054 / NA			0.018 / NA		
AIC	73.8			73.0			17.1		

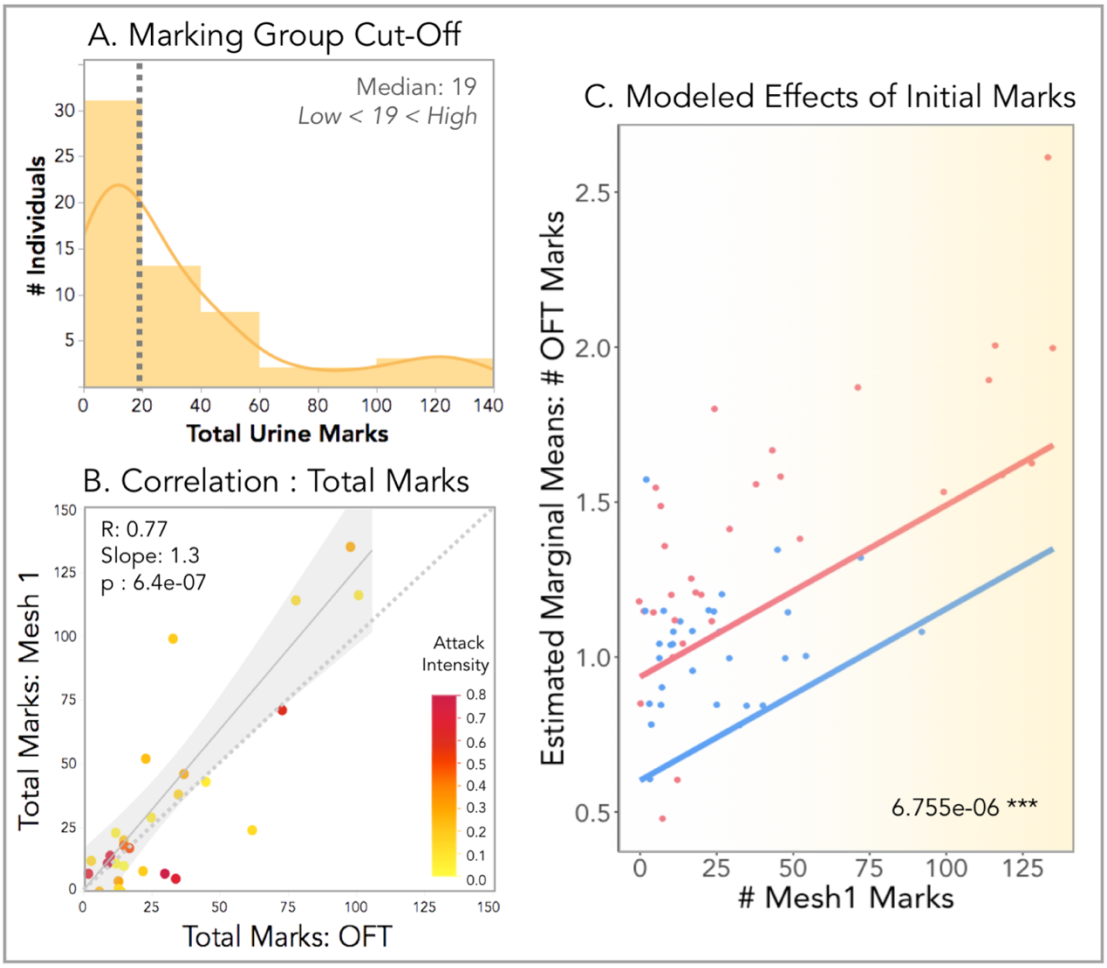

Figure S1. (A) Histogram of the distribution of total urine marks deposited by all males competitors in the Mesh Trial (pre-fight). The median (19) number of marks is indicated with dashed line. High-marking versus low-marking males were categorized based on whether the total marks deposited was either above or below the median. **(B)** Correlation plot of the total number of marks deposited by each winning male prior to the contest trial (Mesh 1) and 1 day after the contest in the open field trial (OFT) (48). The number of marks deposited pre- and post-fight are quite well correlated with each other (R=0.77). This is despite the differences in aggressive experience, arena size, and social stimulus in the environment across these two trials. Individual data points are color-scaled by the proportion of total attacks that were intense (red: high; yellow: low). The males that marked lowly in both trials (clustered in the bottom left corner) tend to perform more intense attacks (more red). One male was removed from this correlation analysis as an outlier (NY3-131), though excluding or including this male does not affect the overall pattern. **(C)** Estimated marginal means of the total number of OFT marks (log-transformed) given fight outcome (winner=red; loser=blue) and initial signal investment (# Mesh 1 marks). Initial signal investment significantly predicts marking levels of winners and losers post- fight. The model p-value of the effect of the # Mesh 1 marks on the total OFT marks indicated in the bottom righthand corner (highly significant).

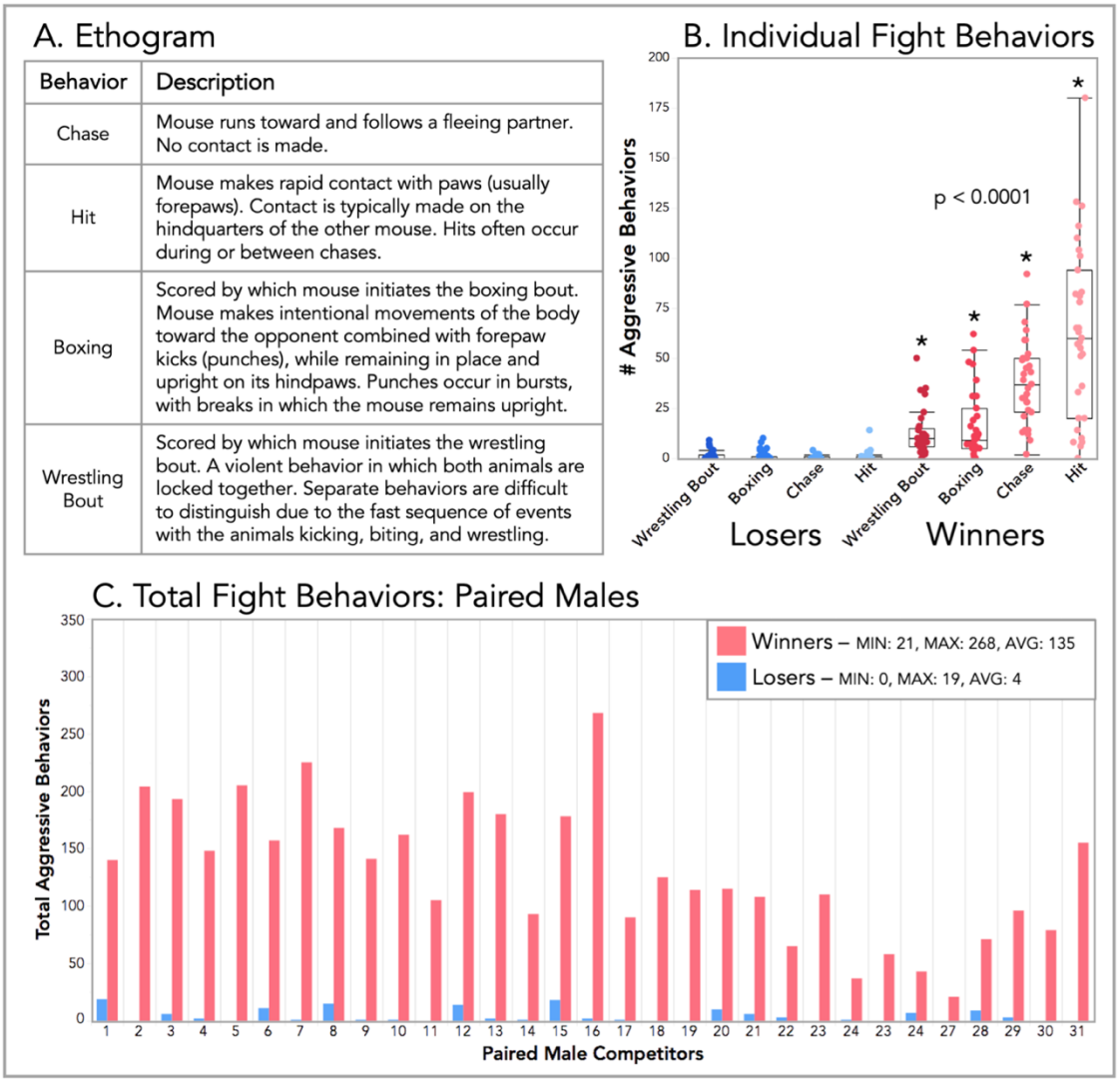

Behavior	Description
Chase	Mouse runs toward and follows a fleeing partner. No contact is made.
Hit	Mouse makes rapid contact with paws (usually forepaws). Contact is typically made on the hindquarters of the other mouse. Hits often occur during or between chases.
Boxing	Scored by which mouse initiates the boxing bout. Mouse makes intentional movements of the body toward the opponent combined with forepaw kicks (punches), while remaining in place and upright on its hindpaws. Punches occur in bursts, with breaks in which the mouse remains upright.
Wrestling Bout	Scored by which mouse initiates the wrestling bout. A violent behavior in which both animals are locked together. Separate behaviors are difficult to distinguish due to the fast sequence of events with the animals kicking, biting, and wrestling.

Figure S2. Fight trial behaviors. (A) Ethogram of scored aggressive behaviors. **(B)** Boxplots of the total counts for individual fight behaviors performed by winning (red) and losing males (blue). Winners performed significantly higher levels of each aggressive behavior compared to losers (* p<0.0001) **(C)** Total aggressive behaviors performed by each paired male competitor (31 pairs). Winners indicated in red and losers in blue. The fight outcome (the categorization of winners and losers) was determined by which male performed more aggressive behaviors within a pair. Across all pairs, winners ranged from performing 21-268 attacks, and losers ranged from performing 0-19 attacks.

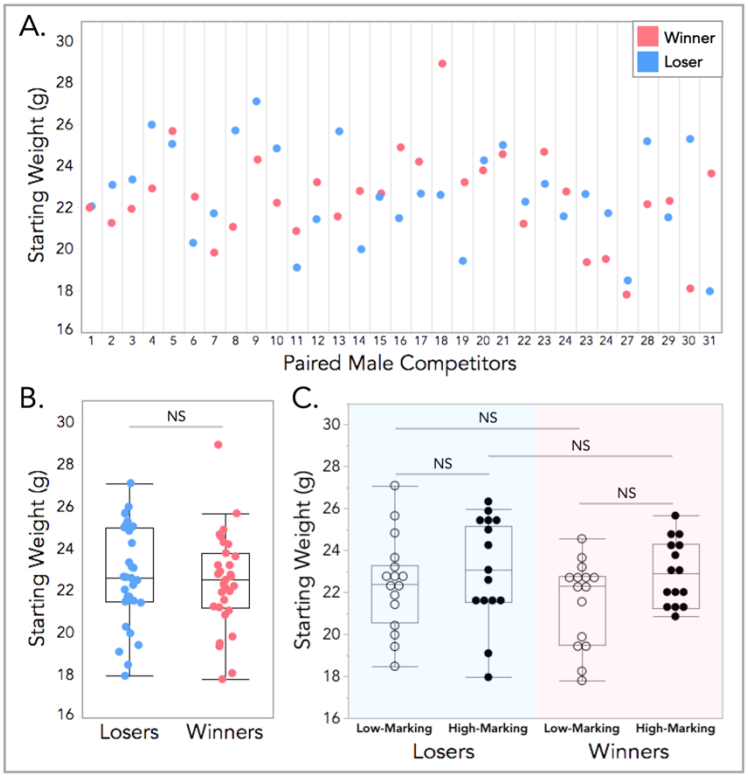

Figure S3. Body weight differences across winning and losing males. All weight measurements (g) were collected the day before trials began, such that competitors were weight-matched as closely as possible. **(A)** Starting weights (g) of each male within a competing pair across trials. **(B)** Boxplot of starting body weights of all losers and winners. Winners and losers did not differ in weight across trials. **(C)** Boxplot of the starting body weight for winners and losers by marking group: high vs. low-marking males. A single male was removed from this analysis as an outlier (NY2-205), however removal of this male did not affect the observed patterns. A LMM was used to model relationships, and analyses of variance were used to test for overall effects. Significance codes: NS p>0.05.

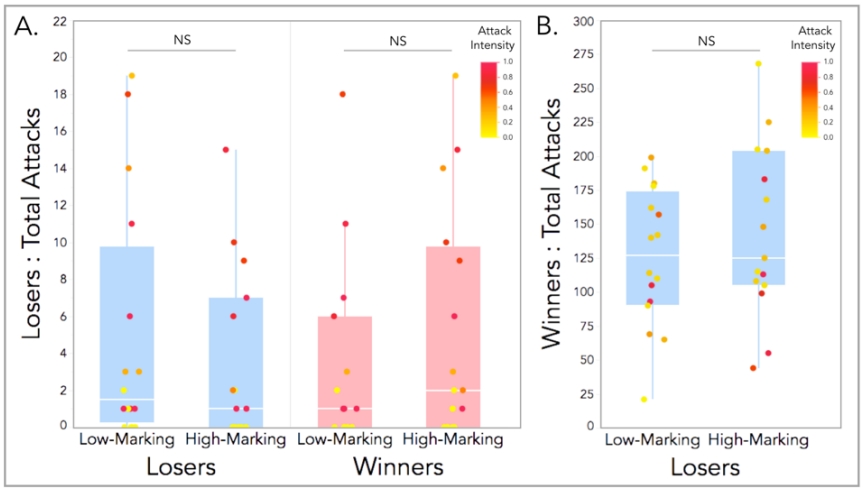

Figure S4. Additional dyadic comparisons of contest aggression and intensity in response to signaling effort. (A) Boxplot of the total attacks performed by losers given either loser or winner marking investment (low vs. high). The initial signaling effort of losers or winners does not predict loser aggression, both in terms of total attacks or intensity. Though losers perform very few attacks and only early on in the trial. **(B)** The initial signaling effort of losers similarly does not predict winner aggression, in total attacks or intensity. LMMs were used to model relationships, and analyses of variance were used to test for overall effects. Significance codes: NS p>0.05.

Declarations

Ethics. All experimental protocols conducted at Cornell University were approved by the Institutional Animal Care and Use Committee (IACUC: Protocol #2015-0060) and were in compliance with the NIH Guide for Care and Use of Animals.

Data accessibility. Data sheets and R code used in all analyses are available on the Dryad Digital Repository.

Authors' contributions. CHM and MJS conceived the study. CHM performed trials and analyses. MFH, JY, BCC, KH and AYL collected samples, scored behavioral trials, and generated tracking data. CHM wrote the initial drafts of the paper. MJS edited the manuscript. All authors contributed to manuscript preparation.

Competing interests. The authors declare no competing interests.

Funding. This research was funded by USDA Hatch Grant (NYC-191428; Michael Sheehan) The funders were not involved in the design of the study; the collection, analysis and interpretation of data; the writing of the manuscript and any decision concerning the publication of the paper.

Acknowledgements. We thank Kevin Besler, Kusuma Anand, Christen Rivera-Erick and Melanie Colvin for crucial technical assistance; Russell Ligon and Caleb Vogt for helping establish recording systems and tracking methods in the lab; James Tumulty, Matthew Zipple and Rose Tatarsky for manuscript feedback.

REFERENCES

1. Parker GA. Assessment strategy and the evolution of fighting behaviour. Journal of Theoretical Biology. 1974 Sep;47(1):223–43.
2. Enquist M. Communication during aggressive interactions with particular reference to variation in choice of behaviour. Animal Behaviour. 1985 Nov;33(4):1152–61.
3. Wagner WE. Fighting, assessment, and frequency alteration in Blanchard's cricket frog. Behav Ecol Sociobiol. 1989 Dec;25(6):429–36.
4. Johnstone RA, Norris K. Badges of status and the cost of aggression. Behav Ecol Sociobiol. 1993 Feb;32(2):127–34.
5. Backwell PRY, Christy JH, Telford SR, Jennions MD, Passmore J. Dishonest signalling in a fiddler crab. Proc R Soc Lond B. 2000 Apr 7;267(1444):719–24.
6. Hurd PL. Resource holding potential, subjective resource value, and game theoretical models of aggressiveness signalling. Journal of Theoretical Biology. 2006 Aug;241(3):639–48.
7. Stapley J, Whiting MJ. Ultraviolet signals fighting ability in a lizard. Biol Lett. 2006 Jun 22;2(2):169–72.
8. Tibbetts EA, Pardo-Sanchez J, Weise C. The establishment and maintenance of dominance hierarchies. Phil Trans R Soc B. 2022 Feb 28;377(1845):20200450.
9. Sheehan MJ, Bergman TJ. Is there an evolutionary trade-off between quality signaling and social recognition? Behavioral Ecology. 2016;27(1):2–13.
10. Grafen A. Biological signals as handicaps. Journal of Theoretical Biology. 1990 Jun;144(4):517–46.

11. Johnstone RA. Behavioural ecology: An evolutionary approach. In: The evolution of animal signals. 1997. p. 155–78.
12. Searcy WA, Nowicki S. The Evolution of Animal Communication: Reliability and Deception in Signaling Systems: Reliability and Deception in Signaling Systems. Princeton University Press; 2010. Available from: https://www.degruyter.com/document/doi/10.1515/9781400835720/html
13. Dunn JC, Halenar LB, Davies TG, Cristobal-Azkarate J, Reby D, Sykes D, et al. Evolutionary Trade-Off between Vocal Tract and Testes Dimensions in Howler Monkeys. Current Biology. 2015 Nov;25(21):2839–44.
14. Lüpold S, Simmons LW, Grueter CC. Sexual ornaments but not weapons trade off against testes size in primates. Proc R Soc B. 2019 Apr 10;286(1900):20182542.
15. Simmons LW, Emlen DJ. Evolutionary trade-off between weapons and testes. Proc Natl Acad Sci USA. 2006 Oct 31;103(44):16346–51.
16. Peters A, Delhey K, Denk AG, Kempenaers B. Trade-Offs between Immune Investment and Sexual Signaling in Male Mallards. The American Naturalist. 2004 Jul;164(1):51–9.
17. Ahtiainen JJ, Alatalo RV, Kortet R, Rantala MJ. A trade-off between sexual signalling and immune function in a natural population of the drumming wolf spider Hygrolycosa rubrofasciata. J Evolution Biol. 2005 Jul;18(4):985–91.
18. Tuttle MD, Ryan MJ. Bat Predation and the Evolution of Frog Vocalizations in the Neotropics. Science. 1981 Nov 6;214(4521):677–8.
19. Roberts SC. Scent-marking by male mice under the risk of predation. Behavioral Ecology. 2001 Nov 1;12(6):698–705.

20. Viitala J, Korplmäki E, Palokangas P, Koivula M. Attraction of kestrels to vole scent marks visible in ultraviolet light. Nature. 1995 Feb;373(6513):425–7.
21. Zuk M, Kolluru GR. Exploitation of Sexual Signals by Predators and Parasitoids. The Quarterly Review of Biology. 1998 Dec;73(4):415–38.
22. Magnhagen C. Predation risk as a cost of reproduction. Trends in Ecology & Evolution. 1991 Jun;6(6):183–6.
23. Rohwer S. Status Signaling in Harris Sparrows: Some Experiments in Deception. Behav. 1977;61(1–2):107–29.
24. Molles LE, Vehrencamp SL. Songbird cheaters pay a retaliation cost: evidence for auditory conventional signals. Proc R Soc Lond B. 2001 Oct 7;268(1480):2013–9.
25. Tibbetts EA, Dale J. A socially enforced signal of quality in a paper wasp. Nature. 2004 Nov;432(7014):218–22.
26. Tibbetts EA, Izzo A. Social Punishment of Dishonest Signalers Caused by Mismatch between Signal and Behavior. Current Biology. 2010 Sep;20(18):1637–40.
27. Dey CJ, Dale J, Quinn JS. Manipulating the appearance of a badge of status causes changes in true badge expression. Proc R Soc B. 2014 Jan 22;281(1775):20132680.
28. Ligon RA, McGraw KJ. Social costs enforce honesty of a dynamic signal of motivation. Proc R Soc B. 2016 Oct 26;283(1841):20161873.
29. Johnson RP. Scent marking in mammals. Animal Behaviour. 1973 Aug;21(3):521–35.

30. Ralls K. Mammalian Scent Marking: Mammals mark when dominant to and intolerant of others, not just when they possess a territory. Science. 1971 Feb 5;171(3970):443–9.
31. Roberts SC. Scent-marking (Ch. 22). In: Rodent Societies. University of Chicago Press; 2007. p. 255–66.
32. Gosling LM. A Reassessment of the Function of Scent Marking in Territories. Zeitschrift für Tierpsychologie. 1982 Jan 12;60(2):89–118.
33. Rich TJ, Hurst JL. The competing countermarks hypothesis: reliable assessment of competitive ability by potential mates. Animal Behaviour. 1999 Nov;58(5):1027–37.
34. Humphries RE, Robertson DHL, Beynon RJ, Hurst JL. Unravelling the chemical basis of competitive scent marking in house mice. Animal Behaviour. 1999 Dec;58(6):1177–90.
35. Hurst JL, Beynon RJ. Scent wars: the chemobiology of competitive signalling in mice. Bioessays. 2004 Dec;26(12):1288–98.
36. Gosling LM, Roberts SC. Scent-marking by male mammals: Cheat-proof signals to competitors and mates. In: Advances in the Study of Behavior. Elsevier; 2001. p. 169–217. Available from: https://linkinghub.elsevier.com/retrieve/pii/S0065345401800073
37. Ferkin MH. Scent marks of rodents can provide information to conspecifics. Anim Cogn. 2019 May;22(3):445–52.
38. Arakawa H, Blanchard DC, Arakawa K, Dunlap C, Blanchard RJ. Scent marking behavior as an odorant communication in mice. Neuroscience & Biobehavioral Reviews. 2008 Sep;32(7):1236–48.

39. Drickamer LC. Urine marking and social dominance in male house mice (Mus musculus domesticus). Behavioural Processes. 2001 Mar;53(1–2):113–20.
40. Hurst JL. Urine marking in populations of wild house mice Mus domesticus rutty. I. Communication between males. Animal Behaviour. 1990 Aug;40(2):209–22.
41. Desjardins C, Maruniak JA, Bronson FH. Social Rank in House Mice: Differentiation Revealed by Ultraviolet Visualization of Urinary Marking Patterns. Science. 1973 Nov 30;182(4115):939–41.
42. Gosling LM, Roberts SC, Thornton EA, Andrew MJ. Life history costs of olfactory status signalling in mice. Behavioral Ecology and Sociobiology. 2000 Sep 12;48(4):328–32.
43. Nelson AC, Cunningham CB, Ruff JS, Potts WK. Protein pheromone expression levels predict and respond to the formation of social dominance networks. J Evol Biol. 2015 Jun;28(6):1213–24.
44. Sheehan MJ, Campbell P, Miller CH. Evolutionary patterns of major urinary protein scent signals in house mice and relatives. Mol Ecol. 2019 Aug;28(15):3587–601.
45. Nevison CM, Barnard CJ, Beynon RJ, Hurst JL. The consequences of inbreeding for recognizing competitors. Proc R Soc Lond B. 2000 Apr 7;267(1444):687–94.
46. Kaur AW, Ackels T, Kuo TH, Cichy A, Dey S, Hays C, et al. Murine Pheromone Proteins Constitute a Context-Dependent Combinatorial Code Governing Multiple Social Behaviors. Cell. 2014 Apr;157(3):676–88.

47. Lee W, Khan A, Curley JP. Major urinary protein levels are associated with social status and context in mouse social hierarchies. Proc R Soc B. 2017 Sep 27;284(1863):20171570.
48. Miller CH, Hillock MF, Yang J, Carlson-Clarke B, Haxhillari K, Lee AY, et al. Dynamic changes to signal allocation rules in response to variable social environments in house mice [Internet]. Ecology; 2022 Jan [cited 2022 May 16]. Available from: http://biorxiv.org/lookup/doi/10.1101/2022.01.28.478242
49. Crowcroft P, Rowe FP. Social organization and territorial behavior in the wild house mouse (Mus musculus L.). Proceedings of the Zoological Society of London. 1963 May;140(3):517–31.
50. Harrington JE. Recognition of Territorial Boundaries by Olfactory Cues in Mice (Mus musculus L.). Zeitschrift für Tierpsychologie. 1976;41(3):295–306.
51. Mackintosh JH. Territory formation by laboratory mice. 1970 Feb;18:177–83.
52. Phifer-Rixey M, Bi K, Ferris KG, Sheehan MJ, Lin D, Mack KL, et al. The genomic basis of environmental adaptation in house mice. Payseur BA, editor. PLoS Genet. 2018 Sep 24;14(9):e1007672.
53. Chalfin L, Dayan M, Levy DR, Austad SN, Miller RA, Iraqi FA, et al. Mapping ecologically relevant social behaviours by gene knockout in wild mice. Nat Commun. 2014 Dec;5(1):4569.
54. Tuttle AH, Philip VM, Chesler EJ, Mogil JS. Comparing phenotypic variation between inbred and outbred mice. Nat Methods. 2018 Dec;15(12):994–6.
55. Cheetham SA, Smith AL, Armstrong SD, Beynon RJ, Hurst JL. Limited variation in the major urinary proteins of laboratory mice. Physiology & Behavior. 2009 Feb;96(2):253–61.

56. Gouveia K, Hurst JL. Reducing Mouse Anxiety during Handling: Effect of Experience with Handling Tunnels. Mintz EM, editor. PLoS ONE. 2013 Jun 20;8(6):e66401.

57. Cheetham SA, Thom MD, Jury F, Ollier WER, Beynon RJ, Hurst JL. The Genetic Basis of Individual-Recognition Signals in the Mouse. Current Biology. 2007 Oct;17(20):1771–7.

58. Sheehan MJ, Lee V, Corbett-Detig R, Bi K, Beynon RJ, Hurst JL, et al. Selection on Coding and Regulatory Variation Maintains Individuality in Major Urinary Protein Scent Marks in Wild Mice. Barsh GS, editor. PLoS Genet. 2016 Mar 3;12(3):e1005891.

59. Friard O, Gamba M. BORIS : a free, versatile open-source event-logging software for video/audio coding and live observations. Methods Ecol Evol. 2016 Nov;7(11):1325–30.

60. Mackintosh JH, Grant EC. A Comparison of the Social Postures of Some Common Laboratory Rodents. Behav. 1963;21(3–4):246–59.

61. Scott JP. Agonistic Behavior of Mice and Rats: A Review. Am Zool. 1966 Nov;6(4):683–701.

62. Van Oortmerssen GA. Biological Significance, Genetics and Evolutionary Origin of Variability in Behaviour within and between Inbred Strains of mice (Mus musculus): A Behaviour Genetic Study. Behavior. 1971;38:1–92.

63. Bates D. Parsimonious Mixed Models. ArXiv. 2018 May 26;arXiv:1506.04967:21.

64. Kuznetsova A, Brockhoff PB, Christensen RHB. lmerTest Package: Tests in Linear Mixed Effects Models. J Stat Soft [Internet]. 2017 [cited 2022 Jan 10];82(13). Available from: http://www.jstatsoft.org/v82/i13/

65. Lenth RV. Least-Squares Means: The *R* Package lsmeans. J Stat Soft. 2016;69(1). Available from: http://www.jstatsoft.org/v69/i01/

66. Lee W, Yang E, Curley JP. Foraging dynamics are associated with social status and context in mouse social hierarchies. PeerJ. 2018 Sep 19;6:e5617.

67. Hissmann K. Strategies of mate finding in the European field cricket (Gryllus campestris) at different population densities: a field study. Ecol Entomol. 1990 Aug;15(3):281–91.

68. Millesi E, Hoffman IE, Huber S. Reproductive strategies of male European sousliks (Spermophilus citellus) at high and low population density. Lutra. 2004;47(2):75–85.

69. Knell RJ. Population density and the evolution of male aggression. Journal of Zoology. 2009 Jun;278(2):83–90.

70. Roberts SA, Davidson AJ, McLean L, Beynon RJ, Hurst JL. Pheromonal Induction of Spatial Learning in Mice. Science. 2012 Dec 14;338(6113):1462–5.

71. Hurst JL. Female recognition and assessment of males through scent. Behavioural Brain Research. 2009 Jun 25;200(2):295–303.

CHAPTER 4

Reproductive state switches the valence of male pheromones in female mice

Caitlin H. Miller*, Tess M. Reichard, Jay Yang, Brandon Carlson-Clarke, Caleb C. Vogt, Melissa R. Warden, Michael J. Sheehan*

Department of Neurobiology and Behavior, Cornell University, Ithaca, NY, USA

*Authors for Correspondence: Caitlin H. Miller: chm79@cornell.edu;
Michael J. Sheehan: msheehan@cornell.edu

Abstract

Internal states shape responses to sensory stimuli. Mammalian female reproductive states are understudied considering they are one of the most regular state changes in the animal kingdom. Here we examine female house mouse preferences toward male odors across the reproductive states of estrus and late-stage pregnancy. In house mice, urine scent marks are salient social odors that convey information about the sex and identity of individuals by major urinary proteins (MUPs). Males secrete a sex-specific pheromonal protein called darcin (MUP20). Additionally, genetically diverse mice secrete unique combinations of MUPs used in individual recognition. Prior work has revealed that male odors are powerful social stimuli for female mice, yet we have a limited understanding of how the valence of such odors change across reproductive states. We discovered a valence shift among estrus and pregnant females toward novel male urine, in which estrus females exhibit preference and pregnant females show strong avoidance. This valence switch also occurs toward darcin alone, providing further support for darcin as a strong sexual signal. However, when presented with familiar male urine, the approach-avoidance response disappears, even when additional darcin is added. In contrast, when a novel identity protein (MUP11) is added to familiar male urine the approach-avoidance response is recovered. This indicates that darcin in the absence of other identity information denotes a novel male and that familiar identity information present in male urine is sufficient to modify responses to darcin. Our findings suggest that the sex and identity information encoded by MUPs are likely processed via distinct, and potentially opposing pathways, that modulate responses toward complex social odor blends. Furthermore, we identify a state-modulated shift in decision-making toward social odors and propose a neural circuit model for this flow of information. These data

underscore the importance of physiological state and signal context for interpreting the meaning and importance of social odors.

Keywords: hormonal state, estrus, pregnancy, valence, social odors, darcin (MUP20), major urinary proteins (MUPs)

Results & Discussion

Internal state shapes the meaning and importance of sensory stimuli. For example, when you're dehydrated a glass of water is much more satisfying than it otherwise would be. Some of the most critical yet understudied state changes are those of mammalian estrus and pregnancy. Reproductive cycles represent rare state shifts that consist of highly regular hormonal changes. These changes facilitate flexible decision-making over both short and long timescales, including adaptive responses to social environments. The value of social encounters thus varies over the course of the estrus cycle and pregnancy [1–6]. While a novel male denotes a mating opportunity for a female mouse in estrus (i.e., close to ovulation) [7,8], a novel male intruder elicits aggression in mothers [3,9,10]. Similarly, the presence of a novel male's odor can induce pregnancy block during early stage pregnancy in house mice, a phenomenon known as the Bruce effect [11,12].

Social odors are a central mode of communication among mammals [13–15]. In house mice, males and females scent mark their environment with urine [7,16–20]. These urine marks convey detailed social information about the sex, competitive status, and identity of individuals [8,21–28], which mice carefully attend to [7,8,27,29,30]. Sexually receptive female mice in estrus find male urine attractive and rewarding [22,31–34]. The component of male urine that stimulates this response is darcin (MUP20), which acts as a male sex pheromone in house mice [1,7,8]. The attractiveness of this odor wanes when females enter the quiescent phase of their estrus cycle (diestrus) [1] and induces aggression in mothers [3]. In contrast, the response of pregnant females toward male social odors is underexplored, particularly during late-stage pregnancy (i.e., the 3rd trimester). The final trimester of pregnancy is intriguing because females are arguably in their least sexually receptive phase and

the physiological shifts occurring during this period may prime females for the profound changes that occur upon giving birth.

Here, we examine the response of female mice in estrus and late-stage pregnancy toward male social odors (**Figure 1A-B**). The objectives of this study were to: (1) investigate the valence of male social odors across reproductive states, and (2) isolate the components of male urine that drive shifts in female responses. Specifically, we were interested in the major urinary protein (MUP) components of mouse urine which convey sex and identity information. In addition to the male pheromone darcin (MUP20), genetically diverse house mice each secrete a unique subset of identity-specific MUPs ('central' MUPs) that are used to recognize individuals [21,23,27,35]. We can synthesize these proteins in the lab as recombinant MUPs (rMUPs) [27,36] and present highly controlled social odor stimuli.

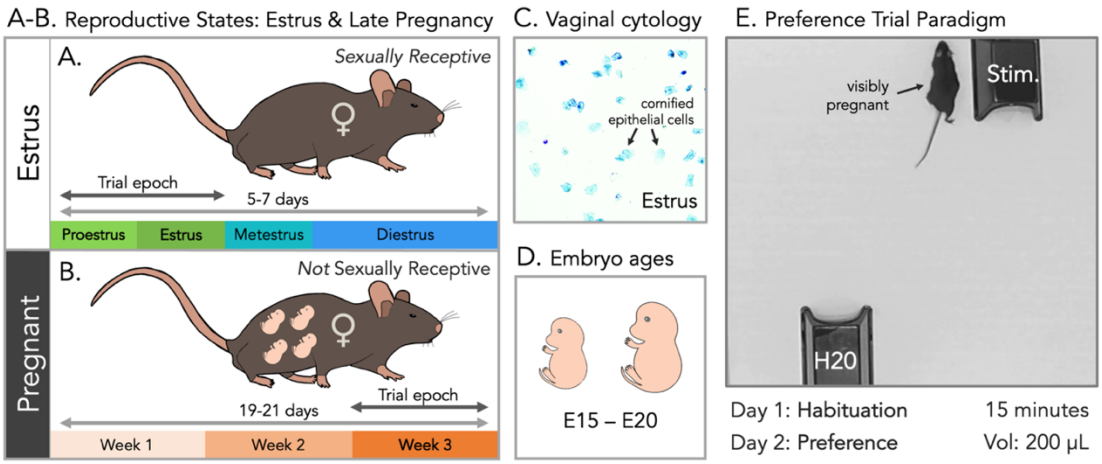

Figure 1. Reproductive states & experimental design. (A) Schematic representing the estrus cycle stages (proestrus, estrus, metestrus & diestrus) of female mice, which typically occur over the course of 5-7 days. Experimental females were close to ovulation, in the proestrus and estrus phases of the cycle, indicated with the "trial epoch" arrow (**Table S1**). **(B)** Schematic representing the 3-week duration of pregnancy. We focus on late-stage pregnancy (3rd trimester), indicated with the "trial epoch" arrow. **(C)** Vaginal cytology was used to track and stage the estrus cycles of females. Cytological swabs of females in estrus were identified by the abundance of cornified epithelial cells. **(D)** Pregnancies were staged such that we carefully tracked the progress of female pregnancies after being paired with a male and ran females with embryos at days 15 -20 of development. **(E)** Preference trial paradigm. Females were placed in an arena for 15 minutes with two huts. Under each hut 200 uL of liquid was deposited in small droplets akin to urine marking. One hut contained a social odor stimulus, and the other a water (H_2O) control. Females were placed in the arena with both huts and stimuli for two consecutive days. The first day was a habituation trial, the second was a preference trial. Time spent in or on top of the huts was scored and preference indexes were calculated as the time spent in the stimulus hut relative to the water hut.

We tracked the reproductive states of naturally-cycling females using vaginal cytology to ascertain the phase of the estrus cycle [37–40] (**Figure 1C, Table S1**). We staged and tracked pregnancies to ensure females were in their 3rd trimester at the time of trials (**Figure 1D**). To examine social odor preferences, we exposed individuals to a two-day preference trial assay (**Figure 1E**). The first day was a habituation trial, as mice will explore novel environments and odors [41,42]. The second day was the preference trial, in which approach-avoidance behaviors were examined (**Table S2**). The arena held two stimulus huts: one contained a social odor, and the other contained a water control (**Figure 1E**). We calculated a preference index based on how much time females spent in or on top of the stimulus hut relative to the water control hut. A zero value indicates a female spent the same amount of time in each hut. Positive values indicate a preference for the stimulus hut while negative values indicate avoidance.

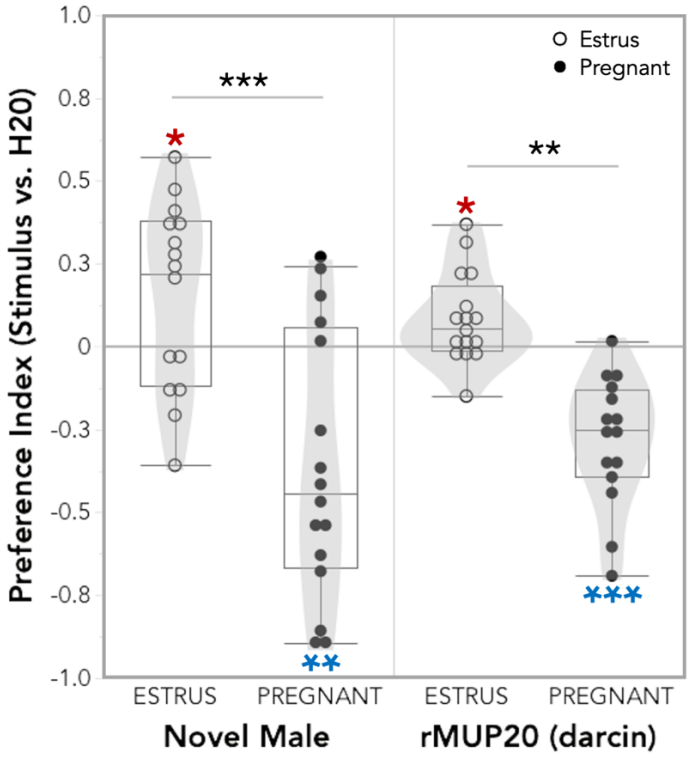

Figure 2. Estrus females show a preference for novel male urine and to rMUP20 (darcin), while pregnant females exhibit strong avoidance to both. All data is from the preference trial day. The preference index: how much time females spent in the stimulus hut relative to the control water hut. Stimulus huts contained either whole novel male urine or the recombinant male urinary protein rMUP20 (i.e., darcin). A zero value means a female spent the same amount of time in each hut. Positive values indicate preference for the stimulus hut, and negative values indicate avoidance. One-sample t-tests (deviation from 0) significance values are indicated with red asterisks (positive deviation or blue asterisks (negative deviation). A linear model was used to examine relationships, analyses of variance were used to test for overall effects, and pairwise comparisons were performed using the *emmeans* package. Estrus: novel male, n=15; rMUP20, n=16. Pregnant: novel male, n=16; rMUP20, n=15. Significance codes: * p<0.05, ** p<0.01, *** p<0.001.

Novel male urine and the male pheromone darcin elicit similar valence shifts across reproductive states

We first tested the response of estrus and pregnant females toward novel male urine. As all experimental subjects were C57BL/6J (C57) females, novel male urine was collected [43] from a genetically distinct wild-derived inbred mouse line (NY3) [44,45]. This was necessary to ensure that the novel male urine stimulus contained a different MUP profile from C57 males, because all individuals of a given inbred strain share identical MUP profiles [46,47]. In the wild different males secrete distinct urine profiles used to recognize individuals [21,23,27,35], and we wanted to present ecologically relevant novel male social odors similar to prior studies [8,48]. Furthermore, all females had prior exposure to adult male C57 urine (via their father and/or stud male).

We predicted that novel male urine would be a potent social odor stimulus for females, given prior research on females in estrus [1,22,31] and mothers [3,9,10]. Similar to what has been previously described [8,22,48], we observed a preference among sexually receptive estrus females toward novel male urine ($t_{1,14} = 2.1$, $p = 0.03$; **Figure 2**). In contrast, late-stage pregnant females showed a strong avoidance to the same stimulus ($t_{1,15} = -3.6$, $p = 0.001$; **Figure 2**). Estrus and pregnant females also differed in their preference for novel male urine (M1: $t_{1,125} = 5.1$, $p < 0.0001$; **Figure 2**). Females therefore exhibit state-dependent changes in decision-making toward social information.

A key component of male house mouse urine is the major urinary protein sex pheromone darcin (MUP20). We next examined if the male sex pheromone darcin on its own was sufficient to elicit the observed approach-avoidance switch in estrus and pregnant females. Following previous studies [1,27], we synthesized and presented

recombinant darcin (rMUP20) as a stimulus. This single urinary protein elicited a similar valence shift across female states when compared to novel male urine (**Figure 2**). We found that females in estrus were attracted to darcin, as previously reported [1,8,48] ($t_{1,15}$ = 2.5, p = 0.01; **Figure 2**). In contrast, pregnant females displayed robust avoidance ($t_{1,14}$ = -5.7, p = 3e-05; **Figure 2**). Females also differed in their preference for darcin across reproductive states (M1: $t_{1,125}$ = 3.6, p = 0.009; **Figure 2**). This response provides further evidence that darcin is a strong social signal in house mice and is a clear example of a valence switch toward a specific and salient sex pheromone.

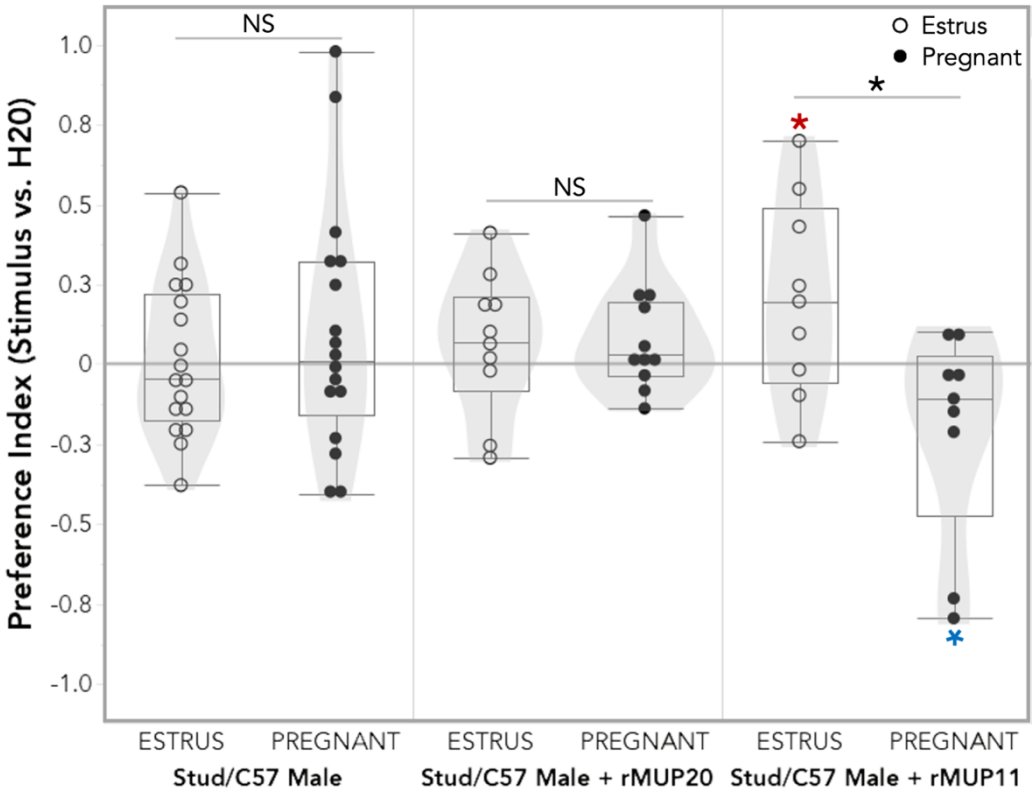

Figure 3. Approach-avoidance behaviors of estrus and pregnant females toward whole stud/C57 male urine, or stud/C57 male urine manipulated with added darcin (rMUP20) or rMUP11. The preference index: how much time females spent in the stimulus hut relative to the control water hut. A zero value means a female spent the same amount of time in each hut. Positive values indicate preference for the stimulus hut, and negative values indicate avoidance. One-sample t-tests (deviation from 0) significance values are indicated with red asterisks (positive deviation or blue asterisks (negative deviation). A linear model was used to examine relationships, analyses of variance were used to test for overall effects, and pairwise comparisons were performed using the *emmeans* package. Estrus: C57, n=17; C57+rMUP20, n=10; C57+rMUP11, n=9. Pregnant: Stud, n=17; Stud+rMUP20, n=11; Stud+rMUP11, n=9. Significance codes: NS p>0.05, * p<0.05.

Altering the identity profile of familiar male urine recovers the approach-avoidance valence switch observed toward novel male urine

There is, however, an important caveat to these results which required further probing – adult males typically secrete darcin in their urine [23,24,49]. This includes the pregnant female's stud male that was co-housed with her during trials. Therefore, darcin itself is unlikely to be aversive to pregnant females because they are consistently exposed to darcin by their stud male. We hypothesized that the observed response toward darcin alone may be due to the absence of other key identity information typically associated with their stud male's urine (i.e., his genotype-specific identity MUP expression pattern).

To address this, we presented pregnant females with urine from their C57 stud male, and estrus females with adult C57 male urine. C57 male urine is not novel to virgin estrus females as they were exposed to it via their fathers. Moreover, because they are from the same inbred line, C57 males and females produce nearly identical MUPs [46,47,49]. The similarity in urine profile conveys relatedness, and females will preferentially mate with unrelated males based on their MUP profile [50]. We manipulated the MUP content of stud/C57 male urine by adding equivalent amounts of either the male-specific recombinant protein darcin (rMUP20) or with a recombinant identity MUP that is found in C57 urine (rMUP11) [27,49]. We predicted that adding rMUP20 to familiar C57 male urine would not alter the urine identity profile, and therefore would not elicit approach-avoidance behaviors in females. Conversely, we predicted that the addition of rMUP11 would alter the perceived identity of the male urine, and thus provoke a valence switch. Importantly, in both cases we add peptides already present in the urine, thus only changing the ratios of MUPs in the stimuli.

When presented with unaltered stud/C57 male urine, neither estrus ($t_{1,16}$ = 0.21, p = 0.83) nor pregnant females ($t_{1,16}$ = 1.1, p = 0.31) displayed any preference, and females did not differ across states (M1: $t_{1,125}$ = -0.90, p = 0.99; **Figure 3**). For estrus females, this is likely because C57 male urine smells like that of a full sibling [50], and is a less attractive mating opportunity in comparison to the urine of a male with a different genotype. For pregnant females this is a male they see daily in their home cage, and hence is a highly familiar odor. The response to stud/C57 male urine with added rMUP20 also revealed no differences across reproductive states (M1: $t_{1,125}$ = -0.14, p = 1.0), and no approach or avoidance among estrus ($t_{1,9}$ = 0.93, p = 0.38) or pregnant females ($t_{1,10}$ = 1.6, p = 0.14; **Figure 3**). This shows that adding additional darcin to familiar male urine does not alter the identity or attractiveness of the stimulus for females. In contrast, when rMUP11 is added to familiar male urine the response toward novel male urine is recovered, and females significantly differ in preference across reproductive states (M1: $t_{1,125}$ = 3.1, p = 0.04; **Figure 3**). Estrus females displayed approach behavior ($t_{1,8}$ = 2.0, p = 0.039), and pregnant females exhibited avoidance ($t_{1,8}$ = -1.9, p = 0.048; **Figure 3**). This is notable given that aside from a single added recombinant identity MUP (rMUP11), everything about the urine stimulus is exactly the same.

Sex and identity information are processed distinctly: a proposed model

Our results reveal that darcin on its own denotes the presence of a novel male. This appears to be driven by the absence of identity information associated with a familiar male. This suggests that sex and identity information are processed via distinct, and potentially opposing, sensory pathways that converge to modulate behavioral

responses. Given the observed preference patterns and existing circuit knowledge, we propose a model of information flow (**Figure 4**).

The robust responses observed toward darcin in this study and by other groups [1,7,8,48], suggest a specialized circuitry ('labeled-line'; **Figure 4B**). This is likely given that a related pheromone (ESP1) that stimulates sexual posturing in females is detected via a labeled-line [51,52]. Our results further demonstrate that this proposed darcin-specific signal cascade is interrupted if a familiar identity-matched 'central' MUP template is present. Darcin is therefore not part of the identity template, but instead acts as a robust male signal that gets suppressed by the presence of familiar male identity information.

Our results provide further evidence that individual recognition is determined by combinatorial coding of 'central' identity MUPs [27,53], as the manipulation of a familiar male MUP ratios with a single identity rMUP (rMUP11) stimulated a response similar to that of a novel male (**Figure 4A**). In this manipulation the template did not match match (due to the altered ratios of identity signaling peptides) and thus the darcin signal cascade was not suppressed. Signal context is consequently crucial for mediating adaptive social and spatial preferences, particularly when determining the presence of a male in the environment and whether that male is familiar or novel.

Pheromonal suppression via individual pattern recognition likely occurs in the accessory olfactory bulb (AOB; **Figure 4**), as MUPs are detected by the accessory olfactory (i.e. vomeronasal) system [1,27,48] and stud male odor memory formation requires a functional AOB but not other downstream limbic regions [12,54,55]. Evidence suggests that this sensory memory is maintained by local modulation of AOB projection neuron membrane excitability [56–58]. We propose a local inhibition of the darcin 'labeled-line' within the AOB (i.e., opposing components; **Figure 4C**),

such that familiar male identities block the darcin circuit cascade, and only upon detection of a novel male are strong neuronal signals sent downstream.

The state-modulated valence switch in decision-making toward novel male odors in estrus and pregnant females likely occurs in the primary downstream limbic targets of the AOB: the medial amygdala (MeA) and/or the bed nucleus of the stria terminalis (BNST). The MeA and BNST receive abundant direct excitatory input from the AOB and have hormone-sensitive neuronal populations [59–62]. These brain regions are primed to facilitate shifts in responses to varying hormone levels by neuromodulatory gain and/or diverging pathways.

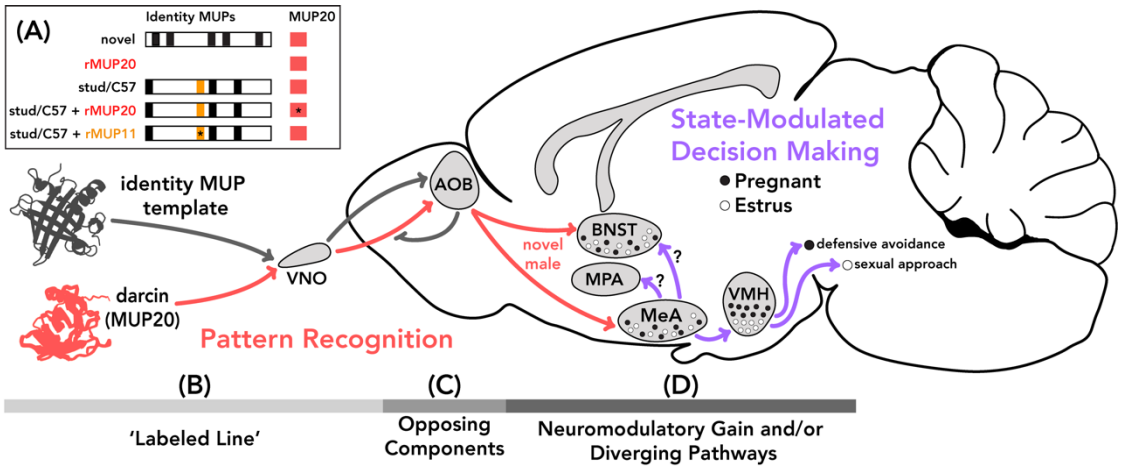

Figure 4. Model of information flow mediating pattern recognition and state-modulated decision-making in female mice toward social odors. (A) Schematic depicting the MUP components of male urine and the recombinant MUP stimuli. For the 'central' identity MUPs protein expression is indicated by black bars, except for MUP11 which is indicated with a yellow bar. Novel male urine has a distinct MUP array compared to familiar stud/C57 male urine. A red bar indicates the presence of the male-specific pheromone MUP20 (darcin). All male urine contains darcin. For manipulated urine stimuli containing additional rMUP an asterisk indicates the added rMUP (rMUP11 or rMUP20). **(B)** Model for the distinct processing of sex (red) and identity information encoded by MUPs (black), in which the male pheromone darcin (red) has specialized circuitry ('labeled line') projecting from the peripheral olfactory vomeronasal organ (VNO) to the accessory olfactory bulb (AOB). **(C)** Templates for familiar male identities are stored in the AOB. When the MUP identity matches the olfactory memory template, this initiates a suppression of darcin-specific signaling cascade. However, if this identity pattern recognition does not occur, the darcin signaling cascade continues to downstream limbic regions and conveys the presence of a novel male. **(D)** Female responses to novel male urine are modulated by their hormonal reproductive state. Females in estrus show a preference for novel male urine, and pregnant females exhibit avoidance. This approach-avoidance valence switch toward the same odor stimuli is likely modulated by activity in one or both of the primary projection targets downstream of the AOB: bed nucleus of the stria terminalis (BNST) or the medial amygdala (MeA). State modulated decision-making is likely mediated by shifts in neuromodulatory gain toward changing hormone levels within the MeA. The MeA in turn gates information to distinct subregions of the ventromedial hypothalamus (VMH) via diverging projections, such that distinct VMH populations are activated during sexual approach (estrus) as opposed to defensive avoidance (pregnant). Alternatively, information may be gated to different downstream limbic brain regions such as the medial preoptic area (MPA) and/or the BNST.

The MeA is a likely target for such modulation given its central location within limbic circuitry, and its role in gating responses to reproductive and defensive stimuli [63,64]. Moreover, the MeA is strongly activated by unfamiliar relative to familiar male urine in female mice [65], and specific MeA neuronal populations are activated by darcin [7] and ESP1 [51]. The MeA in turn sends prominent projections to the ventromedial hypothalamus (VMH), which has abundant estrogen and progesterone-sensitive neurons [51,66–77]. In females, two distinct VMH subpopulations are differentially activated by mating and fighting [68], reminiscent of the approach-avoidance behaviors observed across reproductive states. We propose that neuromodulatory gain within the MeA gates input to the VMH, and thereby activates distinct subpopulations in a state-dependent manner (**Figure 4D**). Alternatively, information may be gated to other brain regions. For example, MeA projections to the BNST may mediate estrus female approach [78], and projections to the VMH may mediate pregnant female avoidance [71,78,79].

This preference paradigm and circuit model provide a unique opportunity to interrogate the neurobiological mechanisms underlying valence processing and hormonal state shifts. The behavioral and physiological changes that occur over the course of reproductive cycles are uniquely regular. Furthermore, pregnancy is one of the most dramatic physiological changes that can occur within an individual's lifetime, and yet is sorely understudied. These results highlight the biomedical importance for considering reproductive state variation as well as how social odors assays are utilized and interpreted. Our findings reveal key insights into how sex and identity information are processed, and open new avenues for investigating recognition mechanisms.

Material & Methods

KEY RESOURCES TABLE

REAGENT or RESOURCE	SOURCE	IDENTIFIER
Experimental Models: Organisms/Strains		
C57BL/6J (*M. m. domesticus*)	The Jackson Laboratory	JAX: 000664
Recording & Imaging Systems		
iDVR-PRO CMS IR security cameras	CCTV Camera Pros	https://www.cctvcamerapros.com/DVR-Remote-Access-non-IE-s/470.htm
40X-2500X Plan Infinity Kohler Laboratory Trinocular Compound Microscope + 18MP USB3.0 Camera	AmScope	T720QC-18M3
Materials & Solutions		
Whatman filter paper (46 x 57 cm)	Sigma-Aldrich	1002-917
Gibco Phosphate Buffered Saline pH 7.4 (1X)	Thermo Fisher Scientific	10010031
JorVet Dip Quick Stain Kit	Jorgensen Labs	J0322
pMAL Protein Fusion and Purification System	New England Biolabs	E8200
Software and Algorithms		
BORIS 8.0	Behavioral Observation Research Interactive Software	https://boris.readthedocs.io/en/latest/
R v.3.6.3	The R Project for Statistical Computing	https://www.r-project.org/
R package *trajr*	(80)	https://cran.r-project.org/web/packages/trajr/index.html
R package *lme4*	(81)	https://cran.r-project.org/package=lme4
R package *lmerTest*	(82)	https://CRAN.R-project.org/package=lmerTest

EXPERIMENTAL MODEL AND SUBJECT DETAILS

Animals

All experimental subjects in this study were C57BL/6J female mice (n=141) obtained from The Jackson Laboratory (JAX stock #000664). At the time of experimentation all females were fully adult (2-5 months old), estrus females were virgin, and pregnant females were in the third week of their first pregnancy. Virgin females used to track estrus cycles were housed in holding cages with other females. Pregnant females were housed in breeding cages with their stud C57BL/6J (C57) male. All holding and breeding cages contained corn cob bedding, cardboard huts, and cotton nestlets. Mice were housed in an Animal Care facility at Cornell University with a 14:10 shifted

light:dark cycle (dark cycle: 10AM–8PM), with food and water provided *ad libitum.* To reduce handling stress confounds, mice were transferred between their home cage and the experimental arena using transfer cups [83].

METHOD DETAILS

Stimuli

The social odors used as trial stimuli consisted of whole urine and/or recombinant major urinary proteins (rMUPs) synthesized in lab: novel male urine, stud/C57 male urine, darcin (rMUP20), stud/C57 male urine with added rMUP20, and stud/C57 male urine with added rMUP11. While darcin is a male-specific major urinary protein [23,24,84], mice secrete many other urinary proteins that mediate identity recognition (also called 'central' MUPs) [21,23,24,27,35]. In the wild, individuals within a population typically excrete distinct combinations of MUPs [23,85]. Individuals within an inbred strain secrete the same combination (as a result of genetic inbreeding) [46,47]. C57 typically express a MUP with molecular weight 18693 Da matching the sequence of MUP11 [27,49], so this was used to shift the identity protein profile of C57 male urine by changing the ratio of MUPs present. Stimuli were all presented as a total 200 µL volume, that was aliquoted in small 25-50 µL droplets to mimic urine marking under specific stimulus huts in the preference trial arena (**Figure 1E**).

Urine collection

Urine collection was performed using the single animal method: males were placed atop a metal grate (an upside down cage hopper) over a clear plastic bag for 30 minutes to 1 hour [43]. Mice were subsequently taken off the plastic bag and returned to their home cage. The urine droplets present on the plastic bag were collected and

stored at -80°C until use. Two types of urine were collected: novel male urine and stud or C57BL/6J male urine. Novel urine was collected from a distinct inbred mouse line (NY3: this strain is related to the SarA/NachJ, SarB/NachJ and SarC/NachJ strains available from the Jackson Lab [44]), to ensure that the urinary protein profile was completely novel to experimental females [21,23,27,46]. For novel male urine we collected a large batch of urine from over 20 adult individuals for each stimulus. This was done such that the exact same novel male genotype urine stimulus was presented to experimental females across trials, without any individual-specific effects of urine odors. Stud and pooled C57BL/6J male urine was also collected. For stud male urine, we collected urine from a pregnant female's specific individual C57BL/6J stud male a week prior to the start of the two-day preference trial. Virgin estrus females by definition did not have a stud male. They were presented adult C57BL/6J male urine. We collected a large batch of urine from over 20 adult male C57BL/6J genotype mice, again to prevent any individual-specific effects of urine odors such that all estrus females received the same C57BL/6J male urine stimulus. For all urine collection, urine was stored on the day of collection at -80°C. Once a sufficient volume was collected to use as stimuli, individual aliquots were thawed on ice, and urine was pooled into a single volume and subsequently aliquoted into trial appropriate volumes (200 µL) and stored at -80°C until use.

Major urinary protein synthesis

Using complementary DNA (cDNA) libraries from adult male house mice, complete MUP cDNAs were obtained from liver tissue. MUP cDNAs were amplified and sequences were checked using Sanger sequencing methods. These MUPs were cloned into an *E. coli* C2523 pMAL-c5X vector and recombinant MUP (rMUP) was

made using pMAL Protein Fusion and Purification System (New England Biolabs) using methods similar to prior studies [27,36]. Mature MUP11 (ENSMUSP00000095654.4) and MUP20 (ENSMUSP00000073667.4) lacking signal peptide [49] were produced as rMUPs to be used as stimuli in preference trials [27,36]. To ensure rMUPs were successfully made, an SDS-PAGE gel was run to verify protein length and compared to male mouse urine. When rMUPs were added to stimuli in behavioral trials, they were presented at a concentration of 5 mg/ml which is comparable to typical urinary protein concentrations found in mouse urine [27].

Vaginal cytology

Rather than removing the ovaries of females and performing hormonal treatments, we wanted to track the natural estrus cycles of females to observe the natural hormonal changes that occur in female mice. Vaginal cytology was used track the estrus cycles of females using standard procedures [37–40], and was performed 1-2 hours prior to the start of the dark cycle (8-9 AM). Vaginal cytology was performed daily for at least two full estrus cycles for each female to ensure careful timing of the proestrus-estrus phase during preference trials. Mice were handled gently to reduce stress, restrained only by the base of their tail and were allowed to rest their forepaws on the cage hopper. A pipette was filled with 25 µL of Gibco Phosphate Buffered Saline (PBS) pH 7.4 (1X), and then gently lavaged at the vaginal opening. The pipette was flushed approximately ten times, or until the solution was cloudy, indicating the presence of cells. The solution was carefully released and spread onto a glass slide. Each mouse had its own slide and pipette to avoid sample contamination. The glass slides were stained with JorVet DipQuick Stain Fixative, Stain Solution, and Counter Stain. Extra stain was rinsed off with a water dip, and subsequently examined under a 10X

resolution microscope (AmScope: T720QC-18M3). Each stage of the estrus cycle is dictated by which cell types are present, leukocytes, cornified epithelial cells, and nucleated epithelial cells, and the proportion of cell types present [37–40] (**Table S1**). Specifically, we looked for females with cornified epithelial cells or nucleated epithelial cells, indicating they were in estrus [37–40] (**Table S1**). As the trials were two days long, on the first habituation trial day we used females that were in the earlier stages of estrus (proestrus or their first day of estrus). On the second preference trial day we timed it such that females were in peak estrus (and close to ovulation).

Pregnancy staging

We set up timed pregnancies because we were interested in studying late stage pregnancy in female mice (females in their 3rd and final week of gestation: 15-21 days pregnant [86]). To do this, adult virgin female mice (at least 1.5-2 months old) were paired with an adult male mouse on a specific date, and their subsequent date for giving birth was predicted to be approximately three weeks after initial breeding cage setup (gestation time of 19-21 days). The day after breeding cages were setup, females were checked to see if she showed signs of successful mating indicated by the presence of a copulatory plug [87]. Females did not always show a plug, so their size was monitored daily until the day of birth [88]. In particular, we carefully tracked the date in which females became visibly pregnant, as this was very predictive of being in their second week of pregnancy. The combination of the predicted birth date based on the breeding cage set up, along with the tracked pregnancy bulge, provided a reliable guide to the pregnancy stage of females. When females were sufficiently large and between 15 and 21 days after the being paired with a male, females entered into the two-day preference trial assay. All pregnant females successfully

gave birth, and the date of birth was used to accurately determine the stage of pregnancy and embryo development (E1-E20) at the time of experimentation.

Females were excluded from trials if they were no longer in estrus on their preference trial day, if pregnant females gave birth on their preference trial day, or if females were actually in their 2nd trimester during the trial period (as determined by the date of birth of their pups).

Preference trials

Because house mice are primarily nocturnal [89], trials occurred during their active dark cycle period, and all experimentation occurred between 11 AM - 2 PM to minimize circadian variation. All trials were performed in two trial chambers that were sound-proofed and fitted with security camera recording systems (iDVR-PRO CMS; 1080p; 30 fps). PVC Trial arenas (50 cm x 50 cm) were placed into these sound-proofed chambers. Large sheets of Whatman filter paper lined the floor of each trial to control the placement and presentation of social odor stimuli. The arena contained two opaque red plastic huts, placed in the lower left corner and the upper right corner. Underneath each hut 200 uL of stimulus or a control were pipetted onto the filter paper in small 25-50 uL droplets, to mimic the pattern of a mouse urine scent marking. In each trial, one hut contained a social odor stimulus (e.g. novel male urine) and the other contained water as a control. The location of the stimulus odor was randomized. Stimuli were aliquoted just prior to the start of the trial. Trials were performed in under mildly aversive full spectrum light to encourage investigation of the huts.

The preference trial assay consisted of two days, in which the mouse was exposed to the same arena and the same stimuli (in the same locations) on both

days. The first day was a habituation trial, as mice will investigate novel environments and odors. The second day was the preference trial, for which approach-avoidance behaviors were examined. Once a mouse was trial ready (i.e., females in late pregnancy or in estrus), mice were transferred in a cup from their holding cage to the center of the arena, to reduce stressful handling. All trials were 15 minutes in duration. At the end of the trial, females were gently removed from the trial arena and returned to their home cage. Between trials, arenas and all chamber surfaces were cleaned thoroughly with 70% EtOH. Experimental females were used once for one preference trial stimulus trial series (i.e., no females were reused across reproductive states or stimuli).

Behavioral scoring and analysis

Behavioral trials were scored using Behavioral Observation Research Interactive Software (BORIS)[90]. Trials were scored blind to the stimulus presentation. The mouse's movements were observed and classified as either under or above the huts (state events; **Table S2**). These classifications were further distinguished on the basis of whether they occurred in the front or back hut in the arena, which contained different stimuli (social stimuli or water control). Using the scored spatial data, similar to a prior study [1] preferences indices (PIs) were calculated as follows: PI = (∑ Time spent investigating stimulus - ∑ Time spent investigating control) / (∑ Time spent investigating stimulus + ∑ Time spent investigating control). Investigations include time spent underneath or on top of huts. Zero value means they spent the same amount of time in each hut. Positive values indicate preference for the stimulus hut (more time was spent in the stimulus hut), and negative values indicate avoidance for the stimulus hut (more time was spent in the water hut).

QUANTIFICATION AND STATISTICAL ANALYSIS

We conducted all statistical analyses in R 3.6.0 (R Development Core Team 2019). We used linear modeling and paired statistical tests to examine relationships between dependent variables (reproductive state and social odor stimuli) and response variables (preference indices). Models were fitted using the package *lme4* [81]. The *lmerTest* package was used to calculate degrees of freedom (Satterthwaite's method) and p-values [82]. We used a type 3 analysis of variance (ANOVA) to test for overall effects of fixed factors or interactions in the models. Post hoc comparisons were conducted using the *emmeans* package [91]. One-sample t-tests were performed to examine whether experimental groups preference indices deviated significantly above or below zero. R script and data sheets used for all statistical analyses are provided.

Declarations

Ethical statement. All experimental protocols conducted at Cornell University were approved by the Institutional Animal Care and Use Committee (IACUC: Protocol #2015-0060) and were in compliance with the NIH Guide for Care and Use of Animals.

Data accessibility. Data sheets and R code used in all analyses are available on the Dryad Digital Repository.

Author contributions. CHM and MJS conceived the study. CHM performed trials and analyses. TMR & JY tracked reproductive cycles and scored behavioral trials. CHM wrote the initial drafts of the paper. MJS and MRW edited the manuscript. All authors contributed to manuscript preparation.

Competing interests. The authors declare no competing interests.

Funding. This research was funded by USDA Hatch Grant (NYC-191428; Michael Sheehan) The funders were not involved in the design of the study; the collection, analysis and interpretation of data; the writing of the manuscript and any decision concerning the publication of the paper.

Acknowledgements. We thank Kevin Besler, Christen Rivera-Erick, Melanie Colvin and Jeremy Cusker for crucial technical assistance; Russell Ligon for helping establish recording systems and tracking methods in the lab; Eileen Troconis for helpful manuscript feedback.

Supplementary information

Table S1. Estrus cycle vaginal cytology images. Vaginal swabs of females in proestrus are characterized by nucleated epithelial cells. Females in estrus have primarily cornified epithelial cells. As females enter the quiescent phase there are more leukocytes, as observed in metestrus. Females in diestrus have almost exclusively leukocytes.

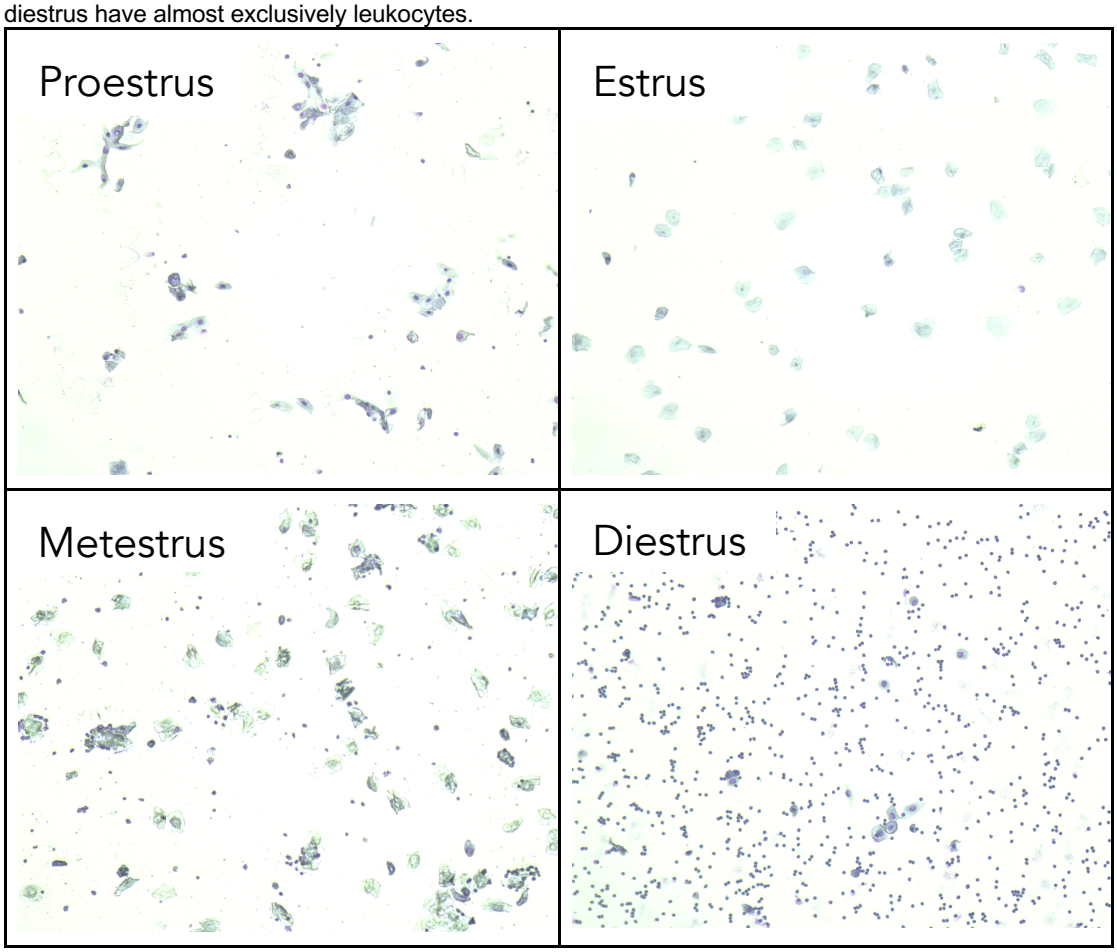

Table S2. Behavioral ethogram for scoring preference trials

Behavior	Description
Under Hut	Mouse goes under the hut and stays under it for a period of time. Behavior was modified based on which hut the mouse went under–front or back hut.
Above Hut	Mouse climbs on top of the hut and remains there for a period of time. Behavior was modified based on which hut the mouse was above–front or back hut.

REFERENCES

1. Dey S, Chamero P, Pru JK, Chien MS, Ibarra-Soria X, Spencer KR, et al. Cyclic Regulation of Sensory Perception by a Female Hormone Alters Behavior. Cell. 2015 Jun;161(6):1334–44.
2. Stowers L, Liberles SD. State-dependent responses to sex pheromones in mouse. Current Opinion in Neurobiology. 2016 Jun;38:74–9.
3. Martín-Sánchez A, McLean L, Beynon RJ, Hurst JL, Ayala G, Lanuza E, et al. From sexual attraction to maternal aggression: When pheromones change their behavioural significance. Hormones and Behavior. 2015 Feb;68:65–76.
4. Beny Y, Kimchi T. Innate and learned aspects of pheromone-mediated social behaviours. Animal Behaviour. 2014 Nov;97:301–11.
5. Ervin KSJ, Lymer JM, Matta R, Clipperton-Allen AE, Kavaliers M, Choleris E. Estrogen involvement in social behavior in rodents: Rapid and long-term actions. Hormones and Behavior. 2015 Aug;74:53–76.
6. Petrulis A. Chemosignals, hormones and mammalian reproduction. Hormones and Behavior. 2013 May;63(5):723–41.
7. Demir E, Li K, Bobrowski-Khoury N, Sanders JI, Beynon RJ, Hurst JL, et al. The pheromone darcin drives a circuit for innate and reinforced behaviours. Nature. 2020 Feb 6;578(7793):137–41.
8. Roberts SA, Davidson AJ, McLean L, Beynon RJ, Hurst JL. Pheromonal Induction of Spatial Learning in Mice. Science. 2012 Dec 14;338(6113):1462–5.
9. St. John RD, Corning PA. Maternal aggression in mice. Behavioral Biology. 1973 Nov;9(5):635–9.

10. Svare B, Betteridge C, Katz D, Samuels O. Some situational and experiential determinants of maternal aggression in mice. Physiology & Behavior. 1981 Feb;26(2):253–8.
11. Bruce HM. An exteroceptive block to pregnancy in the mouse. Nature. 1959 Jul 11;
12. Brennan PA. Outstanding issues surrounding vomeronasal mechanisms of pregnancy block and individual recognition in mice. Behavioural Brain Research. 2009 Jun 25;200(2):287–94.
13. Ralls K. Mammalian Scent Marking: Mammals mark when dominant to and intolerant of others, not just when they possess a territory. Science. 1971 Feb 5;171(3970):443–9.
14. Johnson RP. Scent marking in mammals. Animal Behaviour. 1973 Aug;21(3):521–35.
15. Roberts SC. Scent-marking (Ch. 22). In: Rodent Societies. University of Chicago Press; 2007. p. 255–66.
16. Hurst JL. Urine marking in populations of wild house mice Mus domesticus rutty. I. Communication between males. Animal Behaviour. 1990 Aug;40(2):209–22.
17. Hurst JL. Urine marking in populations of wild house mice Mus domesticus rutty. II. Communication between females. Animal Behaviour. 1990 Aug;40(2):223–32.
18. Hurst JL. Urine marking in populations of wild house mice Mus domesticus Rutty. III. Communication between the sexes. Animal Behaviour. 1990 Aug;40(2):233–43.
19. Hurst JL, Beynon RJ. Scent wars: the chemobiology of competitive signalling in mice. Bioessays. 2004 Dec;26(12):1288–98.

20. Coombes HA, Stockley P, Hurst JL. Female Chemical Signalling Underlying Reproduction in Mammals. J Chem Ecol. 2018 Sep;44(9):851–73.
21. Cheetham SA, Thom MD, Jury F, Ollier WER, Beynon RJ, Hurst JL. The Genetic Basis of Individual-Recognition Signals in the Mouse. Current Biology. 2007 Oct;17(20):1771–7.
22. Roberts SA, Davidson AJ, Beynon RJ, Hurst JL. Female attraction to male scent and associative learning: the house mouse as a mammalian model. Animal Behaviour. 2014 Nov;97:313–21.
23. Sheehan MJ, Lee V, Corbett-Detig R, Bi K, Beynon RJ, Hurst JL, et al. Selection on Coding and Regulatory Variation Maintains Individuality in Major Urinary Protein Scent Marks in Wild Mice. Barsh GS, editor. PLoS Genet. 2016 Mar 3;12(3):e1005891.
24. Sheehan MJ, Campbell P, Miller CH. Evolutionary patterns of major urinary protein scent signals in house mice and relatives. Mol Ecol. 2019 Aug;28(15):3587–601.
25. Lee W, Khan A, Curley JP. Major urinary protein levels are associated with social status and context in mouse social hierarchies. Proc R Soc B. 2017 Sep 27;284(1863):20171570.
26. Desjardins C, Maruniak JA, Bronson FH. Social Rank in House Mice: Differentiation Revealed by Ultraviolet Visualization of Urinary Marking Patterns. Science. 1973 Nov 30;182(4115):939–41.
27. Kaur AW, Ackels T, Kuo TH, Cichy A, Dey S, Hays C, et al. Murine Pheromone Proteins Constitute a Context-Dependent Combinatorial Code Governing Multiple Social Behaviors. Cell. 2014 Apr;157(3):676–88.

28. Ferkin MH. Scent marks of rodents can provide information to conspecifics. Anim Cogn. 2019 May;22(3):445–52.
29. Ferkin MH. The response of rodents to scent marks: Four broad hypotheses. Hormones and Behavior. 2015 Feb;68:43–52.
30. Asaba A, Hattori T, Mogi K, Kikusui T. Sexual attractiveness of male chemicals and vocalizations in mice. Front Neurosci. 2014 Aug 5.
31. Hurst JL. Female recognition and assessment of males through scent. Behavioural Brain Research. 2009 Jun 25;200(2):295–303.
32. Mucignat-Caretta C, Caretta A, Baldini E. Protein-bound Male Urinary Pheromones: Differential Responses According to Age and Gender. Chemical Senses. 1998 Feb 1;23(1):67–70.
33. Drickamer LC. Odor preferences of wild stock female house mice (Mus domesticus) tested at three ages using urine and other cues from conspecific males and females. J Chem Ecol. 1989 Jul;15(7):1971–87.
34. Mossman CA, Drickamer LC. Odor preferences of female house mice (Mus domesticus) in seminatural enclosures. Journal of Comparative Psychology. 1996;110(2):131–8.
35. Hurst JL, Payne CE, Nevison CM, Marie AD, Humphries RE, Robertson DHL, et al. Individual recognition in mice mediated by major urinary proteins. Nature. 2001 Dec;414(6864):631–4.
36. Chamero P, Marton TF, Logan DW, Flanagan K, Cruz JR, Saghatelian A, et al. Identification of protein pheromones that promote aggressive behaviour. Nature. 2007 Dec;450(7171):899–902.
37. Ajayi AF, Akhigbe RE. Staging of the estrous cycle and induction of estrus in experimental rodents: an update. Fertil Res and Pract. 2020 Dec;6(1):5.

38. Byers SL, Wiles MV, Dunn SL, Taft RA. Mouse Estrous Cycle Identification Tool and Images. Singh SR, editor. PLoS ONE. 2012 Apr 13;7(4):e35538.
39. Caligioni CS. Assessing Reproductive Status/Stages in Mice. Current Protocols in Neuroscience. 2009 Jul;48(1).
40. McLean AC, Valenzuela N, Fai S, Bennett SAL. Performing Vaginal Lavage, Crystal Violet Staining, and Vaginal Cytological Evaluation for Mouse Estrous Cycle Staging Identification. JoVE. 2012 Sep 15;(67):4389.
41. Elliot AJ. The Hierarchical Model of Approach-Avoidance Motivation. Motiv Emot. 2006 Oct 6;30(2):111–6.
42. Silverman JL, Yang M, Lord C, Crawley JN. Behavioural phenotyping assays for mouse models of autism. Nat Rev Neurosci. 2010 Jul;11(7):490–502.
43. Kurien BT, Scofield RH. Mouse urine collection using clear plastic wrap. Lab Anim. 1999 Jan 1;33(1):83–6.
44. Phifer-Rixey M, Bi K, Ferris KG, Sheehan MJ, Lin D, Mack KL, et al. The genomic basis of environmental adaptation in house mice. Payseur BA, editor. PLoS Genet. 2018 Sep 24;14(9):e1007672.
45. Miller CH, Hillock MF, Yang J, Carlson-Clarke B, Haxhillari K, Lee AY, et al. Dynamic changes to signal allocation rules in response to variable social environments in house mice. bioxRiv; 2022 Jan.
46. Cheetham SA, Smith AL, Armstrong SD, Beynon RJ, Hurst JL. Limited variation in the major urinary proteins of laboratory mice. Physiology & Behavior. 2009 Feb;96(2):253–61.
47. Nevison CM, Barnard CJ, Beynon RJ, Hurst JL. The consequences of inbreeding for recognizing competitors. Proc R Soc Lond B. 2000 Apr 7;267(1444):687–94.

48. Roberts SA, Simpson DM, Armstrong SD, Davidson AJ, Robertson DH, McLean L, et al. Darcin: a male pheromone that stimulates female memory and sexual attraction to an individual male's odour. BMC Biology. 2010;8(75):21.
49. Mudge JM, Armstrong SD, McLaren K, Beynon RJ, Hurst JL, Nicholson C, et al. Dynamic instability of the Major Urinary Protein gene family revealed by genomic and phenotypic comparisons between C57 and 129 strain mice. Genome Biol. 2008;9(5):R91.
50. Sherborne AL, Thom MD, Paterson S, Jury F, Ollier WER, Stockley P, et al. The Genetic Basis of Inbreeding Avoidance in House Mice. Current Biology. 2007 Dec;17(23):2061–6.
51. Ishii KK, Osakada T, Mori H, Miyasaka N, Yoshihara Y, Miyamichi K, et al. A Labeled-Line Neural Circuit for Pheromone-Mediated Sexual Behaviors in Mice. Neuron. 2017 Jul;95(1):123-137.e8.
52. Haga S, Hattori T, Sato T, Sato K, Matsuda S, Kobayakawa R, et al. The male mouse pheromone ESP1 enhances female sexual receptive behaviour through a specific vomeronasal receptor. Nature. 2010 Jul;466(7302):118–22.
53. Tolokh II, Fu X, Holy TE. Reliable Sex and Strain Discrimination in the Mouse Vomeronasal Organ and Accessory Olfactory Bulb. Journal of Neuroscience. 2013 Aug 21;33(34):13903–13.
54. Kaba H, Rosser A, Keverne B. Neural basis of olfactory memory in the context of pregnancy block. Neuroscience. 1989 Jan;32(3):657–62.
55. Lloyd-Thomas A, Keverne EB. Role of the brain and accessory olfactory system in the block to pregnancy in mice. Neuroscience. 1982 Apr;7(4):907–13.

56. Cansler HL, Maksimova MA, Meeks JP. Experience-Dependent Plasticity in Accessory Olfactory Bulb Interneurons following Male–Male Social Interaction. J Neurosci. 2017 Jul 26;37(30):7240–52.
57. Gao Y, Budlong C, Durlacher E, Davison IG. Neural mechanisms of social learning in the female mouse. eLife. 2017 Jun 16;6:e25421.
58. Oboti L, Schellino R, Giachino C, Chamero P, Pyrski M, Leinders-Zufall T, et al. Newborn Interneurons in the Accessory Olfactory Bulb Promote Mate Recognition in Female Mice. Front Neurosci. 2011;5.
59. Moffitt JR, Bambah-Mukku D, Eichhorn SW, Vaughn E, Shekhar K, Perez JD, et al. Molecular, spatial, and functional single-cell profiling of the hypothalamic preoptic region. Science. 2018 Nov 16;362(6416):eaau5324.
60. Unger EK, Burke KJ, Yang CF, Bender KJ, Fuller PM, Shah NM. Medial Amygdalar Aromatase Neurons Regulate Aggression in Both Sexes. Cell Reports. 2015 Feb;10(4):453–62.
61. Bayless DW, Yang T, Mason MM, Susanto AAT, Lobdell A, Shah NM. Limbic Neurons Shape Sex Recognition and Social Behavior in Sexually Naive Males. Cell. 2019 Feb;176(5):1190-1205.e20.
62. Cooke BM. Steroid-dependent plasticity in the medial amygdala. Neuroscience. 2006 Mar;138(3):997–1005.
63. Choi GB, Dong H wei, Murphy AJ, Valenzuela DM, Yancopoulos GD, Swanson LW, et al. Lhx6 Delineates a Pathway Mediating Innate Reproductive Behaviors from the Amygdala to the Hypothalamus. Neuron. 2005 May;46(4):647–60.
64. Raam T, Hong W. Organization of neural circuits underlying social behavior: A consideration of the medial amygdala. Current Opinion in Neurobiology. 2021 Jun;68:124–36.

65. Binns KE, Brennan PA. Changes in electrophysiological activity in the accessory olfactory bulb and medial amygdala associated with mate recognition in mice. European Journal of Neuroscience. 2005 May;21(9):2529–37.
66. Correa SM, Newstrom DW, Warne JP, Flandin P, Cheung CC, Lin-Moore AT, et al. An Estrogen-Responsive Module in the Ventromedial Hypothalamus Selectively Drives Sex-Specific Activity in Females. Cell Reports. 2015 Jan;10(1):62–74.
67. Falkner AL, Grosenick L, Davidson TJ, Deisseroth K, Lin D. Hypothalamic control of male aggression-seeking behavior. Nat Neurosci. 2016 Apr;19(4):596–604.
68. Hashikawa K, Hashikawa Y, Tremblay R, Zhang J, Feng JE, Sabol A, et al. Esr1+ cells in the ventromedial hypothalamus control female aggression. Nat Neurosci. 2017 Nov;20(11):1580–90.
69. Lee H, Kim DW, Remedios R, Anthony TE, Chang A, Madisen L, et al. Scalable control of mounting and attack by Esr1+ neurons in the ventromedial hypothalamus. Nature. 2014 May 29;509(7502):627–32.
70. Lin D, Boyle MP, Dollar P, Lee H, Lein ES, Perona P, et al. Functional identification of an aggression locus in the mouse hypothalamus. Nature. 2011 Feb;470(7333):221–6.
71. Wang L, Chen IZ, Lin D. Collateral Pathways from the Ventromedial Hypothalamus Mediate Defensive Behaviors. Neuron. 2015 Mar;85(6):1344–58.
72. Yang CF, Chiang MC, Gray DC, Prabhakaran M, Alvarado M, Juntti SA, et al. Sexually Dimorphic Neurons in the Ventromedial Hypothalamus Govern Mating in Both Sexes and Aggression in Males. Cell. 2013 May;153(4):896–909.

73. Yang T, Yang CF, Chizari MD, Maheswaranathan N, Burke KJ, Borius M, et al. Social Control of Hypothalamus-Mediated Male Aggression. Neuron. 2017 Aug;95(4):955-970.e4.
74. Inoue S, Yang R, Tantry A, Davis C ha, Yang T, Knoedler JR, et al. Periodic Remodeling in a Neural Circuit Governs Timing of Female Sexual Behavior. Cell. 2019 Nov;179(6):1393-1408.e16.
75. Nomoto K, Lima SQ. Enhanced Male-Evoked Responses in the Ventromedial Hypothalamus of Sexually Receptive Female Mice. Current Biology. 2015 Mar;25(5):589–94.
76. Pfaff DW, Sakuma Y. Facilitation of the lordosis reflex of female rats from the ventromedial nucleus of the hypothalamus. Journal of Physiology. 1979;288:189–202.
77. Musatov S, Chen W, Pfaff DW, Kaplitt MG, Ogawa S. RNAi-mediated silencing of estrogen receptor α in the ventromedial nucleus of hypothalamus abolishes female sexual behaviors. Proc Natl Acad Sci USA. 2006 Jul 5;103(27):10456–60.
78. Miller SM, Marcotulli D, Shen A, Zweifel LS. Divergent medial amygdala projections regulate approach–avoidance conflict behavior. Nat Neurosci. 2019 Apr;22(4):565–75.
79. Silva BA, Mattucci C, Krzywkowski P, Murana E, Illarionova A, Grinevich V, et al. Independent hypothalamic circuits for social and predator fear. Nat Neurosci. 2013 Dec;16(12):1731–3.
80. McLean DJ, Skowron Volponi MA. trajr: An R package for characterisation of animal trajectories. Tregenza T, editor. Ethology. 2018 Jun;124(6):440–8.
81. Bates D. Parsimonious Mixed Models. ArXiv. 2018 May 26;arXiv:1506.04967:21.

82. Kuznetsova A, Brockhoff PB, Christensen RHB. lmerTest Package: Tests in Linear Mixed Effects Models. J Stat Soft [Internet]. 2017 [cited 2022 Jan 10];82(13). Available from: http://www.jstatsoft.org/v82/i13/
83. Gouveia K, Hurst JL. Reducing Mouse Anxiety during Handling: Effect of Experience with Handling Tunnels. Mintz EM, editor. PLoS ONE. 2013 Jun 20;8(6):e66401.
84. Armstrong SD, Robertson DHL, Cheetham SA, Hurst JL, Beynon RJ. Structural and functional differences in isoforms of mouse major urinary proteins: a male-specific protein that preferentially binds a male pheromone. Biochemical Journal. 2005 Oct 15;391(2):343–50.
85. Beynon RJ, Veggerby C, Payne CE, Robertson DHL, Gaskell SJ, Humphries RE, et al. Polymorphism in Major Urinary Proteins: Molecular Heterogeneity in a Wild Mouse Population. Journal of Chemical Ecology. 2002;18.
86. Pang SC, Janzen-Pang J, Tse MY, Croy BA, Lima PDA. The Cycling and Pregnant Mouse. In: The Guide to Investigation of Mouse Pregnancy [Internet]. Elsevier; 2014 [cited 2022 Jun 6]. p. 3–19. Available from: https://linkinghub.elsevier.com/retrieve/pii/B9780123944450000011
87. Behringer R, Gertsenstein M, Nagy KV, Nagy A. Selecting Female Mice in Estrus and Checking Plugs. Cold Spring Harb Protoc. 2016 Aug;2016(8):pdb.prot092387.
88. Heyne GW, Plisch EH, Melberg CG, Sandgren EP, Peter JA, Lipinski RJ. A Simple and Reliable Method for Early Pregnancy Detection in Inbred Mice. Journal of the American Association for Laboratory Animal Science. :4.
89. Peirson SN, Brown LA, Pothecary CA, Benson LA, Fisk AS. Light and the laboratory mouse. Journal of Neuroscience Methods. 2018 Apr;300:26–36.

90. Friard O, Gamba M. BORIS : a free, versatile open-source event-logging software for video/audio coding and live observations. Fitzjohn R, editor. Methods Ecol Evol. 2016 Nov;7(11):1325–30.

91. Lenth RV. Least-Squares Means: The *R* Package lsmeans. J Stat Soft. 2016;69(1). Available from: http://www.jstatsoft.org/v69/i01/